

**Structural and reactivity studies of new
organophosphorus amides**

by

Susan Laurens

**Structural and reactivity studies of new
organophosphorus amides**

A thesis submitted by

Susan Laurens

In partial fulfillment for the degree of

Philosophiae Doctor
(CHEMISTRY)

School of Physical Sciences
Faculty of Natural and Agricultural Sciences

UNIVERSITY OF PRETORIA

Advisor: Prof. J.C.A. Boeyens

January 2005

INDEX

Abstract	i
Opsomming	iii
1. Introduction	1
1.1 General Background	1
1.2 Objectives	18
1.3 References	19
2. <i>N</i> -Alkylderivatives of 1-oxo-2,8-disubstituted-2,5,8-triaza-1 λ^5 - phosphabicyclo[3.3.0]-octane	22
2.1 Introduction	22
2.2 Results and Discussion	23
2.2.1 Acid catalyzed alcoholysis	23
2.2.2 Base catalyzed alcoholysis	24
2.2.3 Rearrangement of the alcoholysis product	25
2.3 Experimental	27
2.4 References	35
3. Thio analogues of 1-oxo-2,8-diaryl-2,5,8-triaza-1 λ^5 -phosphabicyclo[3.3.0]- octane	36
3.1 Introduction	36
3.2 Results and Discussion	39
3.2.1 Synthesis	39
3.2.2 Acid catalyzed alcoholysis	50
3.2.3 Base catalyzed alcoholysis	52
3.2.4 Rearrangement of the alcoholysis product	52
3.2.5 Derivatives of 1-thio-2,8-diaryl-2,5,8-triaza-1 λ^5 - phosphabicyclo[3.3.0]-octane	59
3.3 Experimental	62
3.3.1 Synthesis of new thio analogues	62
3.3.2 GC-MS Analysis	67
3.4 References	67

4. Structural Analysis	70
4.1 NMR Analysis	70
4.1.1 Introduction	70
4.1.2 Experimental	76
4.1.3 Results and discussion	77
4.2 Crystal Structure Analysis	78
4.2.1 Introduction	78
4.2.2 Experimental	79
4.2.3 Results and discussion	89
4.3 References	92
5. Theoretical Calculations	94
5.1 Introduction to Molecular Modeling	94
5.2 Experimental	97
5.3 Results and Discussion	102
5.4 References	112
6. Conclusion	113
6.1 References	117
<i>Publications originated from this work</i>	118

Acknowledgements

I wish to express my sincere thanks to the following people:

1. Prof. Jan Boeyens for his support and encouragement.
2. Dr. Vimahl Ichharam and Dr. Dave Liles for their help with the crystal structures.
3. Prof. Peet van Rooyen for his encouragement till the end.
4. Prof. Phillip Wessels for his help with the NMR calculations.
5. My family for their continuous support and the sacrifices they had to make.
6. NRF and University of Pretoria for financial assistance.

The experimental work described in this thesis was done under the supervision of Professor T.A. Modro. Part of the work was published by the candidate as co-author with Professor Modro. Composition of the written thesis is the candidate's own work, presented without Prof. Modro's approval of the final draft.

ABSTRACT

The bicyclic substrates 1-oxo-2,8-diaryl-2,5,8-triaza-1 λ^5 -phosphabicyclo[3.3.0]-octane **3** were studied before. The molecular rearrangement of the alcoholysis product of **3** (the eight-membered ring compound 1-oxo-1-ethoxy-2,8-diaryl-2,5,8-triaza-1 λ^5 -phosphacyclooctane) to the five-membered ring isomer (the 1,3,2 λ^5 -diazaphospholidine system) is reasonably well understood for the *N,N*-diaryl substituted substrates. It was decided to expand the studies of the bicyclic system **3** to other derivatives with aliphatic substituents on the nitrogen atoms (R=PhCH₂, Me, Et), as well as the thiophosphoryl and phosphine analogues of **3**.

Differences between the *N*-aryl and *N*-alkyl substrates were observed in the acid and base catalyzed solvolysis of the bicyclic substrate. The reactivity in the rearrangement of the solvolysis product, from an eight-membered ring to the five-membered ring isomer was also different. The *N,N'*-dialkyl substituted compounds rearranged much slower to the corresponding five-membered ring compounds than the *N,N'*-diaryl analogues.

The thiophosphoryl analogue of **3a** (R=Ph), 1-thio-2,8-diphenyl-2,5,8-triaza-1 λ^5 -phosphabicyclo[3.3.0]octane **11a** was prepared by reacting *bis*-(2-phenylamino-ethyl)amine with P(S)Cl₃ in the presence of a base. The alcoholysis product of **11a**, observed in ³¹P NMR (δ_P 76), was the eight-membered ring compound **15**. This compound then rearranged to the five-membered ring isomer **16** during GC-MS analysis. This rearrangement is analogous to the rearrangement observed for the corresponding phosphoryl derivatives. Both the thiophosphoryl bicyclic **11a** and the phosphoryl bicyclic **3a** compounds were detected in the mass spectrum of compound **15**. This could be explained in terms of the thiono (P(S)OR) to thiolo (P(O)SR) rearrangement.

The NMR spectra of the phosphoryl and thiophosphoryl bicyclic compounds **3a** and **11a** proved to have distinct differences in the aliphatic region as far as

coupling constants are concerned. From the crystal structures it was clear that the two halves (two five-membered rings) of **3a** and **11a** had remarkably different dihedral angles. The NMR data represented an average of the two rings, therefore they appear identical on the NMR-scale.

Comparing the dihedral angles as determined from NMR data, by utilization of the Karplus equation, with the dihedral angles obtained from X-ray diffraction data was only approximate. There was very little correlation between the experimental and the calculated dihedral angles for compounds **3a** and **11a**. An average value of the dihedral angles, resulting from NMR data, was not in agreement with the crystal structures.

The MM⁺ force field of HyperChem® was adapted to perform molecular mechanical calculations in an effort to enhance the conceptualization of the properties and the behaviour of these new heterocyclic compounds. The calculated energies of the eight-membered ring and five-membered ring isomers, for all the different derivatives, confirmed that the rearrangement is thermodynamically controlled. The five-membered ring isomer in each case had lower total strain energy than the eight-membered ring isomer.

The thiono and thiole isomers had comparable potential energies. The thiono isomer of the *N*-Benzyl derivative had a slightly lower potential energy than the thiole isomer, for both the eight- and five-membered ring isomers. The calculated energies for both the thiono and the thiole isomers suggested that the five-membered ring isomer was thermodynamically more stable than the eight-membered ring compound.

OPSOMMING

Die bisikliese verbinding 1-okso-2,8-diariel-2,5,8-triasa-1 λ^5 -fosfabisiklo[3.3.0]-oktaan **3**, is voorheen berei en bestudeer. Die molekuleêre herrangskikking van die solvolise produk van **3**, die agtliedring 1-okso-1-alkoksie-2,8-diariel-2,5,8-triasa-1 λ^5 -fosfasiklooktaan na die vyfliedring isomeer, die 1,3,2 λ^5 -diasa-fosfolidine sisteem, word redelik goed verstaan vir die verbindings met aromatiese substituentte op stikstof. Die studie van die bisikliese sisteem **3** is uitgebrei na ander afgeleides met alifatiese substituentte op stikstof sowel as die swawel analoë van **3**.

Die suur en basies gekataliseerde solvolise van **3** verloop verskillend vir die *N*-ariel en *N*-alkiel afgeleides. Verskille is ook waargeneem in die verloop van die agtliedring na vyfliedring herrangskikking. Die *N,N*-dialkiel gesubstitueerde verbindings herrangskik na die ooreenstemmende vyfliedring, maar veel stadiger as die *N,N*-diariel analoë.

Die swawel analoog van **3a**, 1-tio-2,8-difeniel-2,5,8-triasa-1 λ^5 -fosfabisiklo[3.3.0]-oktaan **11a** was berei deur *bis*-(2-fenielamino-etiel)amien met P(S)Cl₃ te laat reageer in die teenwoordigheid van 'n basis. Die alkoholise produk van **11a** wat waargeneem is in ³¹P NMR (δ_P 76) was die agtliedring isomer **15**. Hierdie produk herrangskik onder kondisies van GC-MS analise, na die vyfliedring isomer **16**. Hierdie herrangskikking is in ooreenstemming met die herrangskikking in die ooreenkomstige fosforiel afgeleides. Beide die uitgangstof vir die alkoholise sowel as die suurstof analoog is waargeneem in die massaspektrum. Hierdie waarneming kan verklaar word aan die hand van die tiono (P(S)OR) na tiolo (P(O)SR) herrangskikking.

Die KMR spektra van die fosforiel en die tiofosforiel bisikliese verbindings **3a** en **11a** toon aansienlike verskille in die alifatiese gebied. Die kristalstruktuur data toon dat die twee helftes van die bisikliese verbindings **3a** en **11a** merkbaar

verskil in terme van die dihedrale hoeke. Die KMR data verteenwoordig 'n gemiddelde van die twee ringe, dus vertoon die twee helftes identies op die KMR-skaal. Die vergelyking van die dihedrale hoeke, soos bepaal vanaf KMR data met behulp van die Karplus vergelyking, met die dihedrale hoeke wat verkry is uit X-straaldiffraksie data is in elke geval baie benaderd. Daar is min korrelasie tussen die eksperimentele en berekende dihedrale hoeke vir **3a** en **11a**. Die gemiddelde waarde soos verkry uit KMR data stem nie ooreen met die kristalstrukture nie.

Die MM⁺ kragveld van HyperChem® is aangepas om die eienskappe en reaktiwiteit van die nuwe heterosikliese verbindings verder te bestudeer. Die berekende energieë van die aglidring en vyflidring isomere van al die verskillende afgeleides bevestig dat die herrangskikking termodinamies beheer word. In elke geval het die vyflidring isomeer 'n laer energie as die agtlidring isomeer.

Die tiono en tiolo isomere het vergelykbare potensiële energieë. Die tiolo isomeer van die *N*-Bensiel afgeleide het 'n effens laer energie as die tiono isomeer vir beide die aglidring as die vyflidring isomere. Vir beide die tiono en tiolo isomere, toon die berekende energieë dat die vyflidring isomeer termodinamies meer stabiel is as die aglidring isomeer.

CHAPTER 1

1. INTRODUCTION

1.1 General Background

Phosphorus is an unusual chemical element. In the pure form it can burst into flames spontaneously but is also used in some of the best flame-retarding agents.¹ Tiny amounts of phosphorus play a vital role in all living processes in plants and animals.^{2,3} Gorenstein et.al.⁴ refers to DNA, the genetic tape that guides the reproduction of all species, as the ultimate phosphorus polymer. The essential functions of phosphorus are performed in the form of phosphate esters and diesters⁵. The predominant example of a naturally occurring phosphorus-carbon compound, is 2-aminoethylphosphonic acid, **A** which was isolated from certain protozoa (**Figure 1.1**).

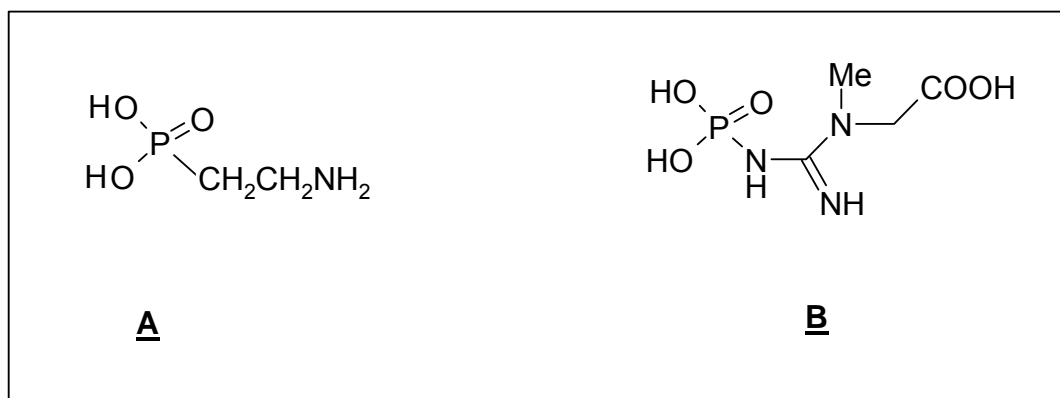


Figure 1.1 Structures of 2-aminoethylphosphonic acid, **A** and phosphocreatine, **B**.

Phosphocreatine **B** is an essential phosphorus-nitrogen compound and this bond may be the reason for its usefulness as a stored form of phosphate⁶. This compound is held in reserve as a reagent for the emergency regeneration of adenosine triphosphate (ATP) **C** (**Figure1.2**). ATP supplies energy for all metabolic pathways important in living organisms.

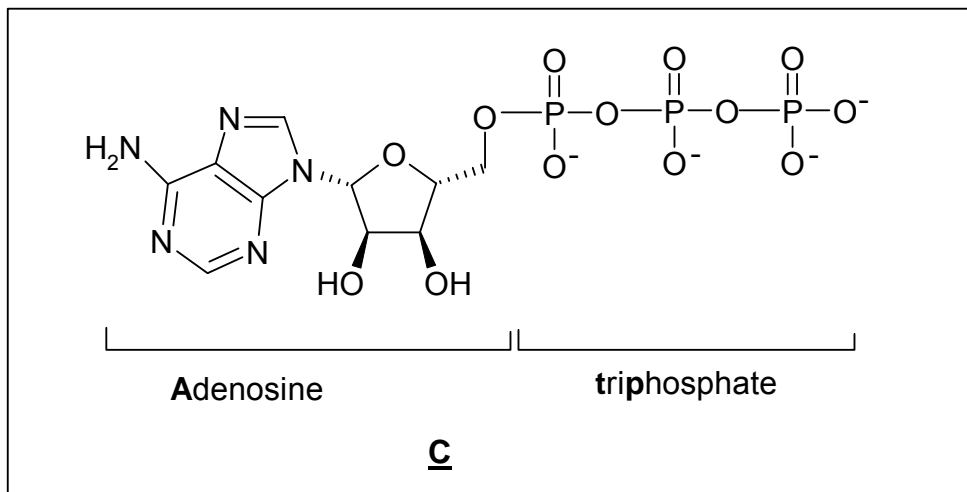


Figure 1.2 Structure of adenosine triphosphate (ATP).

The fact that organophosphorus compounds can form substances with the coordination number of phosphorus ranging from 1 to 6 made a lot of questions arise regarding the stability and reactivity of these compounds. The academic interest in phosphorus compounds made the knowledge of phosphorus chemistry expand enormously since 1960 and the number of phosphorus compounds increased considerably⁷, with diverse practical applications.

Modern investigations of organophosphorus compounds started in 1932 with the preparation of the dimethyl and diethyl phosphorofluoridates⁸. The statement that inhalation of these compounds caused a persistent choking sensation and blurred vision made Schrader⁹ explore this class of compounds for insecticidal activity. This study resulted in preparing the well-known insecticide Parathion¹⁰ (O,O-diethyl O-(4-nitrophenyl)-phosphorothioate) **D**. Further examples are octamethylpyrophosphoramidate (Shradan) **E** and N-acetyl-O,S-dimethylphosphoramidothioate (Orthene) **E** which are systemic and contact insecticides respectively. Prior to the Second World War Schrader established the extremely high toxicity of an organophosphorus compound, O-ethyl *N,N*-dimethylphosphoramidocyanidate (Tabun)¹¹ **G** that became the first of the lethal organophosphorus chemical warfare agents. Tabun is a nerve gas, which causes death by blocking nerve function activity.

McCombie and Saunders¹² synthesized the chemical warfare agent diisopropyl phosphorofluoridate (DFP) **H**, which was the organophosphorus compound studied most extensively by British and American scientists.

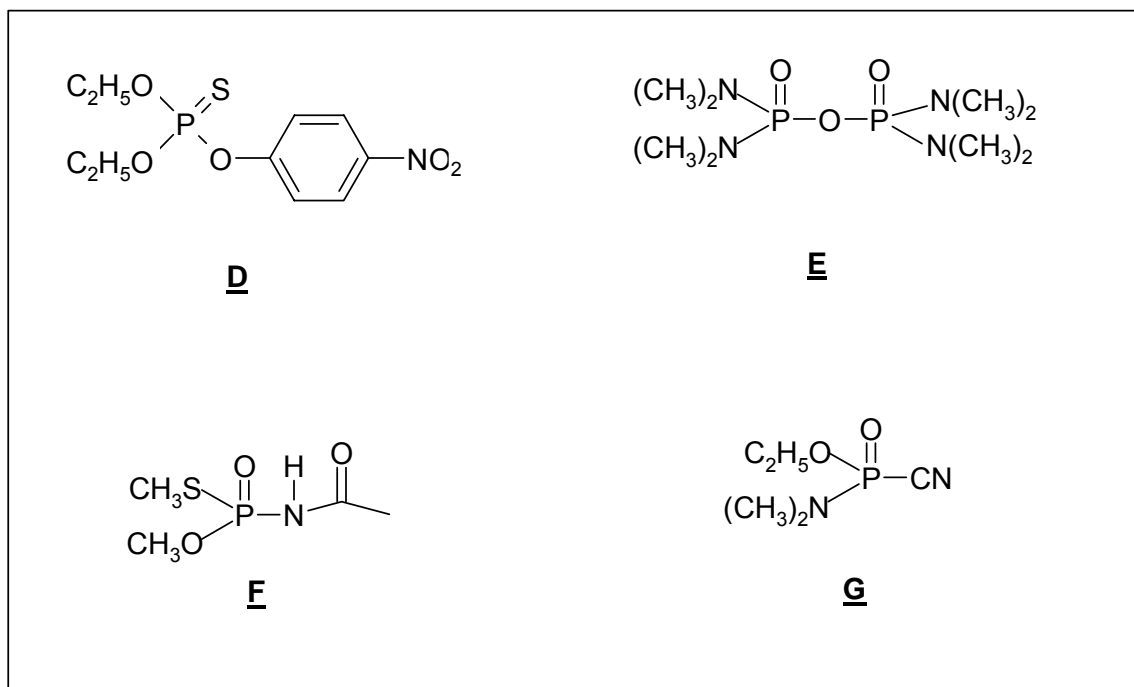


Figure 1.3. Structures of Parathion **D**, Shradan **E**, Orthene **F** and Tabun **G**.

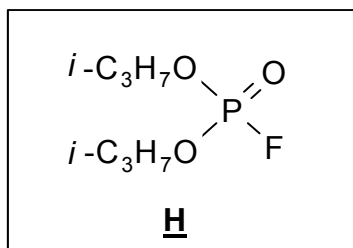


Figure 1.4 Diisopropyl phosphorofluoridate (DFP).

The family of phosphorylated nitrogen mustards, i.e. compounds containing the *bis*-(2-chloroethyl)amino group, are known to be highly effective alkylating agents with respect to a variety of nucleophilic centers, which find application in anti-tumor chemotherapy^{13,14,15}. The alkylating mechanism of these compounds^{16,17,18} like Cyclophosphamide **I**, Ifosfophamide **J** and Trofosphamide **K**, (**Figure 1.5**) has been thoroughly investigated and is well documented.

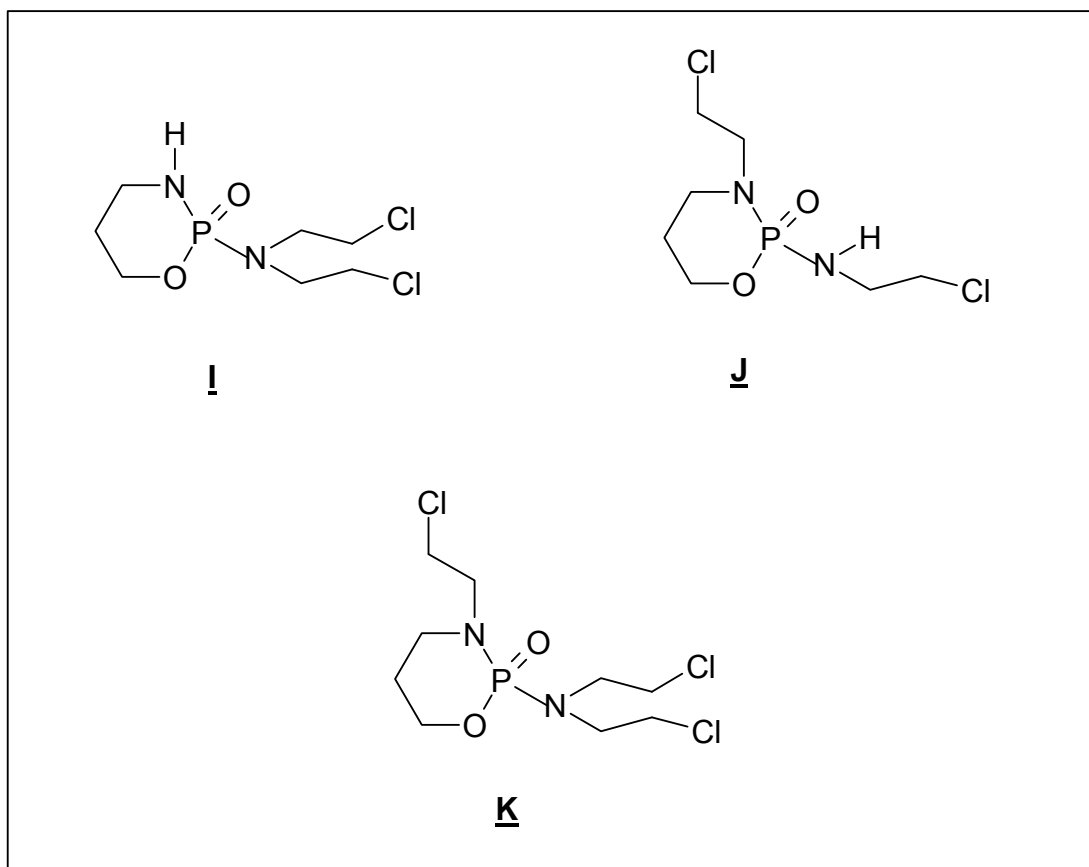
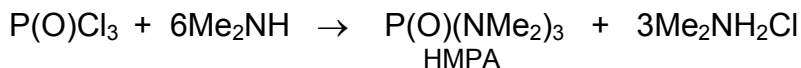


Figure 1.5 Structures of Cyclophosphamide **I**, Ifosfophamide **J** and Trofosphamide **K**.

Compounds containing a nitrogen atom bonded to phosphorus represent an important class of organophosphorus compounds. The field of phosphorus-nitrogen chemistry attracted a lot of attention as phosphorus and nitrogen produce an interesting bonding system. The amine and amide derivatives of four-coordinate pentavalent phosphorus have a formal σ P-N single bond. However this simple bond can have an element of extra bonding, involving a

$2p(N) \rightarrow 3d(P)\pi$ donor system. When the bond distance between phosphorus and nitrogen is relatively short, the nitrogen is sp^3 hybridized (tetrahedral geometry), donating the lone pair of electrons to an empty 3d orbital of phosphorus. As the bond distance increases, the nitrogen loses some of its 's' character to approach ' p^3 ' character. The nitrogen in this 'unhybridized' state has an ideal pyramidal geometry with the lone pair of electrons occupying the 2s atomic orbital of nitrogen. This change in hybridization has a direct effect on the ^{31}P NMR chemical shift. This phenomenon is discussed later in this chapter. The degree of π bonding with phosphorus also reflects the basicity of the nitrogen atom.

Most of the interest in phosphorus-nitrogen chemistry is centered on the phosphoryl derivatives. One such derivative is hexamethylphosphoramide (HMPA) that seems to be the most used compound in this series. HMPA is a good polar aprotic non-aqueous solvent, which is prepared from $\text{P}(\text{O})\text{Cl}_3$ and an excess of dimethylamine (**Scheme 1.1**).

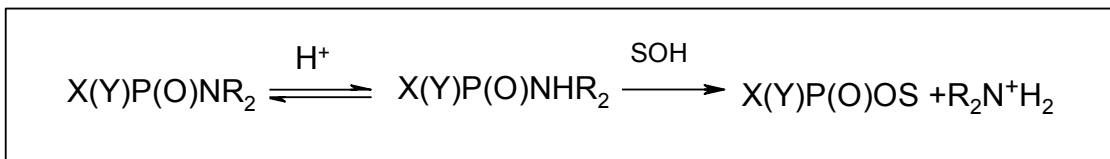


Scheme 1.1 Preparation of hexamethylphosphoramide (HMPA).

The same reaction applies with the use of $\text{P}(\text{S})\text{Cl}_3$ and almost any amine. This type of reaction was the starting point for the synthesis of almost all compounds discussed in this project.

Systems containing the phosphoramidate function $\text{P}(\text{O})\text{N}$ have been the subject of research in our laboratories for many years. The physical and chemical characteristics of the phosphoramidates have been investigated.^{19,20,21} Many features of the P-N bonding in this system have been explored e.g. the nucleophilic cleavage of the P-N bond^{22,23} and the nucleophilicity of the $\text{P}(\text{O})\text{N}$ function²⁴. The remarkably facile fission of the P-N bond under mildly acidic conditions found synthetic application in preparation of chiral organophosphorus

compounds^{25,26} as well as in the modification of the Gabriel procedure of preparing aliphatic amines.²⁷ It was demonstrated that phosphoramidates solvolyze via the N-protonated reactive intermediates, which then undergo bimolecular nucleophilic attack by a solvent molecule^{28,29} (**Scheme 1.2**).



Scheme 1.2 Protonation reaction of the phosphoramidates.

The intramolecular reactivity of a series of phosphorotriamidates with the general structure, $(\text{RNH})_2\text{P(O)NHCH}_2\text{CH}_2\text{Cl}$, was studied.³⁰ Under strongly basic conditions, the *N*-alkyl derivatives ($\text{R}=\text{Me}$, PhCH_2) underwent intramolecular displacement of the chloride yielding the *N*-phosphorylated aziridine **L** (**Figure 1.6**), as the exclusive cyclization product.

For *N*-aryl derivatives ($\text{R}=\text{Ar}$), both the aziridine **L** and the 1,3,2-diazaphospholidine products **L'** could be obtained in comparable yields.

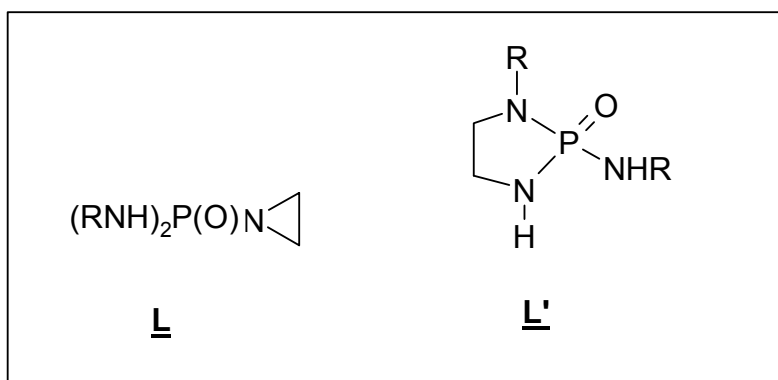


Figure 1.6 Aziridine and 1,3,2-diazaphospholidine derivatives.

The *N*-aromatic cyclic products are mutually interconvertible: 1,3,2-diazaphospholidines rearrange to the corresponding aziridines upon treatment with base, while bromide ion catalyzes the reverse isomerization.

The chemistry of the phosphorylated nitrogen mustards was further investigated by determining the effect of increasing the nucleophilicity of the phosphate moiety, by incorporation of a second nitrogen at the phosphoryl center³¹, on the stability of the system.

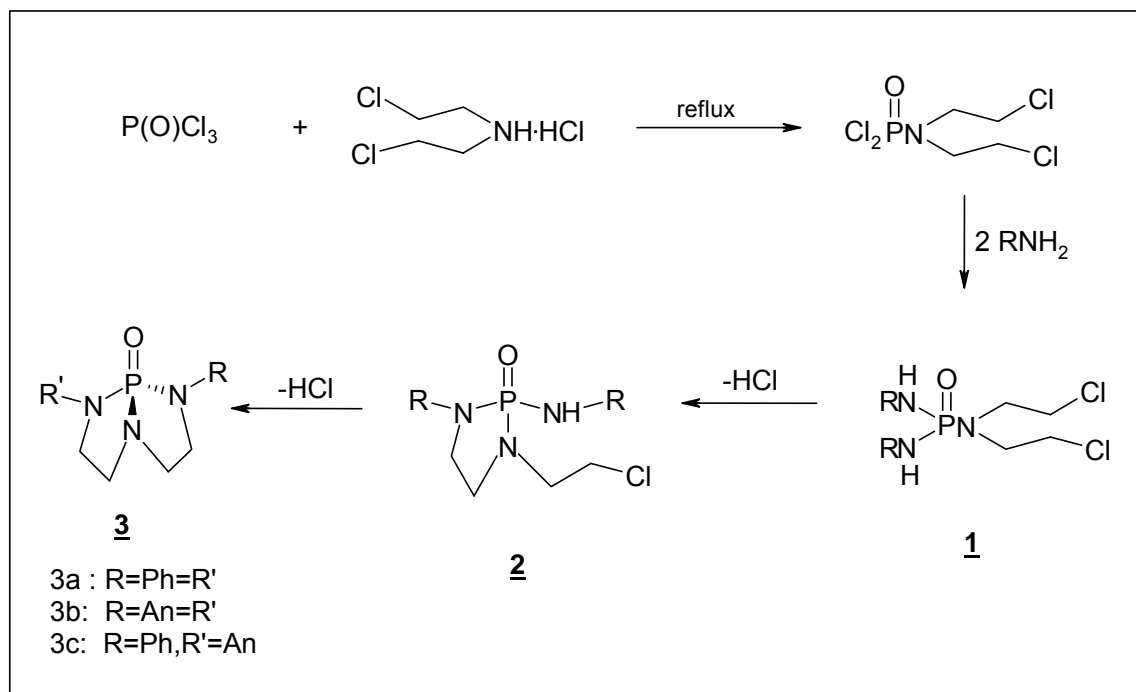
Those preliminary results^{30,31} indicated that the *N*-phosphorylated nitrogen mustards have rich and diverse chemistry, and the potential of those systems had become a major research field in our laboratory.

³¹P and ¹⁵N NMR spectra of eleven cyclic and non-cyclic, closely related phosphoramides were measured and the structures demonstrated a correlation between the bond angles at nitrogen, the ¹⁵N NMR chemical shift and the ¹J(P,N) coupling constants³².

With ¹⁵N NMR spectroscopy it was possible to distinguish between the *exo*- and *endo*-cyclic nitrogens in the monocyclic triamides. ¹⁵N NMR chemical shift values are good indication of the relative basicities of nitrogen atoms in phosphoramidates. This was demonstrated by the rates of acid catalyzed cleavage of the P-N bond in the cyclic substrates.

It was also observed that some phosphoric amides containing a chiral phosphorus atom can act as chiral recognition agents with respect to optically active compounds.³³ By acting as both, donors and acceptors for hydrogen bonding,³⁴ they formed diastereomeric hydrogen bonded complexes with optically active carboxylic and sulphonic acids.

The synthetic potential of the phosphorylated nitrogen mustards was explored by utilizing the two 2-chloroethyl chains of the mustard group to prepare a novel bicyclic system **3** (**Scheme 1.3**). A series of phosphotriamidates were prepared³⁵ which all have the essential structural feature, the -N(CH₂CH₂Cl)₂ group, attached to phosphorus.



Scheme 1.3 Reaction pathway to prepare the bicyclic compound **3**. An = 4-CH₃OC₆H₄.

The preparation of the noncyclic triamides **1** involves three subsequent nucleophilic displacement reactions at the phosphoryl center. The order of the introduction of the nucleophiles is important. The best yields were obtained when the mustard function was introduced first.

The bicyclic derivatives **3** were prepared from the non-cyclic derivative **1** via two successive base promoted cyclization reactions. The deprotonation of the amide hydrogens is followed by the intramolecular displacements of the β -chloro atom of the N-mustard function. The amide hydrogens of the noncyclic triamidate **1** are more acidic than the amide hydrogen of the monocyclic compound **2**, causing the first cyclization to take place more easily. For the second cyclization a stronger base was needed.

Phosphorus and nitrogen form part of the heterocyclic ring in the bicyclic compound. This arrangement of atoms, consisting of two fused rings with the phosphorus and one nitrogen in the bridgehead positions, and the phosphorus

attached to another two nitrogen atoms, represents a completely new heterocyclic system. The compounds with aromatic substituents on nitrogen atoms are stable crystalline compounds and were studied in detail.

The physical characteristics of the phosphoramidates e.g. the bond angles and bond distances (obtained from X-ray crystallographic data) were correlated with ^{31}P NMR data of a series of triamidates.³⁶ This correlation clearly indicated that the ^{31}P NMR chemical shift depends on the bond angles as well as the hybridization of the nitrogen atoms bonded to phosphorus. The noncyclic **1**, monocyclic **2**, bicyclic **3** and tricyclic **4** compounds in this series are characterized by specific values of ^{31}P NMR chemical shifts (δ_{P}).

Triamidate	Structure	δ_{P} Value
Non-cyclic 1 R=Ph		~ 5 ppm
Monocyclic 2 R=Ph		~ 12 ppm
Bicyclic 3 R=Ph		~ 33 ppm
Tricyclic 4		~ 98 ppm

Table 1.1 ^{31}P NMR chemical shifts of the triamidates series.

With the incorporation of each ring (from 0 to 3), there is a regular downfield shift in the ^{31}P NMR chemical shift. (**Table 1.1**). The typical range of the δ_{P} values for

compounds with the phosphoryl function bonded to three nitrogen atoms³⁷ lies between 5 and 33 ppm. Compound **4** however, has a δ_P value of 98 ppm.

The ³¹P chemical shift differences, $\Delta\delta_P$, are described by equation 1.2³⁸, where $\Delta\chi_x$ is the difference in the electronegativity in the P-N bond, Δn_π the change in the π overlap and $\Delta\theta$ the change in the N-P-N bond angle. C, k and A are constants.

$$\Delta\delta_P = -C \Delta\chi_x + k \Delta n_\pi + A \Delta\theta \quad \text{Equation 1.1}$$

With the atoms bonded to phosphorus being constant and the substitution on nitrogen also the same in **1**, **2** and **3**, it can be deduced that the deshielding effect does not result from electronegativity differences, but from changes in the geometry of the P-N tetrahedron. This change in δ_P is a result of the change in geometry of the molecule, which leads to the change in bond angles. This in turn causes changes in the hybridization of the nitrogen atoms. In the series **1**→**4**, the N-P-N bond angles decrease while the P-N bond distance increases. When **4** is compared with the non-cyclic hexaethylphosphoric triamide **4''**, (δ_P 23.3) any differences in polar effects of substituents can be ignored and the dramatic

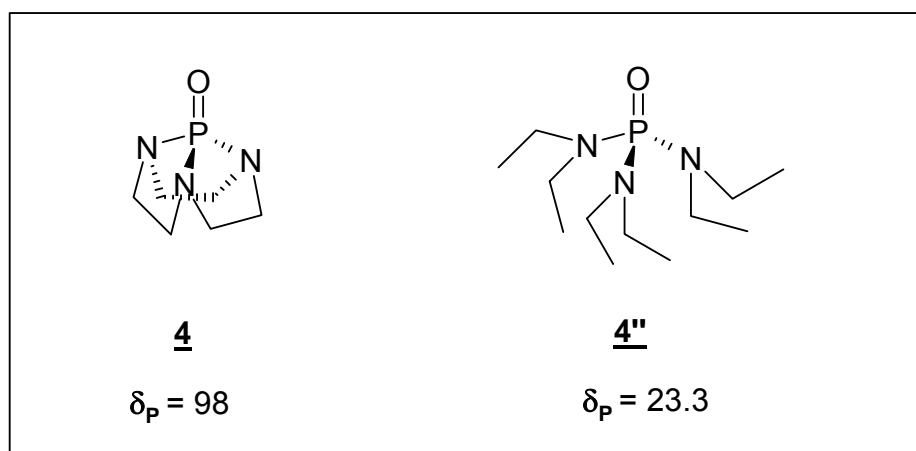


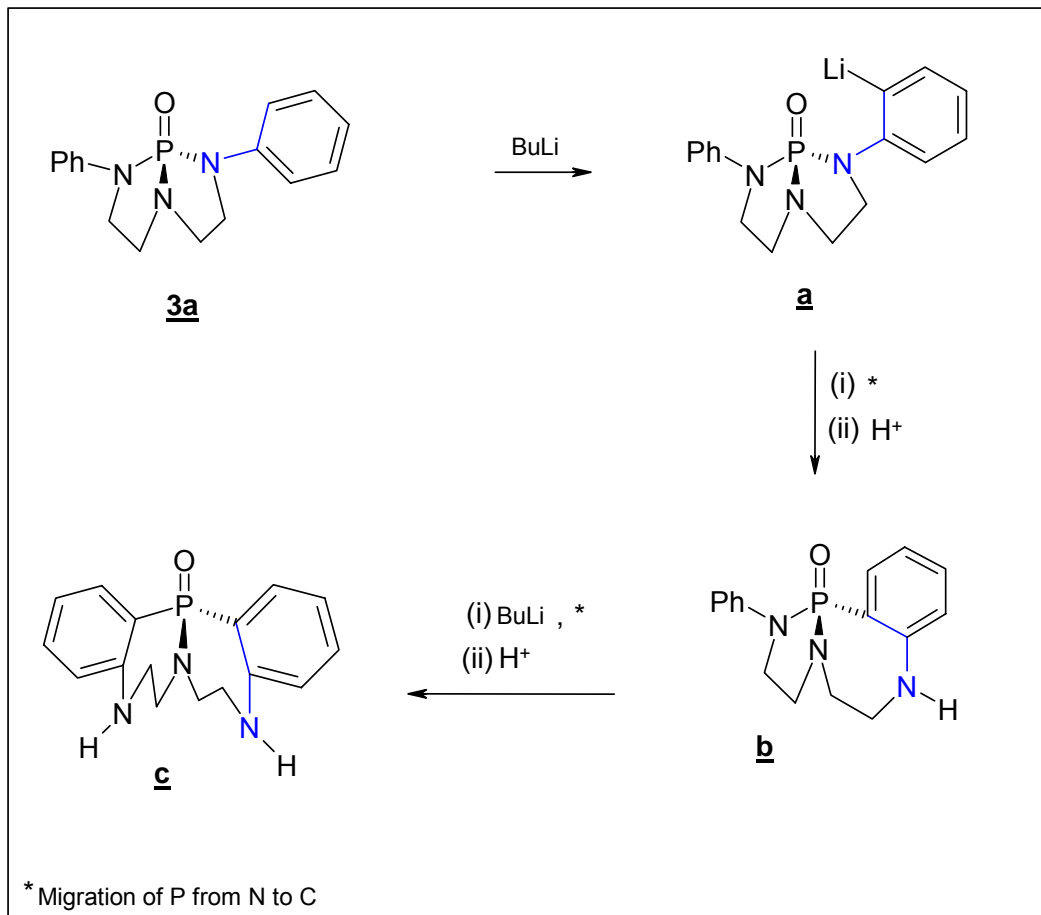
Figure 1.7. Structures of 10-oxo-10-phospha-1,4,7-triazatricyclo[5.2.1.0^{4,10}]-decane, **4** and hexaethylphosphoric triamide, **4''**.

deshielding effect of 74.7 ppm (difference between δ_P values of **4** and **4''**) must solely reflect the difference in geometry.

The δ_P values of compounds **1**, **2**, **3** and **4** are related to the average values of the three N-P-N bond angles present in each molecule, demonstrating that variations in geometry can lead to formidable changes in shielding parameters at the phosphoryl center. This observed variations in the P-N bond characteristics should be reflected by significant differences in the chemical behavior of the individual classes of the new bicyclic system **3**.

The bicyclic system **3** revealed an interesting chemistry, which stimulated the synthesis of new heterocyclic compounds containing nitrogen and phosphorus in the ring skeleton. Metallation induced migration of phosphorus from nitrogen to carbon yields new types of cyclic phosphonic and phosphinic amides³⁹. (**Scheme 1.4**)

The N \Rightarrow C migration of phosphorus in **3a** involves three steps: lithiation of the *ortho*-carbon in the N-Ar group, 1,3-phosphorus shift driven by the formation of a strong P-C bond together with the change of the N-Li bonding, and, finally, quenching of the N-lithiated amide function by a proton donor. In this way new bicyclic systems containing fused five- and seven-, as well as two seven-membered rings (**a**, **b** and **c**) have been prepared.

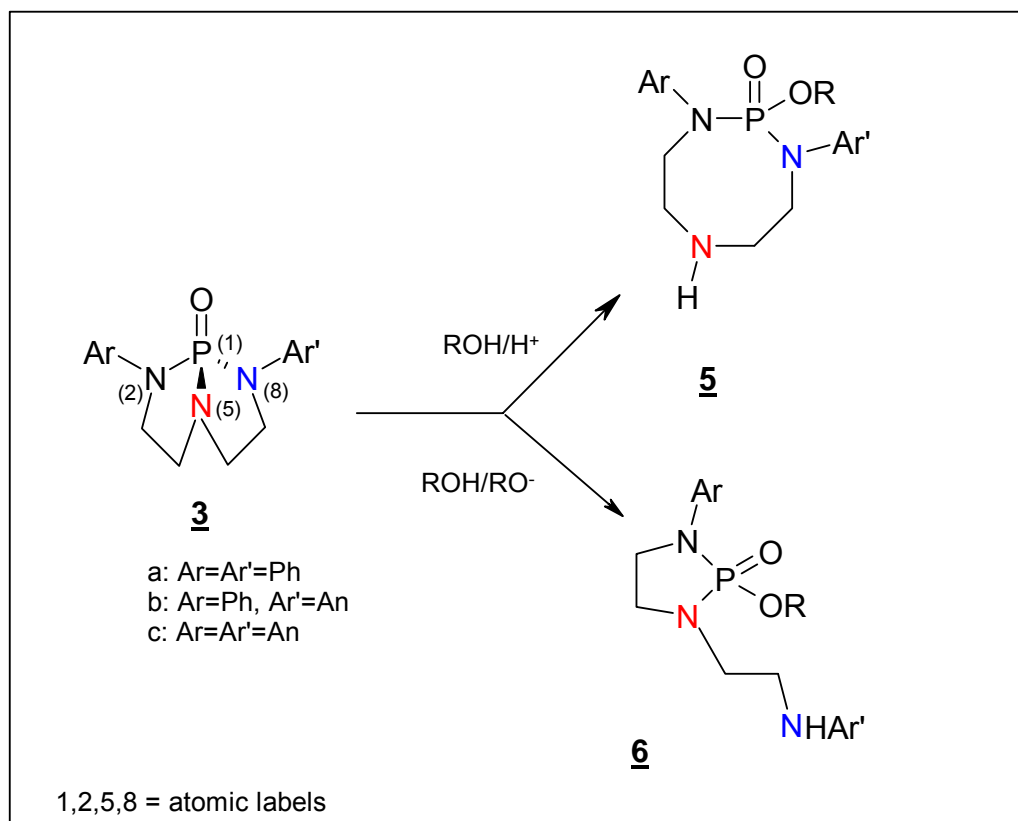


Scheme 1.4 Metallation induced migration of Phosphorus from Nitrogen to Carbon.

The nucleophilic cleavage of one of the P-N bonds in the bicyclic system **3** leads to a novel eight-membered heterocyclic system **5** or to the 1,3,2-diazaphospholidine derivative **6**.⁴⁰ (**Scheme 1.5**)

Quantitative and regioselective cleavage of the “internal” P-N(5) bond was obtained when **3** was treated with an alcohol (R= Me, Et), containing one mole equivalent of HCl. This reaction yielded the hydrochloride salt of the corresponding triazaphosphacyclooctane **5**. The free base of **5** was obtained by neutralization. The regioselectivity of the reaction can be explained in terms of the mechanism of the acid-catalyzed P-N bond cleavage in phosphoric amides, established by Rahil and Haake.⁴¹ According to that mechanism, the first step involves the N-protonation, followed by the direct displacement of the amine by

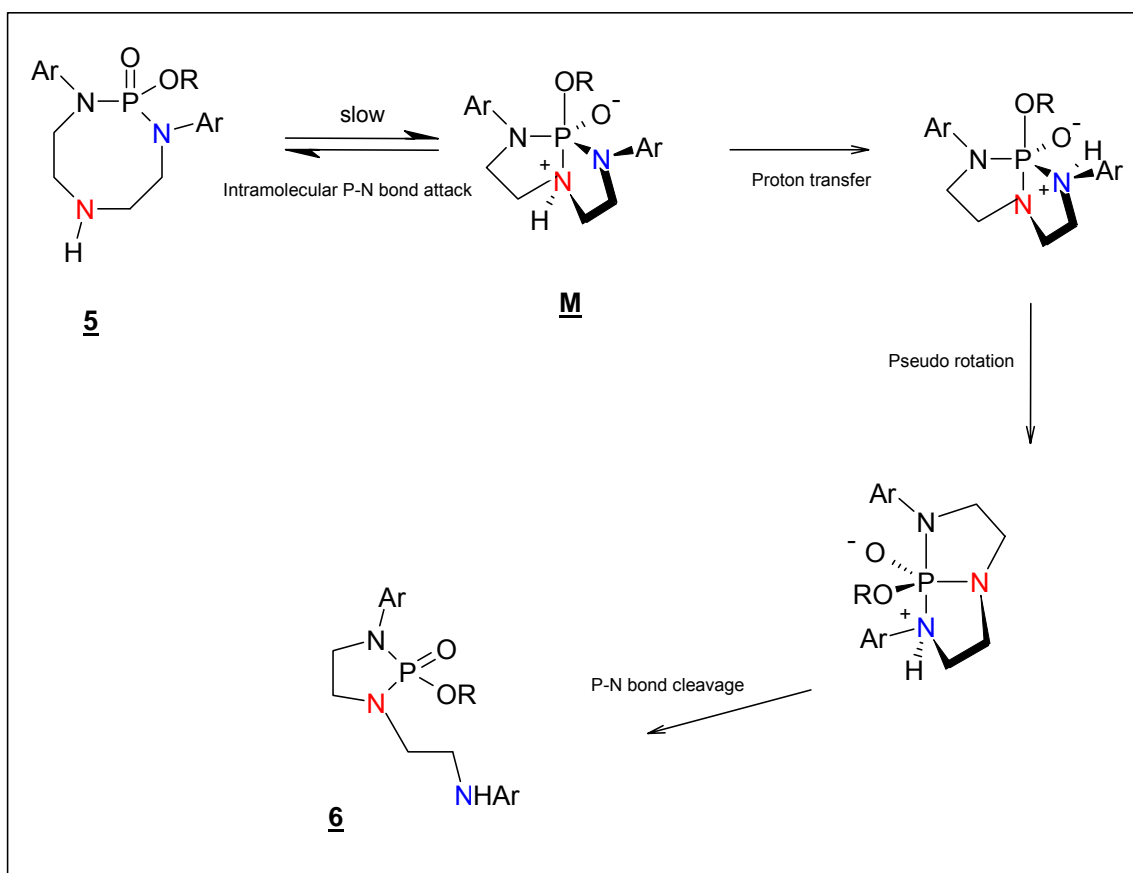
the nucleophilic reagent. In **3a** (R=Ph) the bridgehead nitrogen, N(5), substituted by two alkyl groups, should be significantly more basic than two aryl-substituted nitrogens, thus the substrate should be exclusively activated for the P-N(bridgehead) bond cleavage. ^{15}N NMR studies confirmed the p^3 character of this nitrogen suggesting higher basicity of the bridgehead nitrogen, N(5). Stereoelectronic effects also play a role in the selectivity of the reaction. In the transition state (the P(V) intermediate) of the substitution the N(5) atom is in the apical position which is the most favored location for the leaving group in the trigonal bipyramid structure.



Scheme 1.5 Acid and Base catalyzed cleavage of the P-N bond in **3**.

The eight-membered ring compound **5a** undergoes slow and spontaneous change yielding another P-containing compound **6a**. According to the available data, a mechanism is proposed for this isomerization which involves the rate-determining intramolecular 1,5-nucleophilic attack of the amine nitrogen at the

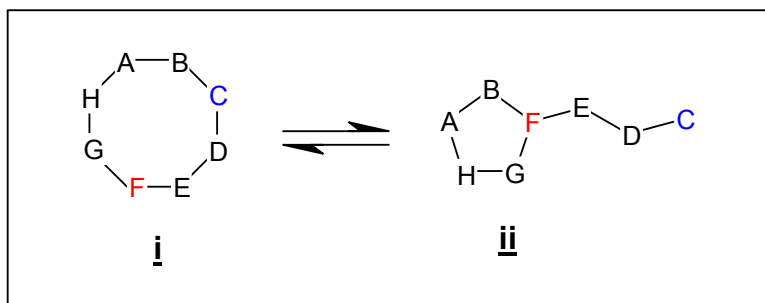
phosphoryl center, resulting in the P(V) intermediate **M** (**Scheme 1.6**), which then undergoes fast proton transfer, pseudorotation, and product determining cleavage of the P-N(8) bond. This mechanism is supported by the structural characteristics (short distance between the N(5) and P atoms) of the *N*-benzoyl derivative of **5a**.



Scheme 1.6 Proposed mechanism of the rearrangement of **5** to **6**.

For the hydrolysis of medium ring phosphate esters, a similar mechanism was postulated. In those cases^{42,43} the transannular N→P interaction in an eight membered heterocyclic system catalyzes the hydrolysis, but the rings stay intact. However for **5a** there is a change in the molecular skeleton. (**Scheme 1.7**) The letters in the scheme are used to demonstrate the ring contraction in this rearrangement where **i** and **ii** represent the 2,5,8-triaza-1λ⁵-phospha-

bicyclooctane and the 3-substituted 1,3,2λ⁵-diazaphospholidine system, respectively. A new bond is formed between atoms B and F and the B-C bond is broken. To our knowledge, this was the first reported case of a rearrangement of this type.

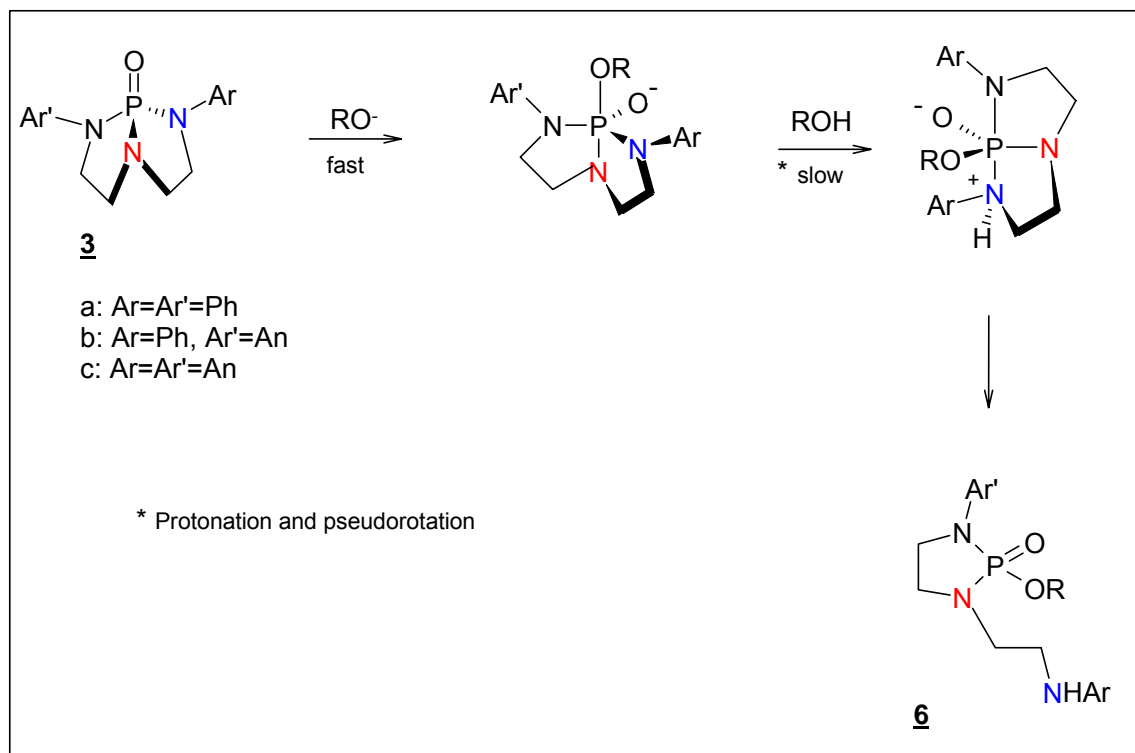


Scheme 1.7 Ring contraction in the rearrangement reaction.

Compounds **5** are stable in the form of their ammonium salts or as the N(5)-acyl derivatives. The nature of the nucleophilic group introduced at the phosphoryl center in the ring-opening reaction, determines the stability and the behavior of the neutral products **5**⁴⁴.

Basic alcoholysis (RO⁻/ROH) of the bicyclic substrate **3** led to the formation of the five membered ring product, **6** as a result of the nucleophilic cleavage of the P-N-Ph bond. The same behavior was observed for another N-aryl substrate where R=4-MeOC₆H₄. The products **6** could be prepared therefore either by direct alcoholysis of **3** or via the rearrangement of **5**.

The mechanism of the base-catalyzed alcoholysis of **3** is much less clear. In the absence of activation of N(5) via protonation, the leaving ability of the departing nitrogen atom determines the regioselectivity of the P-N bond cleavage. (**Scheme 1.8**)



Scheme 1.8 Mechanism of the base catalyzed reaction.

With excess of MeO⁻ the five membered product **6a** undergoes further opening of the second 1,3,2λ⁵-diazaphospholidine ring to give dimethyl di(2-phenyl-aminoethyl)phosphoramidate **7a**.

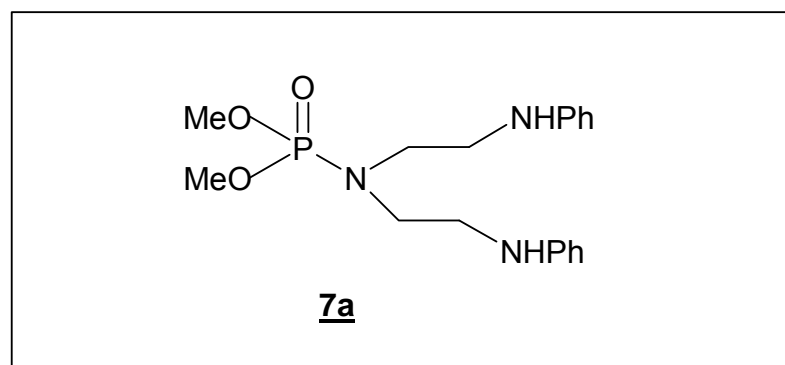


Figure 1.8 Dimethyl di(2-phenyl-aminoethyl)phosphoramidate **7a**.

The **5**→**6** rearrangement indicates greater thermodynamic stability of the five-membered ring **6**. In the further part of this work the results are reported of the

attempts to demonstrate the thermodynamic reasons for the rearrangement using the Molecular Modelling (MM) approach, as well as to show the concerted nature of the reaction.

The ring substituents play a role in both reactions: in the regioselectivity of the P-N bond cleavage by nucleophiles, as well as in the rearrangement reaction. For the base catalyzed substitution in **3a**, the electron-donating substituents in the *N*-Ar function in **5** increase the rate of reaction. When R=R'=4-MeOC₆H₄ (**3b**), the bond cleavage was about 2.5 times faster than for **3a**. The mixed substrate **3c** (R=4-MeOC₆H₄; R'=Ph) showed preference for cleavage of the P-N_{Ar} bond over the P-N_{Ph} bond. The higher basicity of the leaving amine facilitates in this case the proton transfer necessary for the departure of the leaving group.

The opposite was observed for the rearrangement reaction - the bis-*N*-anisyl substrate **3b** proved to be the least reactive. This can be explained according to the different proposed mechanisms for the two processes. In the base catalyzed reaction, the P-O bond formation with a strong nucleophile (EtO⁻) is fast, but the proton-assisted cleavage of the P-N(2) bond is rate determining. The more basic *N*-*p*-anisyl function in **3b** makes the intermediate more reactive in the second, dissociative step of the reaction.

In the rearrangement, on the other hand, the less electron donating phenyl substituents (**3a** and **3c**) make the phosphorus atom more electrophilic thus making **3a** more reactive in the rearrangement. The rate of the rearrangement is determined by the rate of the N(5)-P bond formation, resulting in the P(V) intermediate, which then undergoes fast proton transfer and product determining cleavage of the P-N(2) bond.

With the molecular rearrangement (**5**→**6**) being reasonably well understood for the *N,N'*-diaryl substituted substrates (**3a**, **3b** and **3c**), it was decided to expand

our studies of the bicyclic system **3** to other derivatives with different substitution of the nitrogen atoms.

1.2 Objectives

Against the described background of the previously accumulated results, the objectives of this study were to:

- synthesize some *N*-alkyl derivatives ($R=R'=\text{Me, Et, PhCH}_2$) of the bicyclic system **3** and to study their chemistry relative to the *N*-aryl derivatives
- expand the synthesis to the preparation of new bicyclic models, e.g. the thio analogue of **3**, system **N** as well as any possible analogous compounds:

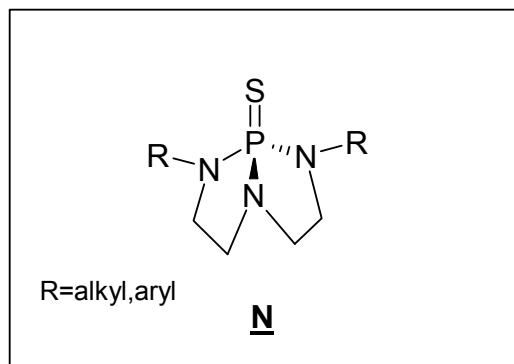


Figure 1.9 Thio analogue of **3**.

- further explore the chemistry of **3** and of any new system of that class with particular interest in the reactivity of the P-N bond towards alcoholysis
- perform a detailed structural analysis on these compounds by X-ray diffraction in order to directly compare the different bicyclic models.

- study wherever possible, the NMR spectroscopic and GC-MS characteristics of those systems
- perform Molecular Mechanical calculations which are anticipated to contribute to better understanding of the properties and the behavior of these new heterocyclic compounds.

1.3 References

1. A.D.F. Toy, E.N. Walsh, *Phosphorus Chemistry in Everyday Living*, Second Ed (1987).
2. Y. Abe, J. Curley-Joseph, M.W.G. De Bolster, J. Feder, T.O. Henderson, R.L. Hilderbrand, H.R. Hudson, H.J. Lubansky in "*Topics in Phosphorus Chemistry*" John Wiley & Sons, Inc., New York, Ch.1 (1983).
3. A.J. Kirby in "*Phosphorus Chemistry Directed Towards Biology*", W.J. Stec, Ed., Pergamon Press, London, p. 82 (1980).
4. D.G. Gorenstein; C. Karlake; J.N. Granger; Y. Cho; M.E. Piotto in "*Phosphorus Chemistry. Developments in American Science*", p 203 (1992).
5. L. Stryder, *Biochemistry*, Fouth Ed. (1995)
6. J. Emsley, D. Hall, in "*The Chemistry of Phosphorus*", Harper and Row, London, Ch. 10, (1976).
7. D.E.C. Corbridge, *Phosphorus. An Outline of its Chemistry, Biochemistry and Technology*, 4th ed., Elsevier:Amsterdam,1990; p 418.
8. P. Taylor in *Goodman and Gilman's The pharmacological Basis of Therapeutics*, Eds. A.G. Gilman, T.W. Rall. A.S. Nies, P.Taylor, Ch. 7, Pergamon Press, Eighth edition (1990).
9. G. Schrader, *Die Entwicklung neuer Insectizide auf Grundlage von Organischen Fluor- und Phosphorverbindungen*, Monographie No. 2, Verlag Chemie, Weinheim (1952).
10. E.E. Kanaga, W.E. Allison, *Bull. Of the Entomological Society of America*, **15 (2)**, 85 (1969).

11. B.C. Saunders, *Some Aspects of the Chemistry and Toxic Action of Organic Compounds Containing Phosphorus and Fluorine*; Cambridge University: Cambridge, England, 1957.
12. H. McCombie, B.C. Saunders, *Nature*, **157**, 287 (1946).
13. O.M. Friedman, A.M. Seligman, *J. Am. Chem. Soc.*, **76**, 658 (1954).
14. T.W. Engle, G. Zon, W. Egan, *J. Med. Chem.*, **25**, 1347 (1952).
15. W.J. Stec, in “*Specialist Periodical Reports: Organophosphorus Chemistry*” The Royal Society of Chemistry, London, Vol. 13, Ch. 8 (1982).
16. W.J. Stec, *Organophosphorus Chemistry*, **13**, 145, (1982).
17. C. le Roux, A.M. Modro, T.A. Modro, *J. Org. Chem.*, **60**, 3832, (1995).
18. P. Calabresi, B.A. Chabner in *Goodman and Gilman’s The Pharmacological Basis of Therapeutics*, Eds. A.G. Gilman, T.W. Rall, A.S. Nies, P. Taylor, Ch.52, Pergamon Press, Eighth edition (1990).
19. M.P. du Plessis, T.A. Modro, L.R. Nassimbeni, *J. Org. Chem.*, **47**, 2313 (1982).
20. B. Davidovitz, T.A. Modro, *J. Chem. Soc. Perkin. Trans. II*, 303 (1985).
21. T.A. Modro, A.M. Modro, P. Bernatowicz, W. Schilf, L. Stefaniak, *Magnetic Resonance in Chemistry*, **36**, S212 (1998).
22. T.A. Modro, B.P. Rijkmans, *J. Org. Chem.*, **47**, 3208 (1982).
23. T.A. Modro, M.A. Lawry, E. Murphy, *J. Org. Chem.*, **43**, 5000 (1978).
24. B. Davidovitz, in “Reactivity Studies of Phosphoric Amides and Esters”, University of Cape Town, PhD Thesis (and references cited therein) (1984).
25. C.R. Hall, T.D. Inch, *Tetrahedron Lett.*, 3761 (1977).
26. T. Koizumi, H. Amitani, E. Yoshi, *Synthesis*, 110 (1979).
27. A. Zwierzak In “Phosphorus Chemistry”, L.D. Quin and J.G. Verkade, Eds., American Chemical Society, Washington, DC, 1980; ACS Symp. Ser. 171, p 169.
28. T. Koizumi, P. Haake, *J. Am. Chem. Soc.*, **95**, 8073 (1973).
29. Y. Kobayashi, T. Koizumi, E. Yoshi, *Chem. Pharm. Bull.*, **27**, 1641 (1979).
30. S. Bauermeister, A.M. Modro, T.A. Modro, A. Zwierzak, *Can. J. Chem.*, **69**, 811 (1991).
31. H. Wan, T.A. Modro, *Phosphorus, Sulfur and Silicon*, **108**, 155 (1996).
32. A.M. Modro, T.A. Modro, P. Bernatowicz, W. Schilf, L. Stefaniak, *Magnetic Resonance in Chemistry*, **35**, 774 (1997).

33. H. Wan, A.M. Modro, T.A. Modro, S. Bourne, L.R. Nassimbeni, *J. Phys. Org. Chem.*, **9**, 739 (1996).
34. D.E.C. Corbridge, *The Structural Chemistry of Phosphorus*, Elsevier: Amsterdam, 1974; Chapter 9.
35. H. Wan, T.A. Modro, *Synthesis*, 1227, (1996).
36. S. Bourne, X.Y. Mbianda, T.A. Modro, L.R. Nassimbeni, H. Wan, *J. Chem. Soc., Perkin Trans. 2*, 83, (1998).
37. *CRC Handbook of Phosphorus-31 NMR Data*, Ed. J.C. Tebby, CRC Press, Boca Raton, 1991.
38. J.H. Letcher, J.R. Van Wazer, *J. Chem. Phys.*, **44**, 815, (1966); *Topics in Phosphorus Chemistry*, **5**, 75, (1967).
39. S. Bourne, Z. He, T.A. Modro, P.H. van Rooyen, *Chem. Commun.*, 853, (1999).
40. X.Y. Mbianda, T.A. Modro, P.H. van Rooyen, *Chem. Commun.*, 741, (1998).
41. J. Rahil, P. Haake, *J. Am. Chem. Soc.*, **103**, 1723 (1981).
42. R.K. Sharma, R. Vaidyanathaswamy, *J. Org. Chem.*, **47**, 1741 (1982).
43. *Conformational Analysis of Medium-Sized Heterocycles*, ed. R.S. Glass, VCH, New York, 1988, Ch. 3.8.
44. Z. He, S. Laurens, X.Y. Mbianda, A.M. Modro, T.A. Modro, *J. Chem. Soc. Perkin Trans. II*, 2589, (1999).

CHAPTER 2

2. N-ALKYL DERIVATIVES OF 1-OXO-2,8-DISUBSTITUTED-2,5,8-TRIAZA-1 λ^5 -PHOSPHABICYCLO[3.3.0]OCTANE

2.1 Introduction

The study on the bicyclic substrates **3** was extended to substrates substituted at the 2,8-nitrogen atoms with aliphatic groups, such as: R= Me, Et, PhCH₂. Of particular interest was the acid-catalyzed solvolysis of *N,N*-dialkyl derivatives **3**.

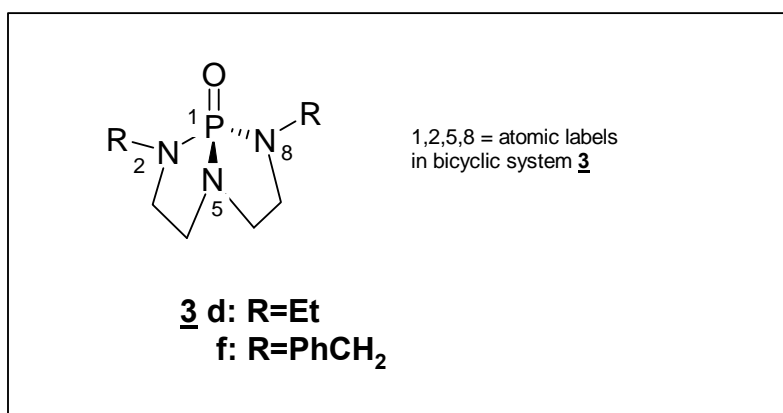


Figure 2.1 General structure of the bicyclic system.

For the *N*-aromatic substrates the observed selectivity of acidic cleavage of the P-N(5) bond was explained in terms of the higher basicity of the bridgehead nitrogen atom (see Chapter 1). In the *N*-aliphatic compounds the basicity of all three nitrogen atoms should be comparable, because all three nitrogen atoms are, apart from the involvement in the P-N bond, bonded to two aliphatic carbon atoms. These differences should have significant effects on the selectivity and the rate of the alcoholysis reaction as well as the **5** → **6** rearrangement.

2.2 Results and discussion

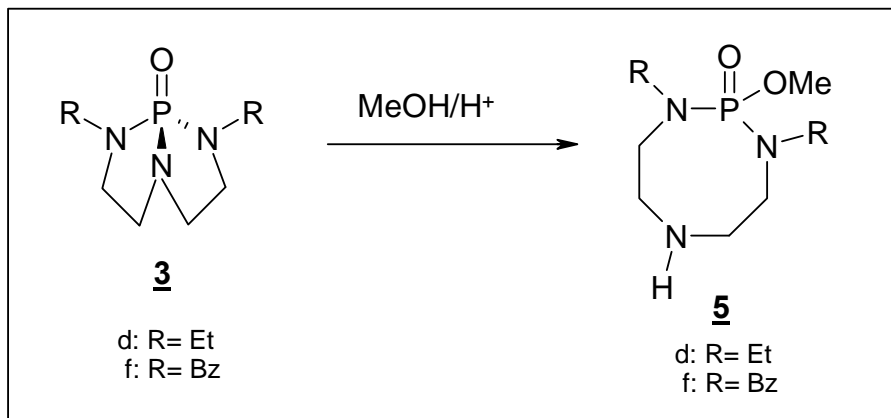
The preparation and the isolation of the *N*-alkyl derivatives of the bicyclic system **3** and their precursors proved to be much more difficult than of those with *N*-aryl substituents.

The pure 2,8-diethyl derivative, **3d** was prepared successfully. Although its immediate precursor was never isolated, it could be detected by ³¹P NMR spectroscopy. In this case the first and second cyclizations proceeded with comparable rates which complicated the isolation of the intermediate products. All attempts to prepare the Me substituted derivative **3e** failed. Its immediate precursor, the triazaphospholidine **2e**, was isolated in a pure state and could be prepared in large quantities. The second cyclization was however unsuccessful under a variety of conditions. The benzyl derivative **3f** was prepared as a spectroscopically pure compound, but the reaction was difficult to reproduce. The yields varied between experiments. The *N*-alkyl derivatives of **3** were isolated as viscous oils and attempts to prepare crystals suitable for x-ray diffraction were unsuccessful.

2.2.1 Acid catalyzed alcoholysis

As with the 2,8-*N*-aryl derivatives, both *N*-alkyl substituted substrates reacted with the HCl-containing methanol according to the reaction shown in (**Scheme 2.1**), yielding the corresponding salts of the products¹ **5d** and **5f**.

The regioselectivity of the alcoholysis of the *N*-aryl substituted derivatives was explained in terms of the basicity of the different nitrogen atoms. In the *N*-alkyl derivatives all the amide nitrogen atoms carry only alkyl substituents and should not differ much in basicity. ¹⁵N NMR studies of the P-N bonding in cyclic amides demonstrated however that the endocyclic nitrogen is always more shielded than the exocyclic nitrogen atom². Following the arguments developed in an important contribution from Von Philipsborn and Müller³, our NMR results suggest that the



Scheme 2. 1 Acid catalyzed methanolysis of **3**.

nitrogen incorporated into the ring should always be more basic, therefore the bridgehead N atom in compounds **3d** and **3f** should be more basic than the other two nitrogen atoms, each located in a single phospholidine ring. However, if the observed selectivity for **3d** (R=Et) and **3f** (R=PhCH₂) depended only on the basicity of the different nitrogens, it would require a pK_a difference of as much as approximately two units between the bridgehead nitrogen and the other two nitrogens. It has to be remembered, however, that in the pentacoordinate intermediate (the transition state) of the substitution, the location of the bridgehead N(5) atom is in the favourable apical position (apical departure). It seems therefore that the selectivity of the acid alcoholysis of all substrates **3** is determined by both the pre-equilibrium protonation step and by stereoelectronic effects.

2.2.2 Base catalyzed alcoholysis

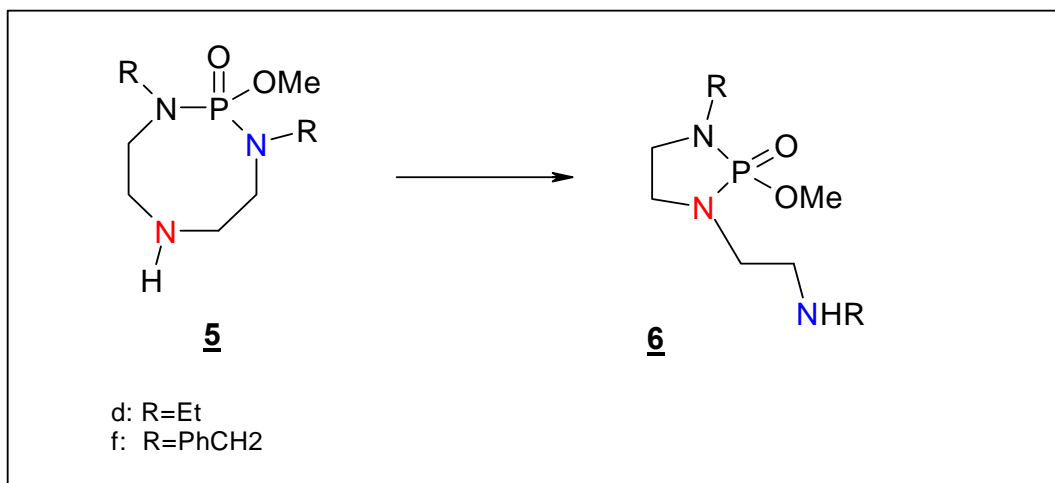
Both prepared *N*-alkyl substrates **3d** and **3f** yielded exclusively the eight-membered cyclic products in the base-catalyzed methanolysis, the same as the products obtained from methanolysis in the presence of HCl. This result suggests that the cleavage of the P-N bond by MeO⁻, follows a mechanism different from that operating for the *N*-aryl derivatives, and is driven by the cleavage of the more strained P-N(5) bond in the bicyclic system. The difference between the *N*-

aryl and *N*-alkyl substrates was also observed for their reactivity in the related **5**→**6** rearrangement (see 2.3.3).

2.2.3 Rearrangement of the alcoholysis product

Both *N,N'*-dialkyl substituted compounds **5d** and **5f** rearranged to compounds **6d** and **6f**, but much slower than in the *N,N'*-diaryl analogues. [Scheme 2.2]

The rearrangement reaction was much less clean for *N*-alkyl than for the *N*-aryl derivatives. Additional signals to those of the rearrangement products appear in the ^{31}P NMR spectrum at higher conversions. In agreement with the trend observed for the *N*-aryl substrates, **5d** (R=Et) was found to be *ca.* five times less reactive than **5a**. The rearrangement of **5f** (R=PhCH₂) was very slow and the reaction did not allow us to isolate and characterize the product **6f**.



Scheme 2.2 Base catalyzed rearrangement of compound **5**.

In the first experiment (**entry 5, Table 2.1**) **3f** was used as a precursor for **5f**. When **3f** was dissolved in MeOH containing NaOMe, it solvolyzed relatively fast to **5f**; after four days the solution contained no **3f**, 98% of **5f** and 2% of the product **6f**. The **5**→**6** interconversion yielded very slowly the final product with an approximate half-life of 960 hours. In the absence of the base (MeO⁻) the rearrangement was too slow to allow any rate determination.

Entry	Substrate	Product	Conditions	$k_1/10^{-5} \text{ s}^{-1}$	$t_{1/2}/\text{h}$
1	<u>5a</u>	<u>6a</u>	Refluxing THF (internal temp. 62 °C). Reaction followed to ca. 85% conversion. $[5a]_0$ (M) = (i) 0.03 (ii) 0.015 M (iii) 0.0075	4.8 ± 0.04 4.5 ± 0.2 3.8 ± 0.08	4.0 4.3 5.1
2	<u>5a</u> <u>5b</u> <u>5c</u>	<u>6a</u> <u>6b</u> <u>6c</u>	Refluxing THF (internal temp. 62 °C). Reaction followed to ca. 90% conversion. $[5a]_0 = 0.050 \text{ M}$	8.9 ± 0.3 3.2 ± 0.1 6.1 ± 0.2	2.2 6.0 3.2
3	<u>5a</u>	<u>6a</u>	CDCl_3 , room temp. $[5a]_0=0.033 \text{ M}$	^a	ca. 1200
	<u>5a·HCl</u>	<u>6a</u>	CDCl_3 , room temp., excess of anhydrous K_2CO_3 $[5a\cdot\text{HCl}]_0=0.033 \text{ M}$	^a	ca. 740
	<u>5a·HCl</u>	<u>6a</u>	CDCl_3 and 1.1 mole-equiv. Et_3N , room temp., $[5a\cdot\text{HCl}]_0=0.033 \text{ M}$	^a	ca. 160
	<u>5c</u>	<u>6c</u> , <u>6c'</u>	CDCl_3 , room temp. Reaction followed to ca. 38% conversion $[5c]_0=0.022 \text{ M}$	^a	ca. 3000
4	<u>5d</u>	<u>6d</u> ^b	Refluxing THF (internal temp. 62 °C). Reaction followed to ca. 55% conversion. ^c $[5d]_0=0.050 \text{ M}$	1.9 ± 0.2	ca. 10
	<u>5d</u>	<u>6d</u> ^b	CDCl_3 , room temp. Reaction followed to ca. 18% conversion. $[5d]_0=0.050 \text{ M}$	^a	ca. 10500
5	<u>5f</u>	<u>6f</u> ^b	In MeOH-MeONa from <u>3f</u> , room temp; $[3f]_0=0.020 \text{ M}$	^a	ca. 960
	<u>5f</u>	<u>6f</u> ^b	Refluxing THF (internal temp. 62 °C). Reaction followed to ca. 60% conversion. ^d $[5f]_0=0.050 \text{ M}$	0.061 ± 0.020	ca. 320
^a Not enough data points collected to determine a reliable value of k_1 . Approximate value of the half-life was determined from the [substrate] vs. time plot. ^b Not isolated and characterized. ^c Additional signals appeared in the ^{31}P NMR spectrum at higher conversions. ^d Approximate value; additional signals appeared in the ^{31}P NMR spectrum during the course of the reaction.					

Table 2.1 Rate data for rearrangement 5 → 6 for *N*-aryl and *N*-alkyl derivatives.

When the free base of 5f was subjected to the rearrangement, the conversion to the product was accompanied by the formation of significant quantities of unidentified phosphorus containing products. The obtained k_1 value demonstrates much lower reactivity of 5f in the rearrangement as compared with the *N,N'*-diaryl and *N,N'*-diethyl analogues.

For the *N,N'*-dialkyl substituted compounds, the rearrangement reaction is much more complex and the structure-reactivity relationship is much less clear than for the *N,N'*-aryl derivatives. The experimental difficulties and the more complex behavior of the *N,N'*-dialkyl derivatives made us to decide not to investigate these compounds further than the experiments discussed above, but, instead, to turn our attention to other, related systems.

2.3 Experimental

Solvents and commercially available substrates were purified by conventional methods immediately before use. Melting points were uncorrected. For column chromatography Merck Kieselgel 60 (0.063-0.200) was used as stationary phase. Mass spectra were recorded on a Varian MAT-212 double focussing inlet spectrometer at an ionization potential of 70 eV. NMR spectra were recorded on a Bruker AC 300 spectrometer in CDCl₃, and the chemical shift values (δ) are given in ppm relative to the solvent (¹H, δ 7.24; ¹³C, δ 77.0). ³¹P NMR chemical shifts are given relative to 85% H₃PO₄ as external standard.

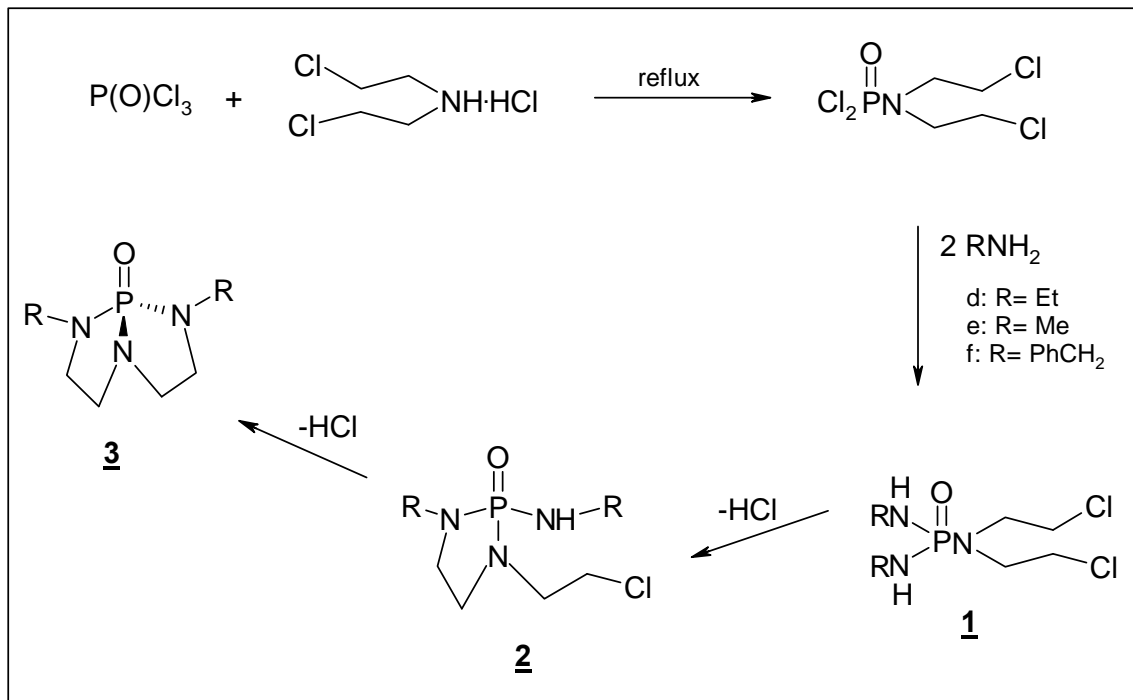
Preparation of substrates

The aliphatic derivatives were prepared via the same route as used for the *N*-aryl derivatives (**Scheme 2.3**)

***N,N*-Bis(2-chloroethyl)phosphoramidodichloride, 0**

The synthetic procedure was reported before⁴.

90% yield, bp. 120-138 °C (~1mmHg), δ_p 18.0, Lit.: 94% yield, bp 98-99 °C (0.05 Torr), δ_p 13.1.



Scheme 2.3 Reaction pathway to prepare the bicyclic compound **3**.

N,N*-Bis(2-chloroethyl)-*N',N''*-dibenzylphosphoric triamide, **1f*

A solution of *N,N*-Bis(2-chloroethyl)phosphoramidodichloride (0.256 g, 1.0 mmol) in ether (20 ml) was added dropwise with stirring at -70°C to a solution of benzylamine (0.439 g, 4.1 mmol) in ether (10 ml). The mixture was kept at -70°C for 2 h, allowed to warm up to room temperature and stirred for another 140 h. The precipitate (benzylammonium chloride) was filtered off and washed with ether (20 ml). The combined ethereal solution was washed with water (2×20 ml) and cooled to 0°C (without drying). Two layers separated, which, after 4 days, yielded the crystalline product at the interface of the layers. Colourless crystals, 0.385 g (97%); mp $83\text{--}85^\circ\text{C}$.

δ_{P} 17.5;

δ_{H} 2.77 (2H, br dt, $^2J_{\text{HP}}$ 9.0, $^3J_{\text{HH}}$ 6.6),

3.60 (4H, t, $^3J_{\text{HH}}$ 6.7),

4.06–4.15 (4H, m),

7.22–7.34 (10H, m)

Elemental Analysis: C₁₈H₂₄Cl₂N₃OP Calculated: C, 54.01; H, 6.04; N, 10.58%.

Found: C, 53.75; H, 6.24; N, 10.18%.

The structure of the product was confirmed by X-ray diffraction.

3-(2-Chloroethyl)-2-oxo-2-benzylamino-1-benzyl-1,3,2λ⁵-diazaphospholidine, 2f

A solution of the above phosphoric triamide (1.119 g, 2.8 mmol) in THF (100 ml) was added dropwise with stirring at room temperature to a solution of Bu^tOK (0.52 g, 4.6 mmol) in THF (100 ml). The mixture was then stirred at room temperature for 48 h. Water (150 ml) was added and the solution extracted with ether (2 × 120 ml). The ethereal solution was dried (MgSO₄), evaporated under reduced pressure and the crude product was purified by column chromatography (ethanol). The product was obtained as a pale-yellow viscous oil (0.64 g, 63%).

δ_P 25.3;

δ_H 2.98-3.04 (2H, m, NCH₂),

3.16-3.26 (4H, m, 2 × NCH₂),

3.51 (1H, t, ³J_{HH} 6.5, one diastereotopic H of CH₂Cl),

3.52 (1H, t, ³J_{HH} 6.5, second diastereotopic H of CH₂Cl),

3.83 (1H, dd, ²J_{HH} 14.9, ³J_{HP} 7.8, one diastereotopic H of CH₂Ph),

3.97 (2H, dd ²J_{HH} 10.7, ³J_{HP} 6.8, two diastereotopic H's of CH₂Ph),

4.07 (1H, dd, ²J_{HH} 14.8, ³J_{HP} 6.8, one diastereotopic H of CH₂Ph),

7.22-7.31 (10H, m, 2 × Ph);

δ_C 42.75 (d, ²J_{CP} 3.6), 44.0 (d, ²J_{CP} 13.1), 45.2 (s), 45.4 (s),

46.7 (d, ²J_{CP} 5.1), 48.5 (d, ²J_{CP} 5.0), 127.1 (s), 127.3 (s), 127.4 (s),

128.2 (s), 128.5 (s), 128.6 (s), 137.6 (d, ³J_{CP} 5.1), 140.0 (d, ³J_{CP} 6.2)

Elemental Analysis: C₁₈H₂₃ClN₃OP requires: C, 59.42; H, 6.37; N, 11.55%.

Found: C, 59.04; H, 6.86; N, 10.92%

1-Oxo-2,8-dibenzyl-2,5,8-triaza-1 λ^5 -phosphabicyclo[3.3.0]-octane (3f).

NaH (3.8 g, 158 mmol; large excess) and Bu₄NHSO₄ (0.1 g, 0.29 mmol) were added to a solution of the above phospholidine in THF (250 ml) and the mixture was stirred at room temperature for 45 h. The THF solution was decanted and the residue was washed several times with THF. The combined THF solution was evaporated under reduced pressure and the crude product was purified by column chromatography (THF). The pure compound was obtained as a slightly grayish viscous oil. (0.43 g, 58%).

δ_P 45.7;

δ_H 2.79-3.01 (4H, m, 2 \times NCH₂),

3.27-3.46 (4H, m, 2 \times NCH₂),

4.02 (2H, dd, ²J_{HH} 15.1, ³J_{HP} 8.1, 2 H's of two CH₂Ph groups),

4.22 (2H, dd, ²J_{HH} 15.1, ³J_{HH} 7.4, 2H's of two CH₂Ph groups),

7.20-7.32 (10H, m);

δ_C 47.9 (d, ²J_{CP} 17.9), 48.5 (d, ²J_{CP} 8.2), 50.2 (d, ²J_{CP} 3.1), 127.2 (s), 128.0 (s), 128.4 (s), 150.1 (s)

Elemental Analysis: C₁₈H₂₂N₃OP·H₂O requires: C, 62.60;H, 7.00;N, 12.17%

Found: C, 61.62;H, 6.98;N, 11.58%.

***N,N*-Bis(2-chloroethyl)-*N',N''*-dimethylphosphoric triamide (1e).**

A solution of *N,N*-Bis(2-chloroethyl)phosphoramidic dichloride (1.00 g, 3.90 mmol) in ether (5 ml) was added dropwise with stirring at –80 °C to a solution of methylamine (7.2 ml, 160 mmol) in ether (10 ml). The mixture was stirred for 2 h at –80 °C and allowed to warm up to room temperature. The solvent and the excess of methylamine was evaporated under reduced pressure, the residue was transferred to a Soxhlet apparatus and extracted with ether for 22 h. The product was obtained as white crystals (0.856 g, 89%), mp 92.1-93.7 °C.

δ_P 20.7

δ_H 2.31b (2H, br s), 2.59 (6H, dd, ³J_{HP} 12.1, ³J_{HH} 5.8), 3.40 (4H, dt, ³J_{HP}

10.6, ³J_{HH} 6.5), 3.62 (4H, t, ³J_{HH} 6.5);

δ_c 26.4 (s), 42.2 (s), 49.0 (d, $^3J_{CP}$ 5.0); the 1H -coupled spectrum showed the expected patterns of q,t,t, for the NMe, NCH₂, and CH₂Cl groups, respectively.

3-(2-Chloroethyl)-2-oxo-2-methylamino-1-methyl-1,3,2λ⁵-diazaphospholidine (2e) .

A solution of MeONa prepared from 0.750 g Na (32 mmol) in MeOH (37 ml) was added dropwise with stirring at 0-5 °C to a solution of the above phosphoric triamide (1.00 g, 4.0 mmol) in MeOH (25 ml). After 1 h the mixture was allowed to warm up to room temperature and was stirred for further 70 h. Methanol was removed under reduced pressure and the crude product was purified by column chromatography (EtOH). Viscous oil (0.428 g, 50%);

δ_P 27.2;

δ_H 2.41 (3H, dd, $^3J_{HP}$ 12.5, $^3J_{HH}$ 5.6, exocyclic NMe), 2.57 (3H, d, $^3J_{HP}$ 9.7, endocyclic NMe), 3.09-3.028 (4H, m), 3.57 (1H, t, $^3J_{HH}$ 6.6, one H of CH₂Cl), 3.58 (1H, t, $^3J_{HH}$ 6.5, one H of CH₂Cl);

MS m/z 213, 211 (M^+ , 5%, 15%), 162 ($M^+ - CH_2Cl$, 100), 133 ($M^+ - CH_2Cl-NMe$, 99), 119 ($M^+ - CH_2Cl - NMe - CH_2$, 56).

***N,N*-Bis(2-chloroethyl)-*N',N''*-diethylphosphoric triamide (1d)**

A large excess (ca. 10 ml) of Et₂NH was distilled off from a 70% aq. solution, dried and condensed in a flask immersed in ice. Ether (20 ml) was added and the solution was added dropwise with stirring to a solution of *N,N*-bis(2-chloroethyl)phosphoramidic dichloride (3.00 g, 11.6 mmol) in ether (20 ml) at -80 °C. The mixture was kept at -80 °C for 2h and left overnight without cooling. Solvent was evaporated under reduced pressure, the residue was transferred to a Soxhlet apparatus and extracted with ether for 55 h. The solvent was evaporated from the extract yielding pure product, 3.09 g (97%); colorless solid, after recrystallization from ether, mp. 69.3-70.5 °C.

δ_P 18.5;

δ_H 1.15 (6H, t, $^3J_{HH}$ 7.1), 2.27 (2H, br s), 2.96 (4H, dq, $^3J_{HH}$, $^3J_{HP}$ 7.2, 8.8),
3.40 (4H, dt, $^3J_{HH}$, $^3J_{HP}$ 6.7, 10.7), 3.63 (4H, t, $^3J_{HH}$ 6.5)

Elemental Analysis: C₈H₂₀Cl₂N₃OP Calculated: C, 34.80; H, 7.30; N, 15.22%

Found: C, 34.55; H, 7.35; N, 15.18%

3-(2-Chloroethyl)-2-oxo-2-ethylamino-1-ethyl-1,3,2λ⁵-diazaphospholidine (2d).

This compound was never isolated and characterized, but its formation and disappearance during the preparation of “bicyclic” **3d** could be followed by ³¹P NMR spectroscopy; δ_P (benzene) = 24.0

1-Oxo-2,8-diethyl-2,5,8-triaza-1λ⁵-phosphabicyclo[3.3.0]octane (3d).

A mixture of the phosphoric triamide described above (1.00 g, 3.6 mol), NaH (prewashed with benzene, 0.400g 16.6 mmol) and Bu₄NBr (0.27 g, 0.18 mmol) was stirred in benzene (100 ml) at room temperature for two days; the reaction progress was monitored by recording directly the ³¹P NMR spectra of samples of the solution. An additional amount of NaH (0.400 g) was added and the stirring was continued for another two days. The ³¹P NMR spectrum demonstrated full conversion and formation of a single phosphorus-containing product. The benzene solution was decanted, the residue was washed several times with benzene and the combined benzene solution was evaporated under reduced pressure. The crude product (viscous oil, 0.886 g, >100%) was purified by bulb-to-bulb distillation (oven temp. 200 °C/0.06 mmHg) yielding 0.475 g (65%) of the almost pure product; second bulb-to-bulb distillation (oven temp. 150-200 °C/0.07 mmHg) afford pure **3d** (0.400 g, 58%) as a colorless viscous oil.

δ_P 45.5;

δ_H 1.08 (6H, t, $^3J_{HH}$ 7.2), 2.65-2.90 (6H, m), 2.90-3.16 (2H, m), 3.24-3.42 (4H, m);

δ_c 14.6 (s), 40.5 (s), 47.6 (d, $^2J_{CP}$ 17.7), 48.5 (d, $^2J_{CP}$ 8.1);

MS, m/z 203 (M^+ , 51%), 188 ($M^+ - CH_3$, 70), 147 ($M^+ - 2C_2H_4$, 29), 146 ($M^+ - C_2H_4 - C_2H_5$, 39), 99 (100)

Elemental analysis: $C_8H_{18}N_3OP \cdot H_2O$ requires: C, 44.08; H, 9.11; N, 18.76%

Found: C, 43.43; H, 9.11; N, 18.99%.

1-Oxo-1-methoxy-2,8-dibenzyl-2,5,8-triaza-1 λ^5 -phosphacyclooctane (5f).

Hydrochloride salt: A solution of **3f** (0.33g, 1.23 mmol) in MeOH (5-20 ml) containing one mole equivalent of anhydrous HCl (ca. 0.1 M solution) was kept at room temperature until the ^{31}P NMR spectrum of a sample of the reaction mixture showed the complete disappearance of **3f**. Reaction time was about 20h. The acidity of the solution (pH= 4-5) was adjusted by the occasional addition of small volumes of methanolic HCl. MeOH was removed under reduced pressure and the hydrochloride salt (**5-HCl**) was isolated and characterized. White solid (96%), purified by crystallization from $CHCl_3$ –benzene (1:1), mp 250.4-256.0 °C.

δ_P 18.7;

δ_H 2.90-3.01 (2H, m) 3.10-3.18 (2H, m), 3.25-3.45 (4H, m), 3.68 (3H, d, $^3J_{HP}$ 11.2), 4.33 (2H, dd, $^3J_{HP}$ 9.5, $^2J_{HH}$ 15.2, two H's of the CH_2Ph groups), 7.24-7.40 (10H, m), 9.98 (2H, br s)

Elemental analysis: $C_{19}H_{27}ClN_3O_3P$ requires: C, 57.65; H, 6.87; N, 10.61%

Found: C, 57.94; H, 7.10; N, 10.07%.

Free base 5f': The salt were then converted to the free base **5f'**. Anhydrous K_2CO_3 (0.69 g, 5.0 mmol) was added to a solution of **5f-HCl** (0.180g, 0.5 mmol) in $CHCl_3$ (20 ml) and the mixture was stirred vigorously at room temperature for 24 h. After filtration, the solution was washed three times with water (3×5 ml),

dried (Na_2SO_4) and the solvent evaporated under reduced pressure. **5f'** was obtained as an oil (69%).

δ_{P} 21.3;

δ_{H} 1.98 (1H, br s), 2.52-2.61 (2H, m), 2.66-2.77 (2H, m), 2.90-3.08 (4H, m), 3.66 (3H, d, $^3J_{\text{HP}}$ 10.9), 4.14 (2H, dd, $^3J_{\text{HP}}$ 8.1, $^2J_{\text{HH}}$ 15.3, two H's of the CH_2Ph groups), 4.32 (2H, dd, $^3J_{\text{HP}}$ 9.4, $^2J_{\text{HH}}$ 15.4, two H's of the CH_2Ph groups), 7.22-7.39 (10H, m).

1-Oxo-1-methoxy-2,8-diethyl-2,5,8-triaza-1 λ^5 -phosphacyclooctane (**5d**).

Hydrochloride salt. Prepared as for **5f**; reaction time 30 minutes. Colorless, hygroscopic crystals (98%).

δ_{P} 18.8;

δ_{H} 1.12 (6H, t, $^3J_{\text{HH}}$ 7.0), 3.08-3.39 (12H, m), 3.64 (3H, d, $^3J_{\text{HP}}$ 11.2);

δ_{C} 14.5 (s), 42.2 (d, $^2J_{\text{CP}}$ 2.6), 43.2 (d, $^2J_{\text{CP}}$ 4.8), 45.3 (s).

Picrate salt, 5d·PicH. The **5d**·HCl (0.067 g, 0.246 mmol) was dissolved in EtOH (0.5 ml) and the solution was added to a solution of picric acid (0.070 g, 0.307 mmol) in EtOH (1.25 ml). The solution was heated at 60 °C for 10 min. and cooled. The precipitate was filtered off, washed with EtOH and dried. Yellow crystals (0.100 g, 81%), mp 144 °C.

δ_{P} (D_2O) 21.1;

δ_{H} (D_2O) 1.08 (6H, t, $^3J_{\text{HP}}$ 7.1), 3.00-3.22 (4H, m), 3.39-3.50 (8H, m), 3.73 (3H, d, $^3J_{\text{HP}}$ 11.4), 8.90 (2H, s)

Elemental analysis: $\text{C}_{15}\text{H}_{25}\text{N}_6\text{O}_9\text{P}$ requires: C, 38.80; H, 5.43; N, 18.06%

Found: C, 38.70; H, 5.51; N, 17.90%.

Free base of **5d**.

Substrate **3d** (0.175 g, 0.86 mmol) was dissolved in MeOH (20 ml), a solution of MeONa (1.3 mole-equiv.) in MeOH (20 ml) was added and the solution was kept

at room temperature, with the ^{31}P NMR spectra recorded periodically (substrate's signal at δ_{P} 47.7 being replaced by the signal at δ_{P} 22.7), $t_{1/2}$ ca. 65 h. After 13 days (ca. 4.8 half-lives) the solution was neutralized with the required volume of 0.73 M methanolic HCl and evaporated under reduced pressure. The residue was extracted with CHCl_3 (4 \times 20 ml) and the combined CHCl_3 solution was evaporated under reduced pressure yielding **5d'** (0.180 g, 89%) as a viscous oil.

δ_{P} 19.9;

δ_{H} 1.13 (6H, t, $^3J_{\text{HH}}$ 7.0), 3.05-3.32 (12H, m), 3.64 (3H, d, $^3J_{\text{HP}}$ 11.1);

δ_{C} 14.4 (s), 42.1 (d, $^2J_{\text{CP}}$ 2.7), 43.0 (d, $^2J_{\text{CP}}$ 4.8), 44.8 (s)

Alternative preparation of hydrochloride salts **5d** and **5f**; general procedure

To a solution of **3** (0.33 mmol) in MeOH (5 ml), Me_3SiCl (0.039 g, 0.36 mmol) was added and the reaction mixture was stirred at room temperature for 4 h. Full conversion was demonstrated by ^{31}P NMR spectroscopy. The solution was evaporated under reduced pressure yielding the corresponding **5·HCl** (100%). The products were sufficiently pure not to require further purification.

2.4 References

1. Z. He, S. Laurens, X.Y. Mbianda, A.M. Modro, T.A. Modro, *J. Chem. Soc. Perkin Trans. 2*, 2589 (1999).
2. A.M. Modro, T.A. Modro, P. Bernatowicz, W. Schilf, L. Stefaniak, *Magn. Reson. Chem.*, **35**, 774 (1997).
3. W. von Philipsborn, R. Müller, *Angew. Chem., Int. Ed. Engl.*, **25**, 383 (1986).
4. S. Bauermeister, A.M. Modro, T.A. Modro, A. Zwierzak, *Can. J. Chem.*, **69**, 811 (1991).

CHAPTER 3

3. THIO ANALOGUES OF 1-OXO-2,8-DIARYL-2,5,8-TRIAZA-1 λ^5 -PHOSPHA-BICYCLO[3.3.0]OCTANE

3.1 Introduction

The synthesis of thiophosphoric amides with general structure Q dates from 1857¹. Most thiophosphoric amides can be prepared via the same routes as their phosphoryl counterparts. Thiophosphoramidates are usually formed via the simple reaction of P(S)Cl₃ or P(S)Br₃ with any primary or secondary amine². Alternatively the aminophosphine can be prepared first which can then be transformed into the corresponding thio analogue with treatment of elemental sulphur^{3,4,5}.

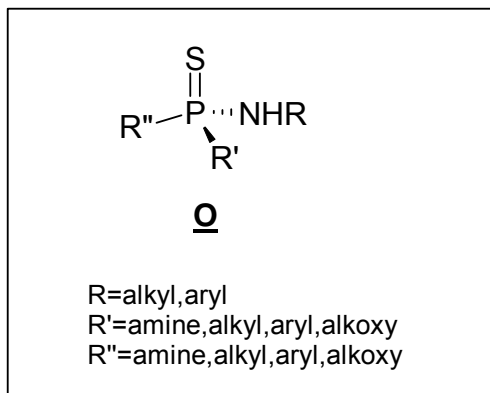


Figure 3.1 General structure of the thiophosphoramidates.

N-Bis(2-chloroethyl)thiophosphoamidodichloridate⁶ 8 and *N,N*-diethylthiophosphoamidodichloridate⁷ 8' are very common substrates for preparing thiophosphotriamidates, but the second and third nucleophilic displacements almost always involve aliphatic amines.

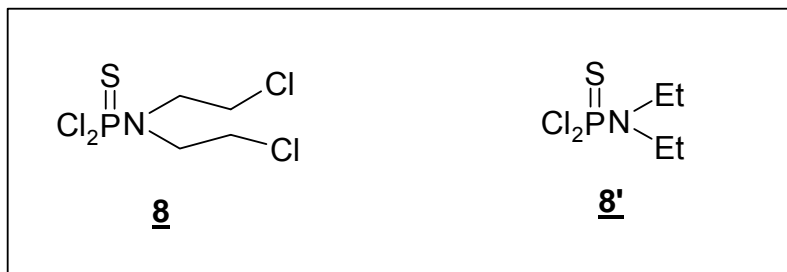


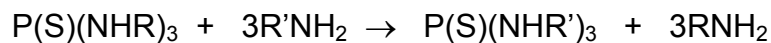
Figure 3.2 Substrates for preparing thiophosphoric triamides.

The phosphoryl oxygen in phosphonic chloro amides of the type RCIP(O)NHR can be exchanged for sulphur when treated with P(S)Cl_3 in the presence of DMF as a catalyst.⁸

Phosphonic diamides with the general structure $\text{R}''\text{P(S)(NHR)(N'HR')}$ ^{9,10} where $\text{R}''=\text{Aryl}$, $\text{R}'=\text{alkyl}$ and $\text{R}=\text{alkyl}$ or aryl substituents, can be prepared from $\text{R}''\text{P(S)Cl}_2$.

Numerous thiophosphorotriamides have been prepared over the years, but most attention was given to the symmetrically substituted thiophosphoric amides, $(\text{RNH})_3\text{P(S)}$ ^{5,11,12} or unsymmetrical triamides containing only aliphatic substituents on nitrogen¹³. Compounds of the type $(\text{R}_2\text{NH})_3\text{P=S}$, as well as N,N',N'' -trialkyl- N,N',N'' -triarylphosphoric triamides^{3,14} are synthesized in very simple substitution reactions. The symmetrical thio derivatives can sometimes be prepared by treating the corresponding phosphoryl compound with P_4S_{10} . Existing examples are phosphorotriamides which contain either aliphatic or aromatic substituents on nitrogen.

Primary amine derivatives can undergo transamination in which aryl groups can be replaced by more strongly bonded alkyl groups, or in which a more volatile amine can be boiled off and the equilibrium shifted to the desired side. (**Scheme 3.1**) This method is also only applicable to symmetrically substituted compounds like P(S)(NHR)_3 .



Scheme 3.1 Transamination of thiophosphorotriamidates.

No examples have been reported of thiophosphorotriamidates with general structure **P** (**Figure 3.3**) where only one of the *N*-substituents is aliphatic and the other two substituents are aromatic. This situation is similar to our compound **9a**, which was used as substrate in attempts to prepare our model compound **11a**.

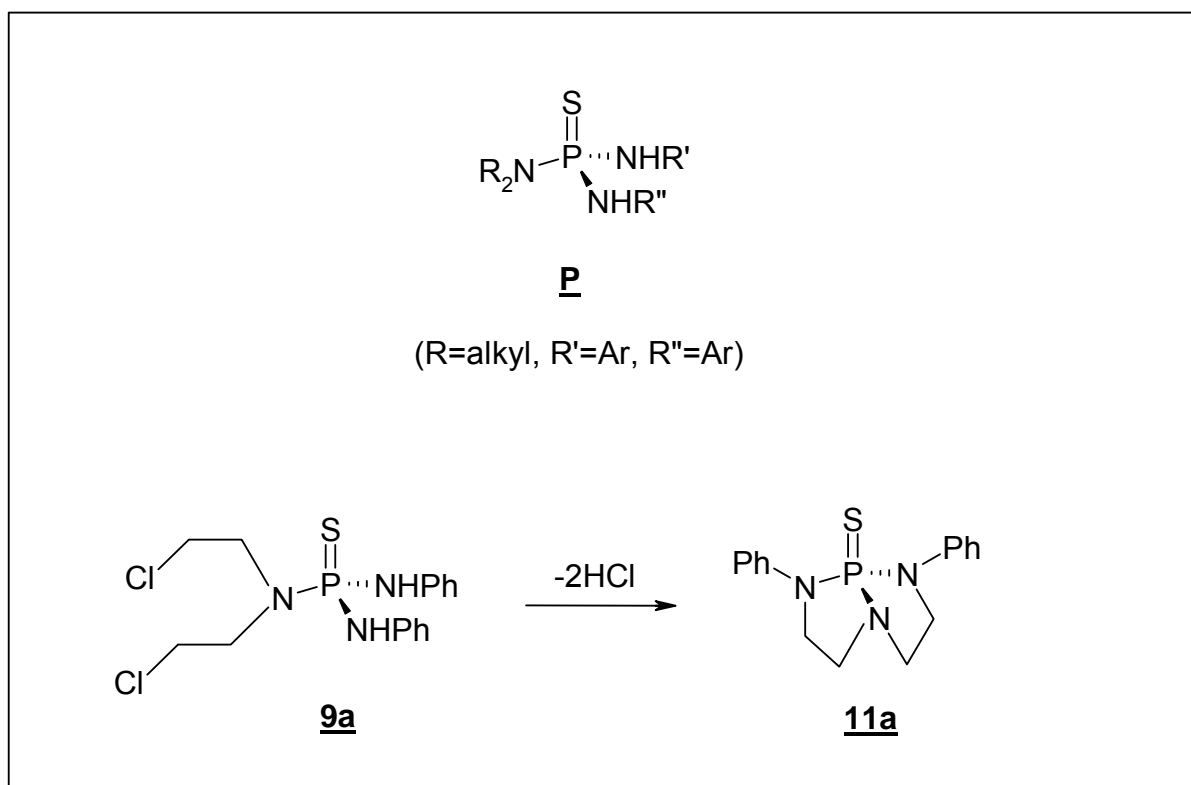


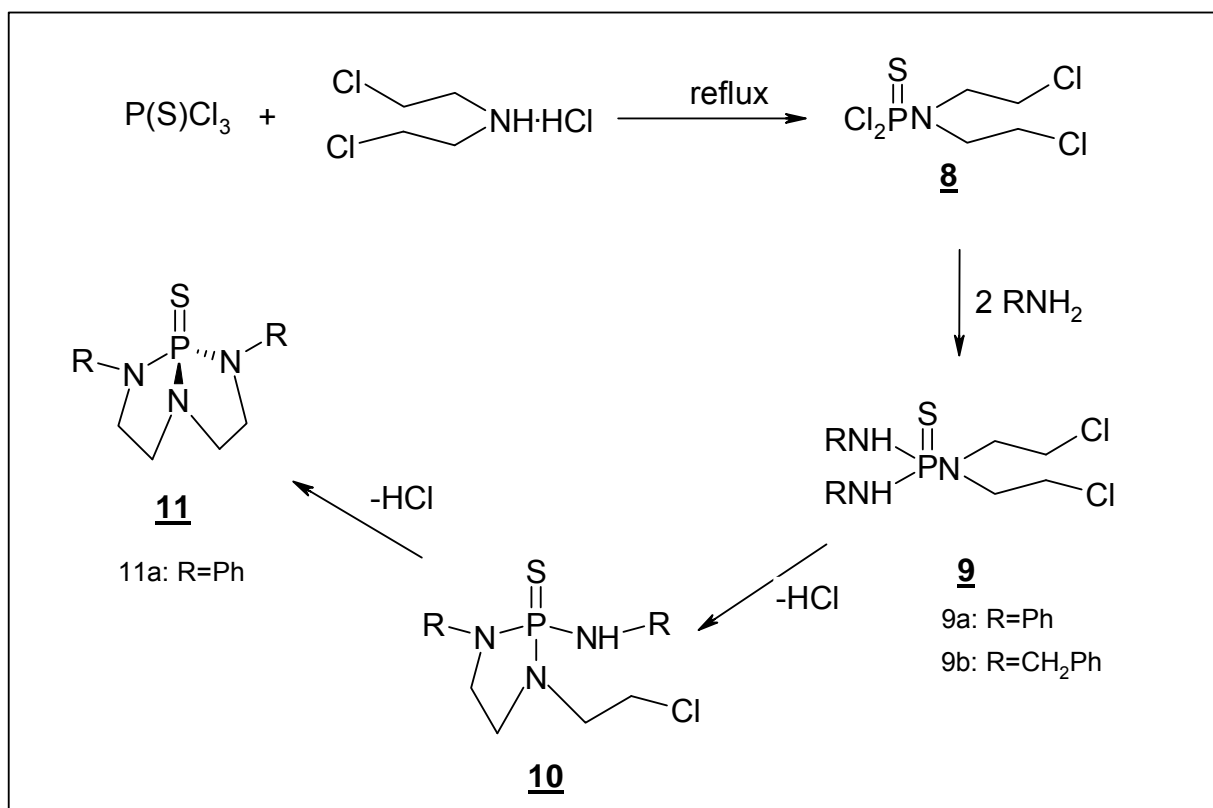
Figure 3.3 Thiophosphorotriamidates.

Although some of the thiophosphoamidodichloridates of the type $R_2NP(S)Cl_2$ are very resistant to nucleophilic attack, no problems were anticipated in obtaining the corresponding thio analogue **11a** via the same synthetic route as for the phosphoryl analogue **3a**.

3.2 Results and Discussion

3.2.1 Synthesis

The attempted route to product **11a**, according to the general sequence shown in **Scheme 3.2** turned out quite disappointing.



Scheme 3.2 Reaction pathway attempted for the preparation of the bicyclic thio analogue **11**.

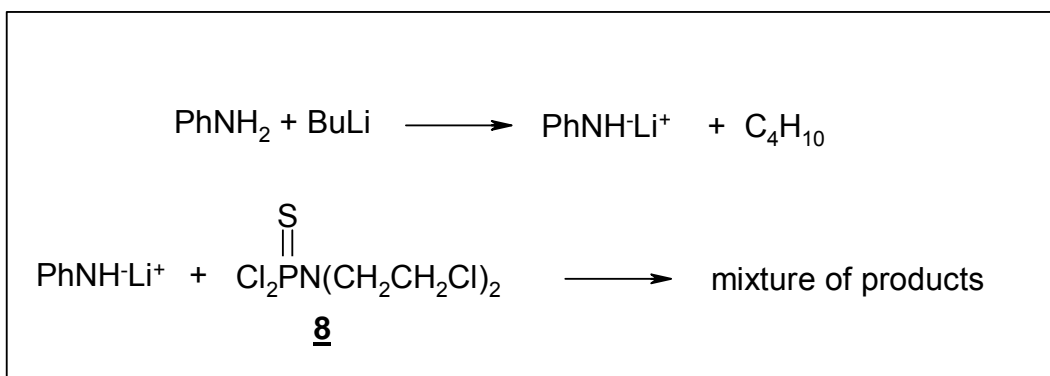
The first compound in the series, namely the *N*-bis(2-chloroethyl)-thiophosphoramidodichloridate **8** was prepared with a satisfactory yield and with the melting point in good agreement with the value reported in literature. All the attempts to substitute the two remaining chlorines for aniline residues were unsuccessful.

The known route to synthesize the noncyclic precursor **9** by reacting the *N*-bis(2-chloroethyl)thiophosphoramidodichloridate **8** with two moles of aniline and two moles of a base, failed under a variety of reaction conditions. The final product

couldn't be isolated in a state of satisfactory purity and with acceptable yield. The aniline in the presence of triethylamine proved to be not a strong enough nucleophile to replace the second and third chlorine atoms at the thio phosphoryl centre in compound **8**. This observation remains in disagreement with the reported preparations of thiophosphoric trianilides, $(\text{ArNH})_3\text{PS}$ from $\text{P}(\text{S})\text{Cl}_3$ and the aromatic amines. The phosphorous anilides, $(\text{PhNH})_2\text{PNMe}_2$, were prepared via the transamination reaction, but it was due to the much higher reactivity of the P(III) substrates relative to the phosphoryl or thiophosphoryl analogues.

The noncyclic triamidate with aliphatic substituents on nitrogen (**9b**, $\text{R}=\text{PhCH}_2$) was prepared via the route shown in **Scheme 3.2**, but attempts to cyclize the compound led to the formation of an unexpected phosphorus containing product with a δ_{P} value of 5. The ^{31}P chemical shift of the desired product was expected to be much more down field¹⁵. No attempts were made to identify that product.

Different synthetic methods were then applied in order to introduce the two *N*-phenyl groups at the thiophosphoryl centre to arrive at the non-cyclic precursor **9a** ($\text{R}=\text{Ph}$). Lithium anilide was prepared to force the nucleophilic attack at phosphorus (**Scheme 3.3**), but this reaction was also unsuccessful. The reaction resulted in a complicated mixture of compounds and no single product could be isolated from the mixture.



Scheme 3.3 Attempted lithium anilide route to prepare substrate **9a**.

When the *N*-phenyl groups were introduced first to the P(S)Cl_3 , in order to prepare the *N,N'*-diphenylphosphorothiochloridate **12a** (Figure 3.4), a crystalline, unidentified phosphorus containing compound was formed.

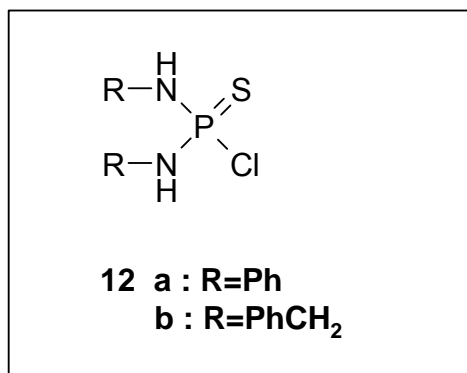
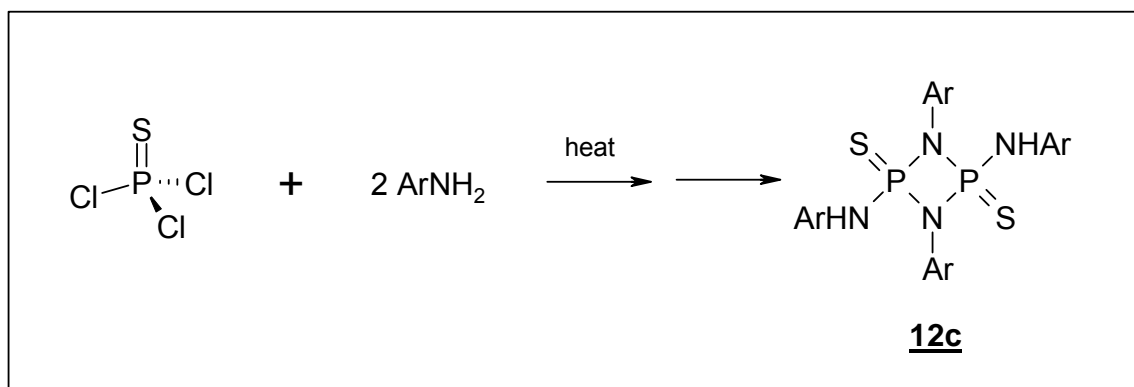


Figure 3.4 *N,N'*-disubstituted phosphorothiochloridate.

Most aromatic amines react with PCl_3 / PCl_5 / P(O)Cl_3 / P(S)Cl_3 to form dimers rather than monomers. Our unknown compound could be the dimeric cyclophosphazane **12c** (Scheme 3).

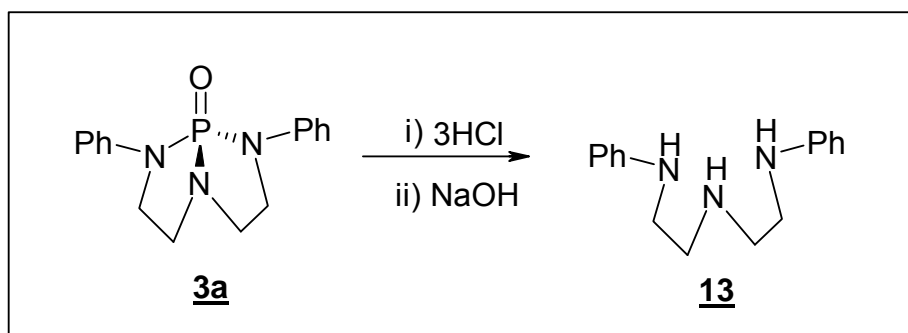


Scheme 3.4 Reaction of aniline with P(S)Cl_3 .

The benzyl analogue **12b** was prepared in very pure state and in good yield, but attempts to replace the last chlorine at phosphorus by the mustard group, failed. No attempts were made to further investigate these reactions.

In the next attempt, the phosphoryl bicyclic compound **3a** was treated with $P(S)Cl_3$ in the presence of DMF in order to exchange the oxygen for sulphur, according to the report on the catalytic activity of DMF in that type of reactions. The crude product of that reaction contained a mixture of phosphorus containing compounds with the desired product (recognized by its characteristic ^{31}P NMR chemical shift, δ_P 81) only as a minor component. No attempts were made to isolate any of the reaction products. After standing on the shelf for more than a year, one product separated from the mixture as a semi-solid. The ^{31}P NMR revealed a single phosphorus containing compound with $\delta_P \sim 100$ ppm, much more low field than the desired product which has $\delta_P \sim 81$ ppm). Time didn't allow us to identify and characterize this compound.

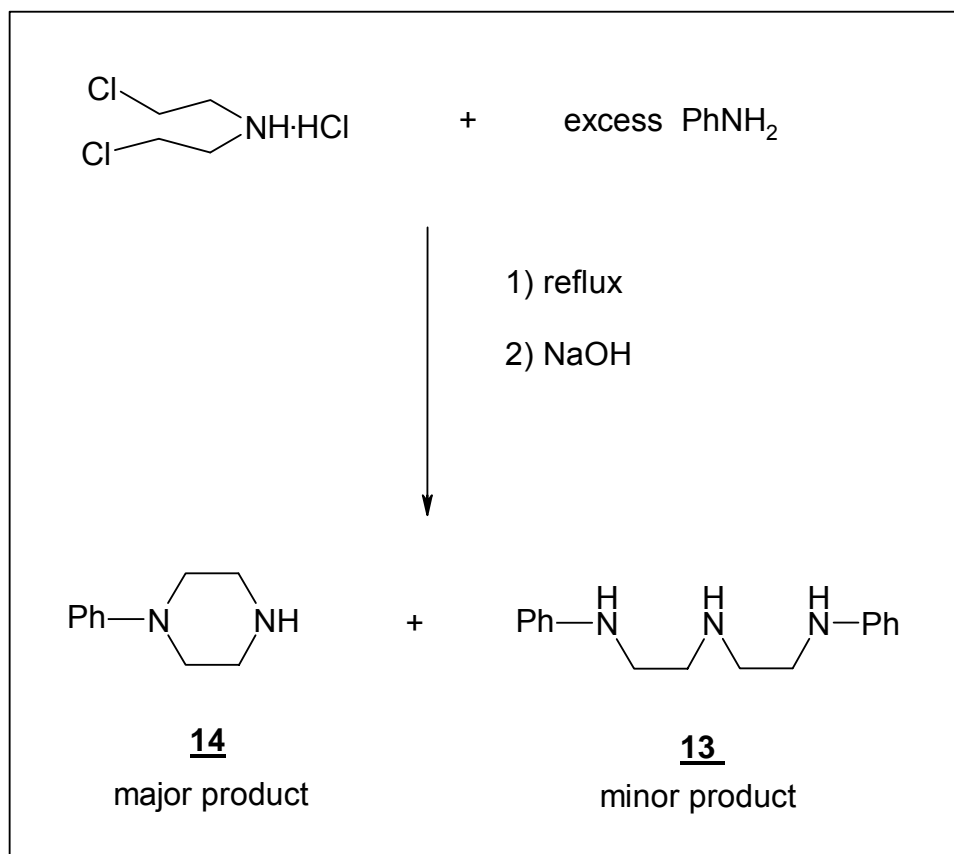
In the course of this work, triamine **13**, *N,N'*-diphenyl-bis(2-aminoethyl)amine, was prepared in our laboratory¹⁶ which was then used to prepare the thio bicyclic derivative in a one pot reaction. The triamine was originally prepared by hydrolysis of all three P-N bonds in the phosphoryl bicyclic compound **3a** (R=Ph) by reacting it with concentrated aqueous hydrochloric acid (**Scheme 3.5**). The triamine trihydrochloride salt **13'** was isolated from this reaction in quantitative yield and needed no further purification.



Scheme 3. 5 Preparation of triamine **13** from phosphoryl bicyclic **3a**.

Cleavage of the three P-N bonds could also be achieved by reacting the bicyclic substrate with an excess of Me_3SiCl in MeOH. This is even a better reaction as all side products could be evaporated.

The *obvious* route for preparing the triamine **13** is reacting the mustard amine hydrochloride salt, bis(2-chloroethyl)ammonium chloride, with two moles of aniline. In agreement with the early experiment of Prelog and Driza¹⁷ reported in 1933 we have demonstrated that the desired triamine is only formed as a minor product (~10%) and N-phenylpiperazine **14** is the major product of the reaction. After the first substitution by aniline, an intramolecular substitution is favoured above the second substitution by aniline, leading to the main product **14** (Scheme 3.6).



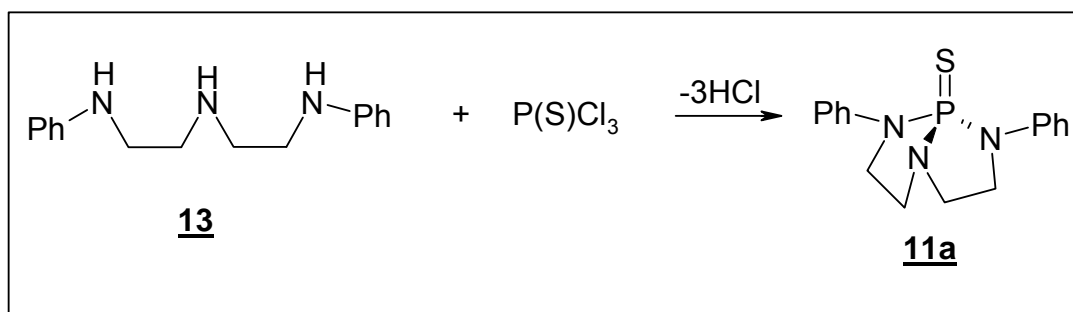
Scheme 3.6 Preparation of triamine **13**.

Triamine **13** attracted our attention as a possible substrate in our quest for the product **11a**. It seemed reasonable that the condensation of **13** with $P(S)Cl_3$ in the presence of excess base, and under sufficient dilution, could serve as a

feasible route to **11a**, the compound which we have still failed to prepare via other routes.

The novel synthesis of the triamine **13** developed in our laboratory was however very time consuming and gave an overall yield of only 34% after six steps. A rather unconventional approach was applied to arrive at the triamine in large quantities. The “*N*-phenylpiperazine reaction” was carried out on a large scale (~60 g of substrate) in order to prepare a reasonable quantity of the triamine. The mustard amine hydrochloride salt and a large excess of aniline were refluxed in toluene for twenty four hours. The resultant mixture of amine salts was treated with large excess of aqueous NaOH to liberate the free bases, which were extracted with CH₂Cl₂. The triamine **13** was then precipitated with diethyl ether, together with some impurities, from the bulk of the *N*-phenylpiperazine. The triamine **13** (free base) was extracted from the precipitate with hot methanol from which it crystallizes out upon cooling. ¹H NMR and elemental analysis showed that in this way **13** can be prepared in a very pure state, and can be used in the planned synthesis of **11a**. It was possible therefore to demonstrate that the direct preparation of the triamines of the type **13** from the nitrogen mustard and aromatic amines can be of practical use, provided that one accepts great losses of the substrates which are converted to the piperazine derivative **14**.

The bicyclic compound **11a** was then prepared by reacting the triamine **13** with P(S)Cl₃ (Scheme 3.7)¹⁸ in the presence of a base.



Scheme 3. 7 Preparation of the thio-bicyclic compound **11a** from triamine **13**.

Triamine **13** has very low solubility in most organic solvents which limited the choices of reactions conditions. Triethylamine was chosen as a base necessary to neutralize three equivalents of HCl expected to be released. The substrate **13**, $P(S)Cl_3$ and Et_3N were mixed in a final molar ratio of 1:1.1:6 and with high dilution (7.5 mg of **13**/mL, 0.03 M). The high dilution was necessary to prevent the triamine molecule to react with $P(S)Cl_3$ at more than one reactive centre which might result in the formation of undesired chain products e.g. **13x**.

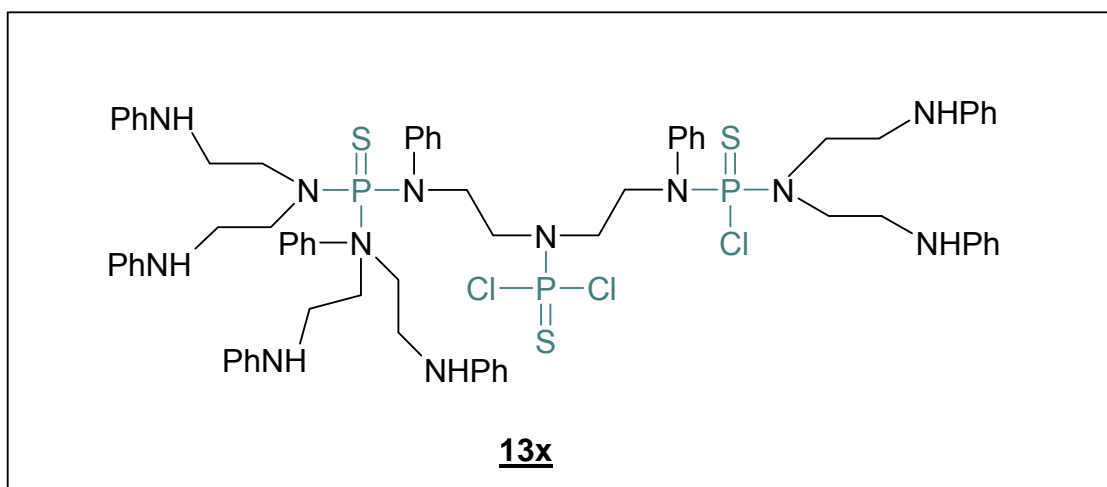


Figure 3. 5 Expected condensation product from reaction of $P(S)Cl_3$ and triamine **13**.

A low boiling solvent (diethyl ether) was found to be possible as the medium for the first attempt of the reaction. Since we also expected polymerization to occur more likely at high temperatures, the boiling point of the solvent secured the low temperature of the reaction.

One mol of triamine **13** and 6 mol of triethylamine were dissolved in 50 mL of anhydrous diethyl ether. $P(S)Cl_3$ (1.1 mol) in 10 mL ether was added dropwise while stirring ($-10\text{ }^\circ\text{C}$). The mixture was left to warm up to room temperature and then refluxed for ten days. Like before, the progress of the reaction was followed by ^{31}P NMR of the reaction mixture. The reaction was very slow but the intensity of the $P(S)Cl_3$ resonance signal was decreasing while new signals were growing. Finally all the intermediate signals were gone and only the signal of the product **11a** at 81 ppm was observed. The triethylammonium chloride was filtered off

and the filtrate washed with a 10% aqueous K_2CO_3 solution to keep the pH between 7 and 8. The solvent was evaporated and the crude product purified by column chromatography.

This reaction was repeated in anhydrous THF which lead to the formation of the product in shorter time, but resulted in a mixture of side products causing a much lower yield.

During one of these experiments, the water flow in the laboratory was cut off and the temperature of the reaction mixture ran out of control. All the solvent evaporated. After workup a very pure product **11a** was isolated with the yield comparable to previous experiments. This made us realize that the experiment can be carried out at much higher temperature without damaging our product. The synthesis of **11a** was then adjusted according to this observation. The triamine and $P(S)Cl_3$ were refluxed in toluene without using a base. The HCl which was formed in the reaction was boiled off while refluxing. After cooling, the insoluble side products were filtered off and the mixture washed with a 10% K_2CO_3 solution. The mixture was dried over $MgSO_4$ and the toluene evaporated under reduced pressure. A reasonably pure product **11a** crystallized from this mixture. A very pure compound was obtained after repeated crystallizations from toluene.

Another possible route to arrive at **11a**, which was not explored here, is to use tris(imidazolyl)thiophosphoric amide as starting material.

Attempts to prepare the unsubstituted bicyclic compound (R=H) via the route shown in **Scheme 3.7** using bis-(2-aminoethyl)amine as the substrate, resulted in a crystalline product with a ^{31}P NMR signal at $\delta_P \sim 100$ ppm. This compound decomposed upon attempts of isolation.

NMR Analysis

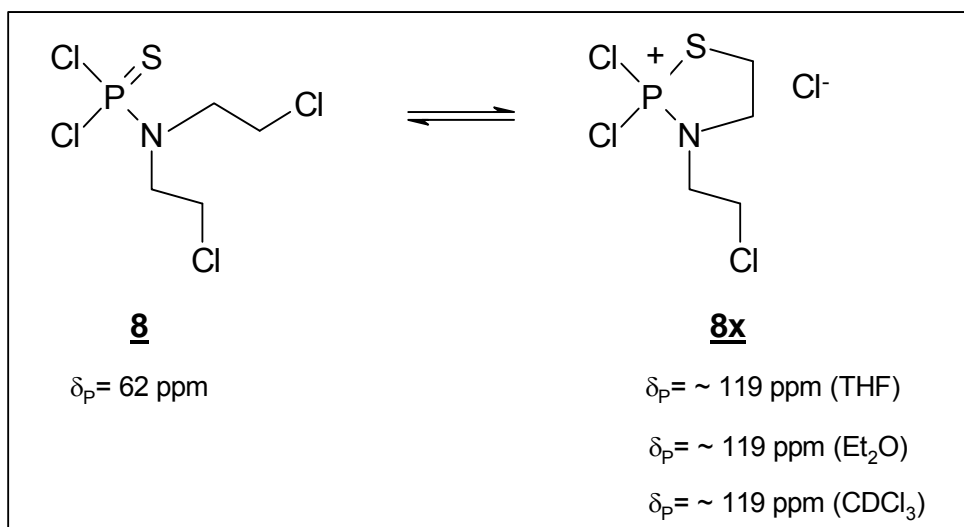
For the phosphoryl derivatives, the ^{31}P -NMR spectroscopy was very valuable in determining the chemical changes around phosphorus. As discussed in the introduction in Chapter 1, there is a correlation between the ^{31}P -NMR chemical shift and the structural differences in the phosphotriamidate series. This could be used to distinguish, with very high certainty, between the different compounds in the series without isolation of the individual compounds. The values reported in literature for those thio compounds which are most like the ones studied in this project, showed the same trend as in the phosphoryl derivatives. A regular downfield shift was observed for thio compounds with increasing number of nitrogens attached to phosphorus, but the differences are much smaller. With the thio-derivatives obtained in this work, it was not possible to unambiguously assign δ_{P} values to the different compounds. E.g. the ^{31}P chemical shift of substrate **8** differs from the next compound in the series, **9b** (R=Benzyl) by less than 1 ppm, but in the phosphoryl family the $\Delta\delta_{\text{P}}$ for the corresponding compounds was ~ 5 ppm.

Additional experiments

In the many attempts to prepare the phosphotriamide **9a** a new signal (δ_{P} 119) was sometimes observed in the ^{31}P NMR spectrum of the reaction mixture but after evaporation of the solvent, the signal disappeared completely. The substrate **8** used as the starting material to prepare **9a** was heated alone in THF, Et₂O and CDCl₃ respectively. The same signal (δ_{P} ~ 119) was observed in the solution, but after evaporation of the solvent the only signal observed was that of the substrate **8** at δ_{P} 62 ppm, and the ^1H NMR spectrum was unchanged.

The only plausible explanation for this observation is that substrate **8** is capable of entering some reversible reaction of which the product **8x** can be formed only at higher temperatures, and then return to the initial stable compound **8**. The most likely reaction would be the intramolecular displacement of the chloride ion

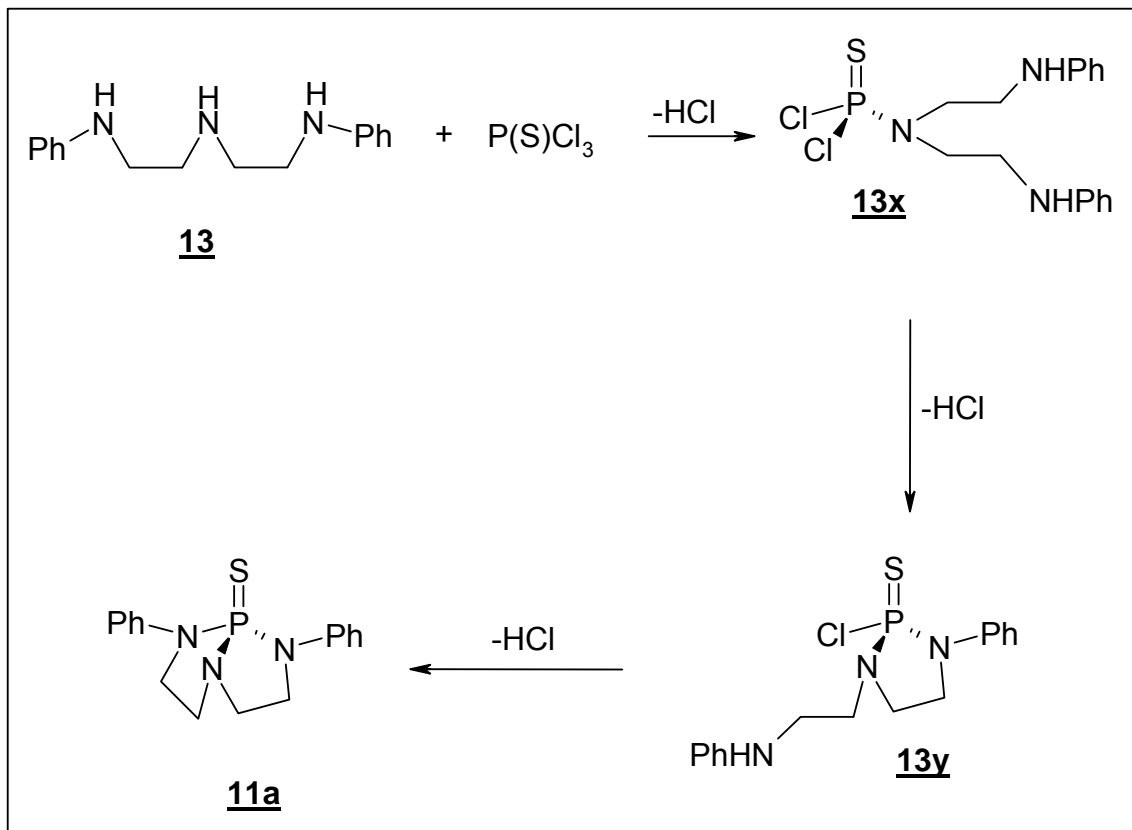
(Scheme 3.8)¹⁹. The nucleophilicity of the thiophosphoryl group will be discussed later in this chapter.



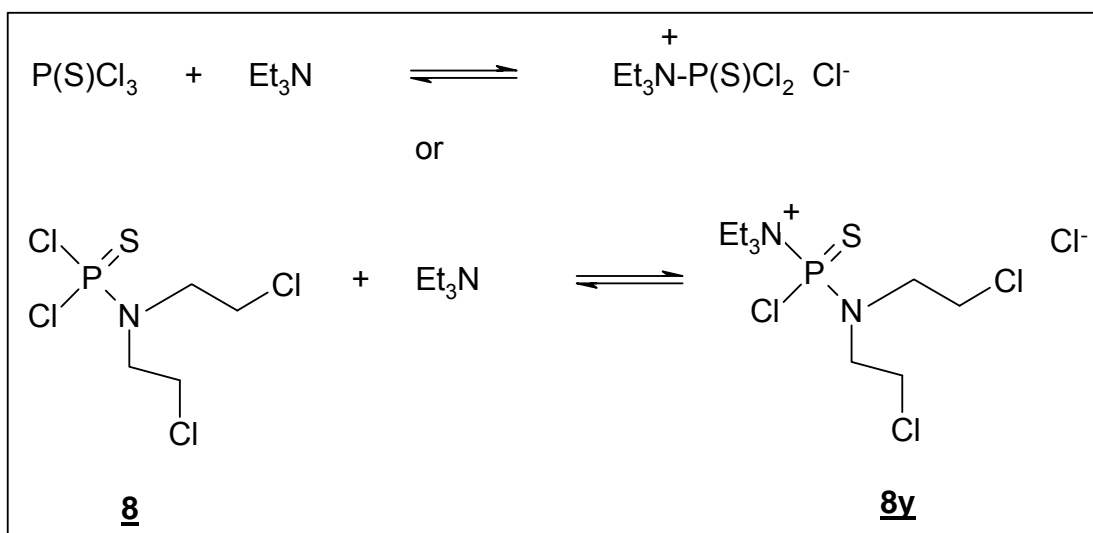
Scheme 3.8 Intramolecular displacement reaction of substrate **8**.

In almost all of the reaction mixtures where compound **8** or P(S)Cl₃ (δ_P 32) were used as a substrate and when triethylamine (Et₃N) was used as a base, a signal at $\delta_P \sim 43$ was observed in the ³¹P NMR spectra.

The resonance signal ($\delta_P \sim 43$) also appeared in the reaction of triamine **13** with P(S)Cl₃. At first it was believed to be one of the intermediate substitution products **13x** or **13y** (Scheme 3.9), but these compounds were never isolated. The ³¹P NMR signal at 63 ppm should rather be the monosubstituted intermediate **13x** because the chemical environment of phosphorus is basically identical as in compound **9a** which has δ_P 62.



Scheme 3. 9 Stepwise preparation of the thiobicyclic compound **11a** from triamine **13**.



Scheme 3. 10. Proposed equilibrium for reactions of **8** and P(S)Cl₃ and Et₃N.

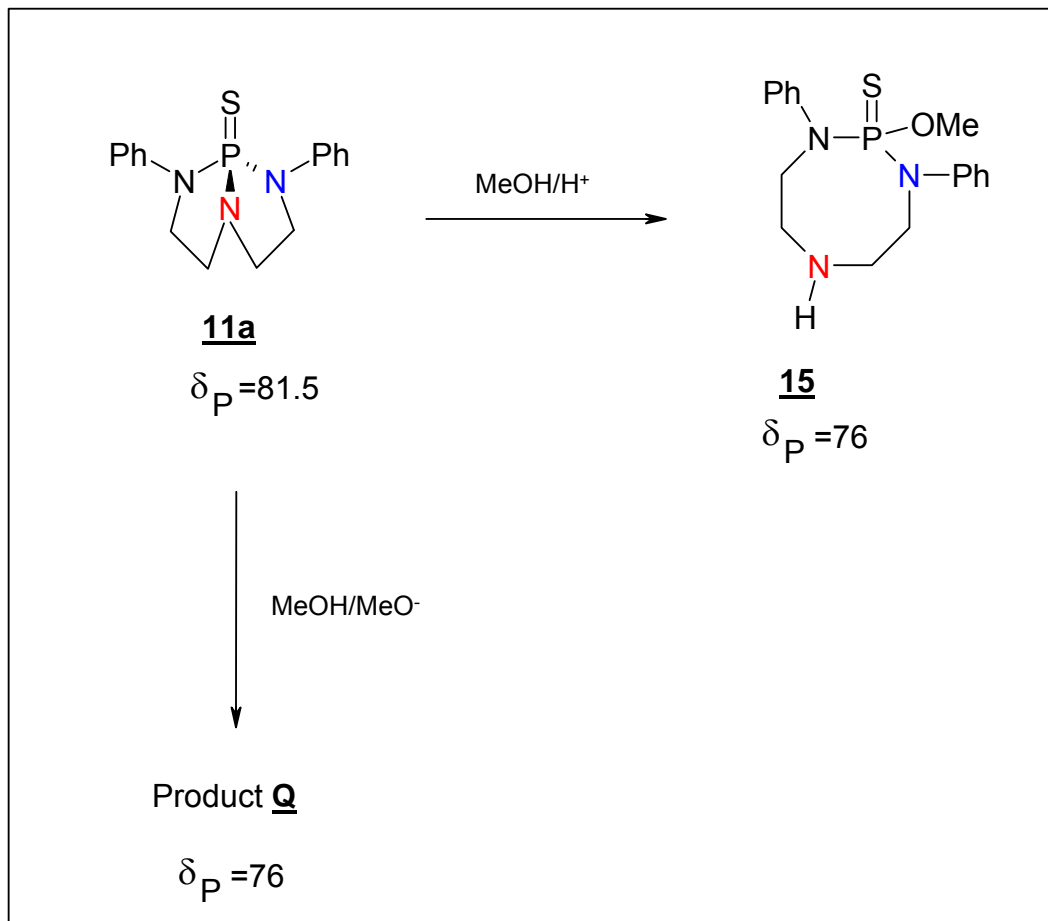
Equilibria like that shown in **Scheme 3.10** can be proposed. The ammonium species could be stabilized by adding SbCl_5 and formation of the non-nucleophilic SbCl_6^- -anion. This was not investigated any further.

3.2.2 Acid catalyzed alcoholysis

The first reaction studied for the new bicyclic compound **11a** was the acid catalysed solvolysis of the amide bond. A similar substitution reaction was expected like for the phosphoryl derivatives because the P-N bond is very unstable under acidic conditions²⁰ in a variety of amides derived from phosphorus acids. When the thiobicyclic compound **11a** was treated with methanol containing one mol equivalent of HCl, we observed the appearance of a new signal, only 5 ppm up field in the ^{31}P -NMR spectrum of the crude reaction mixture, with complete disappearance of the signal of the substrate. Reaction was completed in less than five minutes.

Under acidic conditions the product was stable in solution and could be isolated as a white solid after evaporation of methanol. ^1H -NMR spectrum indicated that it is the substitution product, the eight membered ring compound **15** (**Scheme 3.11**). The isolated product was not pure enough to give a reliable ^{13}C NMR spectrum. Therefore the crude product was analysed by GC-MS without further purification to confirm the structure of the compound.

The product **15** of the acid catalyzed reaction is stable as the neat hydrochloride salt. The hydrochloride salt was dissolved in chloroform and treated with aqueous K_2CO_3 to liberate the free amine. After decanting the aqueous layer, the organic layer was dried and without evaporation of the solvent, the ^1H -NMR of the sample was recorded. ^1H -NMR spectrum of the free amine **15'** did not correspond to the ^1H -NMR spectrum of the eight-membered ring compound **15** and ^{13}C NMR was not very useful because of the impurity of the sample.



Scheme 3.11 Alcoholysis of thiophosporyl bicyclic **11a**.

The splitting pattern of the aliphatic protons of the free base was distinctly different from that of the hydrochloride salt. The characteristic doublet for the methoxy protons has moved down field with 0.3 ppm and the coupling constant $^3J_{\text{HP}}$ changed from 13.9 Hz to 14.5 Hz. When the free base was isolated from the solvent as a grey viscous oil, and then sent for NMR, the ^{31}P NMR spectrum indicated a mixture of phosphorus containing compounds which changed with time. ^1H NMR spectrum indicated the major fraction is the compound which results in the doublet with $^3J_{\text{HP}}=14.5$ and only 18 % of the product with $^3J_{\text{HP}}=13.9$. The corresponding free amine **15'** was never isolated in the pure form.

3.2.3 Base catalyzed alcoholysis

The change of the alcoholysis medium from the MeOH/H⁺ system to a solution of sodium methoxide in methanol gave a ³¹P-NMR signal at δ_P 76, the same as for the acidic methanolysis. This alcoholysis product is not the same as for the acidic alcoholysis. The ¹H NMR spectrum of product **Q** showed some distinct differences from the ¹H NMR spectrum of compound **15**.

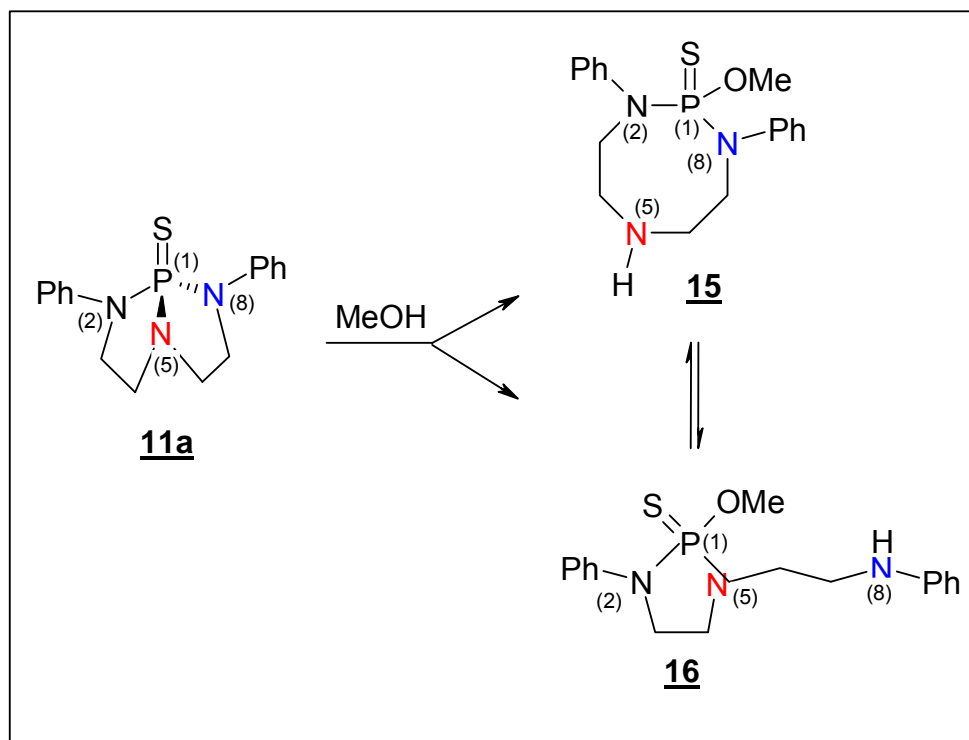
3.2.4 Rearrangement of the Alcoholysis Product , **15**

Liberation of the free base of the alcoholysis product **15** resulted in a mixture of unknown phosphorus compounds. The free base was never isolated as a pure compound and therefore it was not possible to study the kinetics of the rearrangement of the eight-membered ring compound in analogy to the phosphoryl derivative.

Gas Chromatography-Mass Spectrometry (GC-MS) was employed to acquire information on the alcoholysis product **15**. Gas chromatography (GC) in combination with mass spectrometry (MS), is a technique with which the components of a complex mixture can be separated and identified even if present in amounts as low as 10⁻¹² g. All forms of chromatography involve the partitioning of compounds between two phases, one mobile and one stationary. Each compound in a mixture partitions to a different degree between these two phases so that as they are carried along over a bed of the stationary phase, separation occurs. The components separated by gas chromatography are then eluted directly into the detector, in this case the mass spectrometer.

In the mass spectrometer the molecules are ionized in vacuum by a bundle of electrons. The fragmentation produces characteristic groups of ions of different masses. If the ions are separated according to their mass, a definite pattern of the number of ions present at each mass will be found. This pattern, the mass spectrum, is unique to a compound as fingerprints are to people. A compound can be identified by the mass spectrum.

From GC-MS analysis we got rather unexpected results. The analysis showed that the product contained two major compounds. One fraction contained the molecular ion of our expected product **15** (M^+ 347), but the fragmentation pattern revealed that *it is not* the substitution product, but in fact its isomer **16**. To form compound **15**, the P-N(5) bond is broken in compound **11a** and to form compound **16** the P-N(2)/P-N(8) bond is broken, giving the five-membered ring. The mass spectrum of that fraction, and the proposed fragmentation pattern are presented in **Figure 3.6** and **Scheme 3.13**, respectively.



Scheme 3.12 Cleavage of the P-N bonds in **11a**.

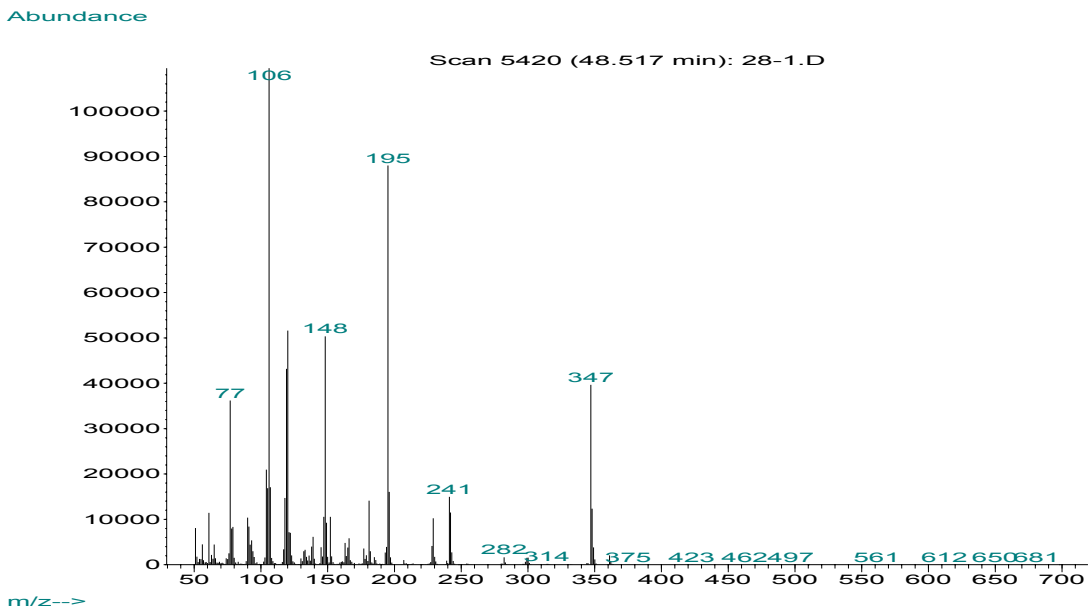


Figure 3.6 MS spectrum of fraction containing M⁺ 347.

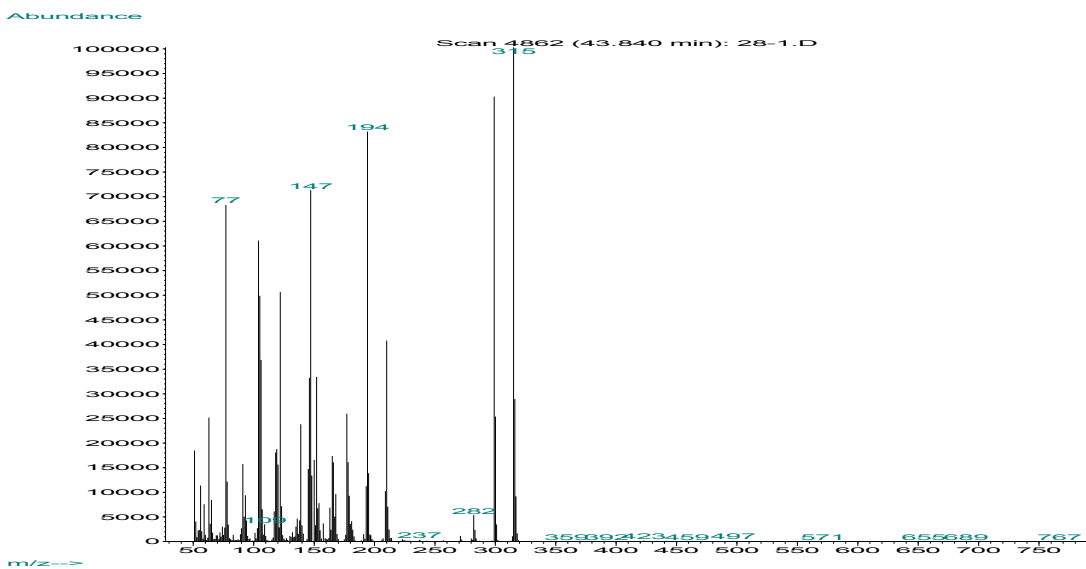
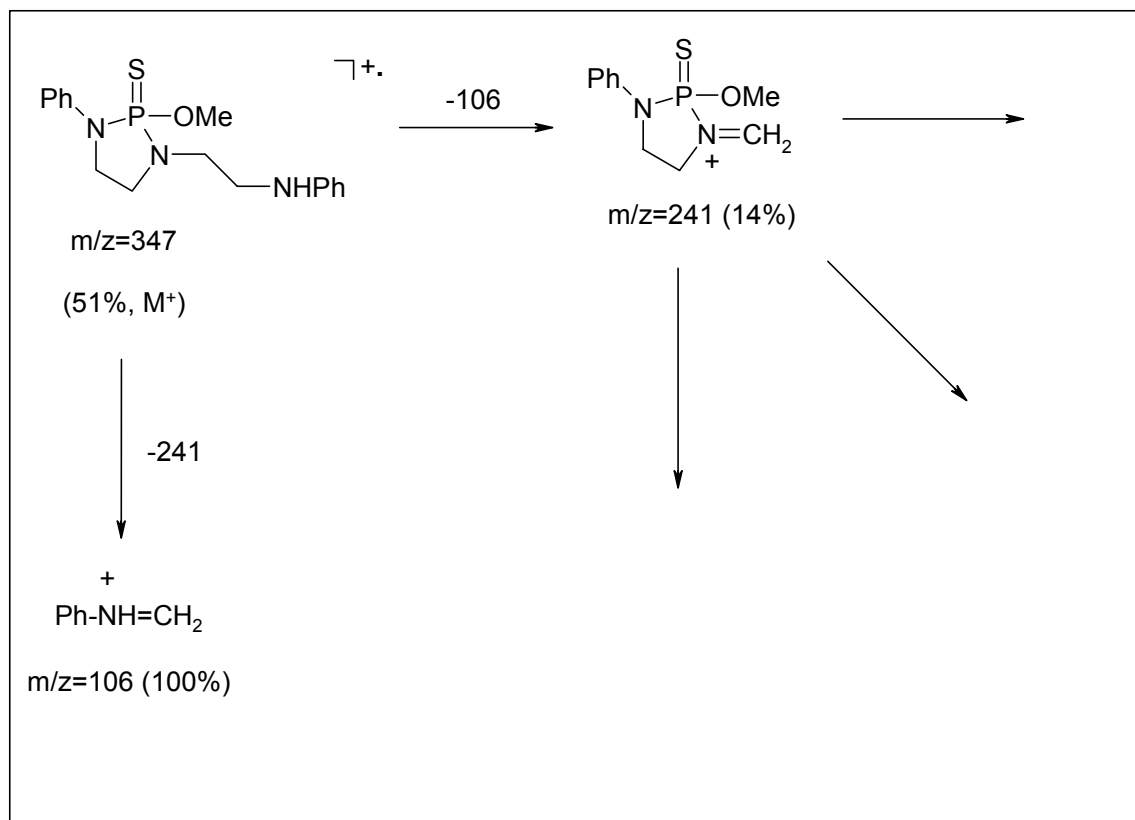


Figure 3.7 MS spectrum of fraction containing M⁺ 299 and M⁺ 315.



Scheme 3.13 Proposed MS fragmentation pattern of product **15**.

All the main fragments and mass losses can be explained accepting for the first fraction the structure of **16**. It is known that compounds with a heteroatom attached to an aliphatic chain, undergo α -cleavage²¹, i.e. the molecule is cleaved between the α - and β -carbon with respect to the heteroatom. The substitution product **15** wouldn't give the same fragmentation pattern after α -cleavage.

The molecular ion loses a fragment with a mass of 241 resulting in a base peak with a mass to charge ratio (m/z) of 106. At the same time, the mass loss of 106 and the appearance of a low intensity peak of $m/z=241$ is also observed. These peaks ($m/z=241$ and $m/z=106$) are both generated by the α -cleavage with different distribution of electrons into both fragments.

The compound that was detected in the ^{31}P -NMR spectrum (δ_{P} 76), is the substitution product **15**. Product **15** is then rearranging to its isomer **16** under

conditions of GC-MS analysis due to the high temperature or the basic groups present on the GC column. This rearrangement is in analogy with the rearrangement observed for the corresponding phosphoryl derivatives.

The other fraction obtained in the GC-MS experiment contained the molecular ion of the starting material **11a** (M^+ 315) as well as of its phosphoryl analogue **3a** (M^+ 299) (**Figure 3.7**). This was very surprising, because the signal of substrate **11a** disappeared completely in the ^{31}P -NMR spectrum of the reaction product. What was even more confusing was the presence of the oxygen analogue, which was never present in the reaction system in the first place!

If the two standard mass spectra of **11a** and **3a** (obtained independently from the genuine samples of those compounds; (**Fig. 3.8 & 3.9**) are superimposed, they give exactly the same result as that obtained for the second fraction (RT 43.840 min.) of our compound **15**.

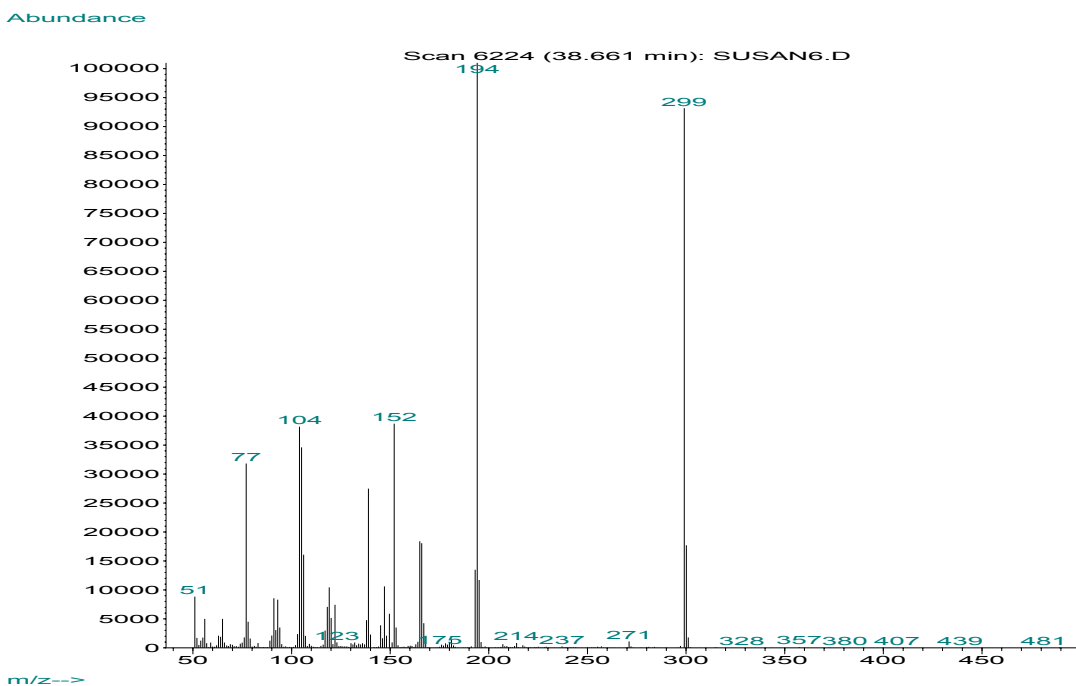


Figure 3.8 Standard MS spectrum of compound **3a**.

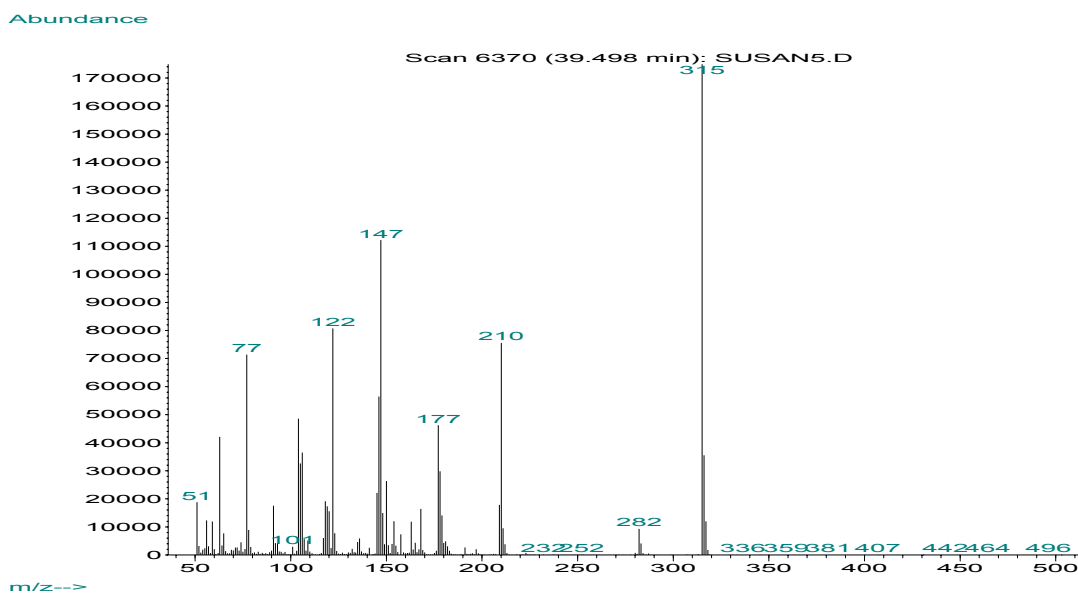
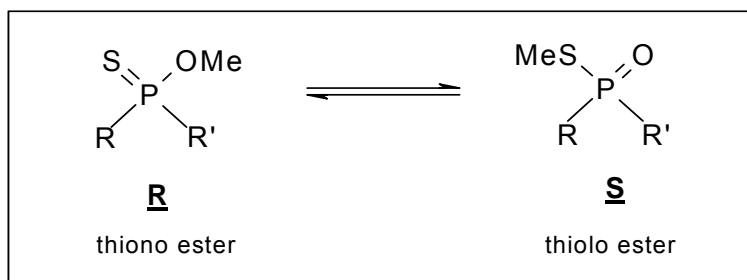


Figure 3.9. Standard MS spectrum of compound **11a**.

All the fragments and mass losses correspond to that of the standard spectra of the P=S (**11a**) and P=O (**3a**) containing bicyclic compounds.

Our explanation of the observed results is as follows. At high temperature, methyl esters of thiophosphoric acid, the thionophosphoric ester **R** can rearrange to the thiolo phosphoric ester²² **S** (**Scheme 3.14**).



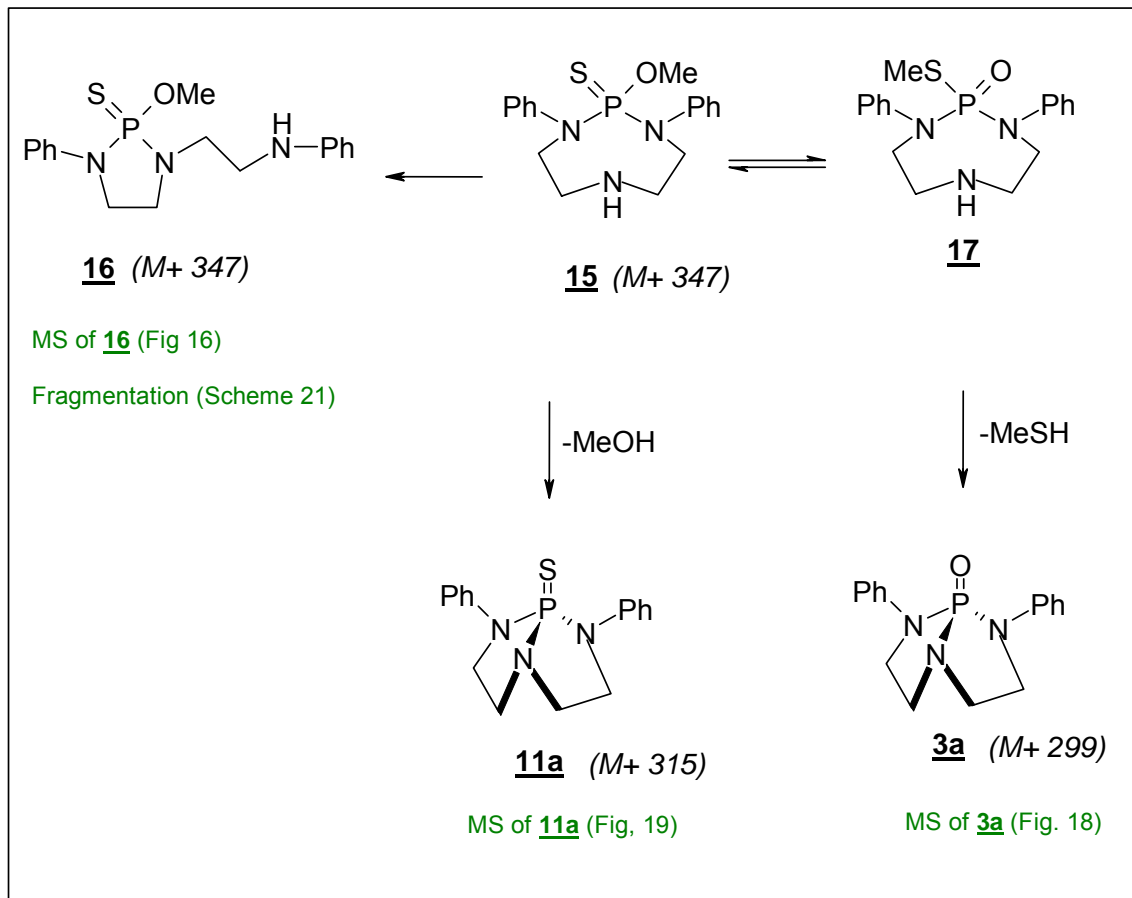
Scheme 3.14. Thermal rearrangement of methyl thiophosphoric esters.

This rearrangement was also observed in the mass spectra of a series of thionophosphate esters and amides studied by Cooks and Gerrard^{23,24}. They

have established three important generalizations.

1. The molecular ion can rearrange before any fission occurs (**Scheme 3.14**). Spectra of thiono and thiolo esters were not identical. In the thiono isomer the ion $M - CH_3$ is more prominent which indicated that the equilibrium between thiono and thiolo is not complete in the ion source. Spectra obtained at source temperatures of 60 and 200 degrees indicated that the rearrangement is of electron impact and not of thermal origin.
2. Rearrangement can give ions formed by joining two substituents, e.g. in the mass spectra of $P(S)(OPh)_2OMe$ were found ions of composition $PhSPh$, C_7H_7 and $PhSMe$. Ions of the composition $PhOH$ and $PhSH$ were also formed by hydrogen abstraction by one substituent from another.
3. Compounds with NHC_6H_6 substituents formed the base peak by loss of SH directly from the molecular ion. Deuteration of NH as well as the other substituents indicated that H is abstracted from the cyclohexyl ring; the loss of SH competes successfully with the McLafferty rearrangement, e.g. in compounds $i-C_3H_8O-P(S)-$, the ion $M - SH$ was the base peak and the ion $M - C_3H_8$ was less than 5%.

According to our experimental results and the observations made by Cooks and Gerrard, our solvolysis product **15** (thiono ester) rearranges to the thiolo isomer. It can either lose methanol to form the substrate **11a** again, or the thiolo ester can lose $MeSH$ directly to form the phosphoryl bicyclic compound **3a**. The following mechanism is proposed to explain the reappearance of the substrate **11a** as well as the phosphoryl bicyclic **3a** (**Scheme 3.15**).



Scheme 3.15 Proposed mechanism of the rearrangement of the thionoester **15**.

The alcoholysis reaction product **15** can therefore rearrange via three different reaction pathways. Firstly it can rearrange to the isomeric compound, the five membered ring **16**, lose MeOH to form substrate **11a** again or rearrange to the thiolo ester which can lose MeSH to form the phosphoryl bicyclic analogue **3a**.

3.2.5 Derivatives of 1-Thio-2,8-diphenyl-2,5,8-triaza-1 λ^5 -phosphabicyclo-[3.3.0]octane, **11a**

Benzoylation

The hydrochloride salt **15** was treated with benzoylchloride in pyridine in order to prepare the *N*-benzoylated derivative **18**. ^1H NMR integrated for fifteen aromatic protons and eight aliphatic protons which was good indication that we have the benzoylated product. ^{31}P NMR spectrum contains a signal with the same

chemical shift as that of the substrate (compound **15**). All attempts to grow crystals suitable for X-ray analysis failed.

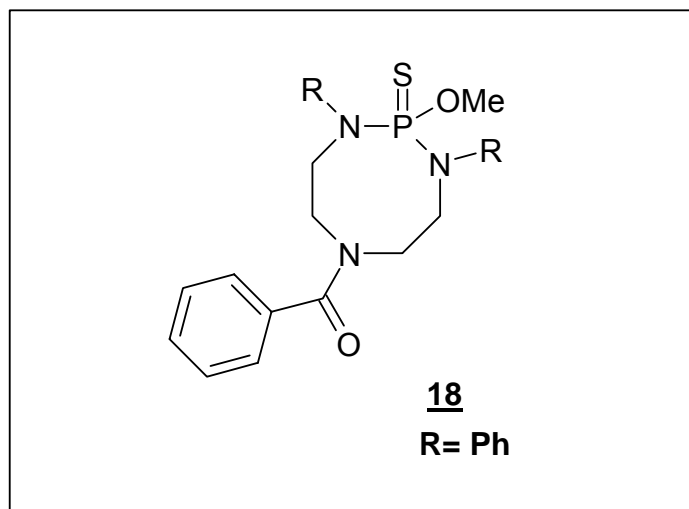
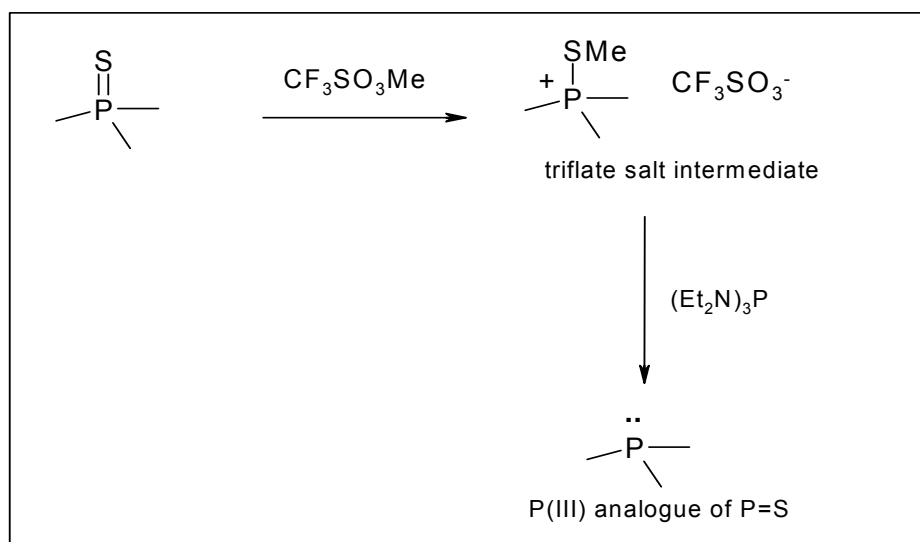


Figure 3.10 N-Benzoylated **15**.

Reduction of the P=S bond

Omelanczuk^{25,26} and co-workers described the reduction of thiophosphorus compounds by treating the 'P=S' compound with methyltriflate to form a stable intermediate product and then breaking the phosphorus-sulphur bond, leaving the phosphine [P(III)] analogue of the substrate.



Scheme 3.16 Reduction reaction to prepare P(III) analogues.

Compound **11a** was subjected to this same reaction conditions in order to prepare the phosphine triamide **19**, which we failed to prepare via the conventional route.

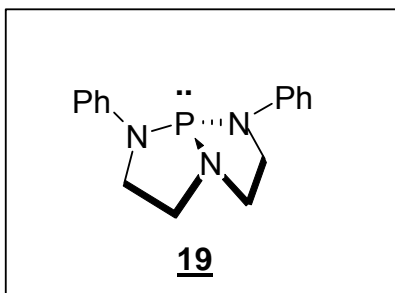


Figure 3.11 Phosphine derivative of bicyclic compound

Although the desired compound **19** was never isolated the reaction products were examined further. When the bicyclic compound **11a** was treated with the methyltriflate, a nonhomogeneous CF_3SO_3^- salt was formed in 60 % yield (^{31}P 77.7 ppm. In attempts to crystallize the salt, it was hydrolyzed, cleaving the P-N(5) bond, which lead to the thiolester **20**.

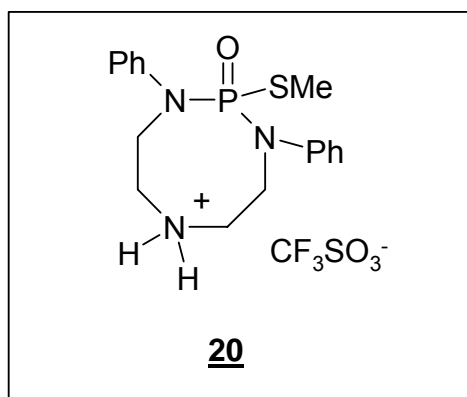


Figure 3.12 Triflate salt of the thiolester.

The desulfurization reaction of the triflate salt resulted in many byproducts. The ^{31}P NMR signal at 104.5 ppm could possibly be assigned to the bicyclic

phosphine derivative **19**. The final reaction product couldn't be isolated in a state of satisfactory purity to do further analysis.

3.3 Experimental

3.3.1 Synthesis of new thio analogues

N,N*-Bis(2-chloroethyl)thiophosphoramidic dichloride, **8*

Rigorously dry bis(2-chloroethyl)ammonium chloride was dissolved in four mol-equivalents of freshly distilled P(S)Cl₃ and the solution was heated under reflux for 16 h. The excess of P(S)Cl₃ was distilled off and the product was purified by bulb-to-bulb distillation (20 °C/1 mm Hg); mp 32-34 °C (literature, mp. 33-34°C), 71%.

δ_P (CDCl₃): 62.6;

δ_H 3.87-4.04 (overlapping t and dt, 4 x CH₂).

The structure of the compound was confirmed by X-ray diffraction. (**Chapter 4**)

1-Thio-2,8-diphenyl-2,5,8-triaza-1 λ^5 -phosphabicyclo[3.3.0]octane, **11a**

Bis(2-phenylaminoethyl)amine **13** (0.450 g, 1.8 mmol) and triethylamine (0.725 g, 7.2 mmol) were dissolved in rigorously anhydrous ether (50 mL). The solution was cooled to -10 °C, and freshly distilled P(S)Cl₃ (0.430 g, 2.5 mmol), dissolved in ether (10 mL), was added dropwise with stirring and cooling in the atmosphere of dry argon. The temperature of the mixture was kept between -20 and -10°C and was then allowed to warm up to room temperature. The precipitated triethylammonium chloride was filtered off and the filtrate was washed with a slightly basic aqueous solution (K₂CO₃). The filtrate was dried (MgSO₄), evaporated under reduced pressure, and the crude product (72%) was purified by column chromatography (CH₂Cl₂). The product (0.228 g, 41%) was obtained as colourless, crystalline material; m.p. 153 °C.

δ_P (CDCl₃): δ_P 81.5;

δ_H 3.21-3.31 (m, 2H), 3.62-3.78 (m, 4H), 3.83-3.92 (m, 2H), 7.01-7.06

(t, $J=7.0$ Hz, 2H), 7.16-7.25 (m, 8H);
 δ_{C} 47.8 (s), 49.6 (d, $J=16.2$ Hz), 121.7 (s), 123.5 (s), 128.9 (s).

Elemental Analysis: $\text{C}_{16}\text{H}_{18}\text{N}_3\text{PS}$: Calculated: C, 60.93; H, 5.75; N, 13.32; S, 10.17% Found: C, 60.70; H, 5.85; N, 13.28; S, 9.98%.

The structure of the product was confirmed by X-ray diffraction. (**Chapter 4**)

Alternative procedure for the preparation of 11a

8.76 g of triamine **13** (free base) and 6.08 g of freshly distilled $\text{P}(\text{S})\text{Cl}_3$ was refluxed in toluene (480 ml) for 14 days. The reaction mixture was allowed to cool down to room temperature, the undissolved material filtered off and the toluene solution washed with 10% K_2CO_3 (2x100 ml) and evaporated. The crude product was recrystallized from toluene several times to afford very pure colourless crystals. Yield: 57%, identical to previous product.

Bis(2-phenylaminoethyl)amine Trihydrochloride salt, 13'

1-Oxo-2,8-diphenyl-2,5,8-triaza-1 λ^5 -phosphabicyclo-[3.3.0]-octane **3a** which was used as the substrate was prepared as described before.²⁷ The product **3a** was not isolated, but the decanted reaction mixture was treated with 3 mol-equivalents of concentrated aqueous HCl. The solids were filtered off and washed with water. The product did not need further purification.

Yield: 86.5%, mp 220 °C (Lit. 203-206 °C).

δ_{H} (MeOD): 3.28 T, 4H, $J_{\text{HH}}=5.9$ Hz, 2 NCH_2), 3.49 (t, 4H, $J_{\text{HH}}=6.0$ Hz, 2 ArNCH_2), 6.67-6.71 (m, 6H, 4 o- H_{arom} , 2 p- H_{arom}), 7.15 (t, 4H, $J_{\text{HH}}=6.0$ Hz, 4 m- H_{arom})

δ_{C} (MeOH) 41.1 (s, NCH_2), 48.1 (s, ArNCH_2), 114.3 (s, o- C_{arom}), 119.1 (s, p- C_{arom}), 130.3 (s, m- C_{arom}), 149.1 (s, ipso- C_{arom}).

Free base, 13

The trihydrochloride salt (1.47 g) was mixed with 7 mL of 10 % aqueous NaOH. The mixture was stirred for several hours until the free amine separated out as an oil. The amine was extracted with CH₂Cl₂ (4 x 20 mL). The CH₂Cl₂ solution was dried (MgSO₄) and the solvent evaporated leaving a dark brown oil.

Yield 0.662 g, 45%.

δ_{H} 2.88(t, 4H, $J_{\text{HH}}=5.7$ Hz, 2NCH₂), 3.21 (t, 4H, $J_{\text{HH}}=5.7$ Hz, 2 ArNCH₂),
4.01 (br s, 3H, 3NH), 6.63 (d, 4H, $J_{\text{HH}}=8.0$ Hz, 4 o-H_{arom}), 6.71 (t, 2H,
 $J_{\text{HH}}=7.5$ Hz, 2 p-H_{arom}), 7.18 (dd, 4H, $J_{\text{HH}}=8.0, 7.5$ Hz, 4 m-H_{arom})
 δ_{C} 44.3 (s, NCH₂), 49.1 (s, ArNCH₂), 113.6 (s, o-C_{arom}), 118.1 (s, p-C_{arom}),
129.9 (s, m-C_{arom}), 149.0 (s, ipso-C_{arom})

Alternative procedure for the preparation of 13

Rigorously dry bis(2-chloroethyl)ammonium chloride (60g) and 208g aniline (24 moles excess) was mixed with 500 mL toluene and refluxed gently for 24 hours. The mixture was cooled to room temperature and the white precipitate filtered off. The precipitate was washed with toluene. The white solid (mixture of amines HCl salts) was stirred in 700 mL solution of 10% NaOH for 24 hours, to liberate the free amines. The mixture was extracted with CH₂Cl₂ (3 X 240 mL), dried over MgSO₄ and the solvent was evaporated. Ether was added to the dark brown oil to precipitate the desired triamine from the mixture. The triamine was further purified by extraction with hot methanol which gave a very pure white solid.

Yield 4.9 g, 11.8% ,mp 240-244 °C.

Elemental analysis: C₁₆H₂₁N₃ Calculated: C 75.30, H 8.24, N 16.47%,

Found: C 75.15, H 8.4 ,N 16.01%

N,N-Bis(2-chloroethyl)-N',N''-dibenzylthiophosphoric triamide, 9b

1.468g (5.3 mmol) of substrate, *N,N*-bis(2-chloroethyl)thiophosphoramido dichloride was dissolved in 15 ml of anhydrous benzene. A mixture of 1.142 g (10.6 mmol) benzylamine and 1.08 g (10.7 mmol) triethylamine in 15 ml

anhydrous benzene was added dropwise while stirring. The mixture was refluxed on a waterbath for 10 hours and left to cool down to room temperature. The white precipitate which contained the product as well as triethylammoniumchloride was filtered off and washed with 10 mL benzene and then with 100 ml ice-cold water. The solid product was dried under vacuum and then recrystallized from CH₂Cl₂. Yield 74%, mp 163-164 °C (Lit. yield 70-82%, mp.160,5-161,5 °C).

δ_P 64.1;
 δ_H 2.77 (2H, br dt, ²J_{HP} 9.0, ³J_{HH} 8.19),
 3.19-3.33 (6H, m.),
 4.10-4.37 (4H, m),
 7.22-7.34 (10H, m)
 7.80-7.95 (2H, m)

Elemental Analysis: C₁₈H₂₄N₃PSCl₂ Calculated: C 51.9, H 5.77, N 10.1, S 7.7%

Found: C 51.78, H 5.9, N 10.00, S 7.32%.

***N,N'*-dibenzylthiophosphoro diamidochloride, 12b**

Benzylamine (1.96 g, 0.02 mol) and triethylamine (2.2 g, 0.022 mol) was dissolved in 50 mL of anhydrous THF and cooled down to -10 °C. P(S)Cl₃ (1.70 g, 0.010 mol) in 100 mL of THF was added dropwise while cooling. The reaction mixture was kept at low temp for 2 hours and then left to warm up to room temperature. The white ppt was filtered off and the solvent evaporated. The crude product was dissolved in CHCl₃, washed with water (2x 50 mL) and dried (MgSO₄). After evaporation of the solvent the product was recrystallized from MeOH.

Yield: (70%), mp. 160-163 °C

δ_P 65.1
 δ_H 4.22-4.26 (4H, d, ³J_{HP}),
 7.33-7.45 (10H_{arom}, m),
 δ_C 46.1 (s, ArNCH₂), 127.7 (s, o-C_{arom}), 128.0 (s, p-C_{arom}),
 129.0 (s, m-C_{arom}), 140.2 (s, ipso-C_{arom})

Elemental Analysis: C₁₄H₁₆N₂PSCI. Calculated: C 54.1, H 5.15, N 9.02, S 10.3%
 Found: C 54.9, H 5.30, N 8.85, S 9.99%.

Alcoholysis product Hydrochloride salt 15?

Compound 11a (1.347 g, 4.28 mmol) was dissolved in 1000 mL of anhydrous methanol. A solution of Me₃SiCl in anhydrous methanol was added (0.477g) and stirred for 5 minutes. The solvent and volatile reaction products were evaporated. Yield 100% , mp 180 –182 °C .

δ_P 75

δ_H 3.21 (3H, d, ³J_{HP} 13.81), 3.25-3.55 (4H, m), 3.8-4.05 (2H, m), 4.1-4.28 (2H, m), 7.2-7.55 (10H_{arom}, m)

Elemental analysis: C₁₇H₂₃N₃OPSCI Calculated C 53.2, H 6.0, N 11.0, S 8.3%
 Found: C 53.17, H 6.12, N 10.11, S 7.80%.

Free base

0.285 g of the hydrochloride salt 15 was dissolved in 20 mL of CHCl₃. The solution was washed with 2 x 15 mL of 10 % K₂CO₃ , dried and the solvent evaporated. This product was used immediately for the benzoylation reaction. Yield: 73%.

***N*-Benzoylated alcoholysis product, 18**

0.188 g (0.5 mmol) of product 15 and 3 mL of dry pyridine was dissolved in 15 mL benzene. Benzoylchloride (0.250 g, 1.8 mmol) in 15 mL benzene was added dropwise while cooling (0 °C) and stirring . The reaction mixture was refluxed on a waterbath for 1 hour. A bright yellow precipitate was formed. The benzene solution was decanted and the yellow precipitate washed with benzene (2x20mL). The benzene was discarded. The yellow solid was dissolved in CHCl₃, washed with water, dried and the solvent evaporated under reduced pressure. The product was recrystallized from toluene. Yield 26.8%, mp. 161-165 °C.

δ_P 75 (74.9918)

δ_H 3.35 (3H, d, $^3J_{HP}$ 13.9), 3.44-3.56 (2H, m), 3.75-3.9 (3H, m), 3.95-4.15 (3H, m), 7.15-7.4 (15H, m)

δ_C (s, OCH₃), 46.86 (s, CH₂), 49.49 (s, CH₂), 51.64 (s, CH₂), 51.84 (s, CH₂), 127.04 (s, o-C_{arom}), 128.07 (s, p-C_{arom}), 129.21 (s, m-C_{arom}), 136.26 (s, ipso-C_{arom}), 172.1 (s, C=O)

Elemental analysis: C₂₄H₂₆N₃O₂PS Calculated C 53.2, H 6.0, N 11.0, S 8.3%

Found: C 53.0, H 6.1, N 11.5, S 8.7%

3.3.2 GC-MS Analysis

A 1 μ L aliquot of the sample was injected into the injection port of a Hewlett Packard 5890 series II “plus” gas chromatograph, using a HP 7683 auto injector. Data collection and instrument control was performed with a HP 59970 MC ChemStation. The injector port temperature was set to 250°C, and splitless injection was performed. Separation was achieved with a DB-1 capillary column, J & W Scientific (30m x 0.25 mm and 0.1 μ m film thickness) at a helium flow rate of 1.0 mL/min. An initial oven temperature of 100°C was held for 3 minutes and subsequently raised at a rate of 5 °C/minute, up to 250°C, and then held for 40 minutes at that temperature. The column outlet was inserted directly into the ion source of a HP 5973 Mass Selective Detector (Hewlett Packard). The mass spectrometer was operated with a filament current of 300 μ A and electron energy of 70 eV in the electron ionisation (EI) mode. The mass range scanned was 50-800 atomic mass units (amu). The transfer line was set at 280°C, and the quadrupole and source temperatures were 150°C and 230°C, respectively.

3.4 References

1. H. Schiff, *Ann.*, **101**,299 (1857).
2. J. Emsley, D. Hall, in “*The Chemistry of Phosphorus*”, Harper and Row, London, (1976).
3. C. Stuebe, H.P. Lankelma, *J. Am. Chem. Soc.*, **78**, 976 (1956).

4. H-J. Vetter, *Z. Naturforsch*, **196**, 72 (1964).
5. H-J. Vetter, H. Nöth, *Chem. Ber.*, **96**, 1308 (1962).
6. V. Dorn, H. Welfle, *J. Prakt. Chem.*, **313(2)**, S218 (1971).
7. K. Sasse in *Organische Phosphor-Verbindungen*; Thieme: Stuttgart, 1964; part 2, p 749.
8. M.P. Coogan, M.J.P. Harger, *J. Chem. Soc. Perkin Trans. 2*, 2101 (1994).
9. C. Tang, H. Lang, Z. He, R. Chen, *Phosphorus, Sulphur and Silicon*, **114**, 123 (1996).
10. E.J. Reist, I.G. Junga, B.R. Baker, *J. Org. Chem.*, **25**, 666 (1960).
11. W. Autenrieth, P. Rudolph, *Ber.*, **33**, 2112 (1900).
12. P. Rudert, *Ber.*, **26**, 565 (1893).
13. S. Fischer, J. Hoyano, L.K. Peterson, *Can. J. Chem.*, **54**, 2710 (1976).
14. A. P. Marchenko, A.M. Pinchuk, N.G. Feshchenko, *J. General Chem. USSR*, **43**, 1900 (1973) (Engl. 1887) *Russian Journal of General Chemistry*.
15. Phosphorus-31 NMR Spectroscopy in Stereochemical analysis, J.G. Verkade, L.D. Quin Ed (1987).
16. D.P. Pienaar, T.A. Modro, A.M. Modro, *Synthesis*, 1315 (2000).
17. V. Prelog and G.J. Driza, *Coll. Czech. Chem. Commun.*, **5**, 497 (1933).
18. S. Laurens, V. Ichharam, T.A. Modro, *Heteroatom Chem.*, **12 (5)**, 327 (2001).
19. I.M. Aladzheva, D.I. Lobanov, O. V. Bykhovskaya, P. V. Petrovskii, T.A. Mastriukova, *Doklady Chemistry (Translation of the chemistry section of Doklady Akademii Nauk)*, **30-32**, 3881 (2003).
20. J. Rahil, P. Haake, *J. Am. Chem. Soc.*, **103**, 1723 (1981).
21. F.W. McLafferty, *Interpretation of Mass Spectra*, 3rd ed.; University Science Books: Mill Valley, 1980.
22. K. Sasse in *Organische Phosphor-Verbindungen*; Thieme: Stuttgart, 1964; part 2, pp 597, 668-670, 784.
23. R.G. Cooks, A.F. Gerrard, *J. Chem. Soc. B*, 1327 (1968).
24. R.G. Gillis, J.L. Occoclowitz in *Analytical Chemistry of Phosphorus Compounds*, Ed. M. Halmann (1972).
25. J. Omelanczuk, M. Mikolajczyk, *Tetrahedron Lett.*, **25**, 2493 (1984).
26. J. Omelanczuk, M. Mikolajczyk, *J. Am. Chem. Soc.*, **101**, 7292 (1979).
27. H. Wan, T.A. Modro, *Synthesis*, 1227, (1996).

CHAPTER 4

4. STRUCTURAL ANALYSIS

4.1 NMR Analysis

4.1.1 Introduction

The bicyclic system **11a** as well as its phosphoryl analogue **3a** showed similar and interesting ^1H NMR spectra (**Figure 4.2 and 4.3**), with one distinct difference in the aliphatic region.

There is high non-equivalency of the individual hydrogen atoms of the ring methylene protons. This suggest a high degree of rigidity on the NMR time scale which made it possible to compare dihedral angles determined from solution state NMR with those of X-ray diffraction data.

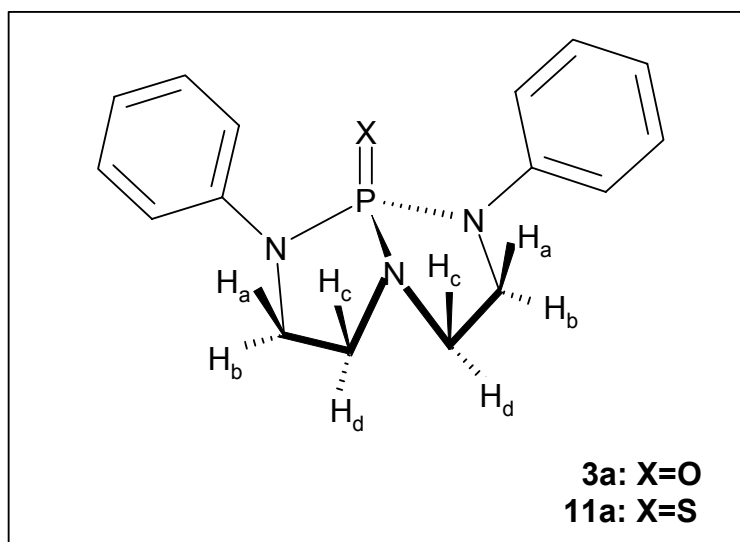


Figure 4. 1 Orientation of the methylene ring protons in **3a**, **11a**.

In the ^1H NMR spectrum of bicyclic compound **3a** only four sets of multiplets for the eight aliphatic hydrogens were observed. For the aliphatic protons of these compounds there is a dramatic separation into low-field and high-field spectral regions. The appearance of four sets of multiplets is due to the molecular plane

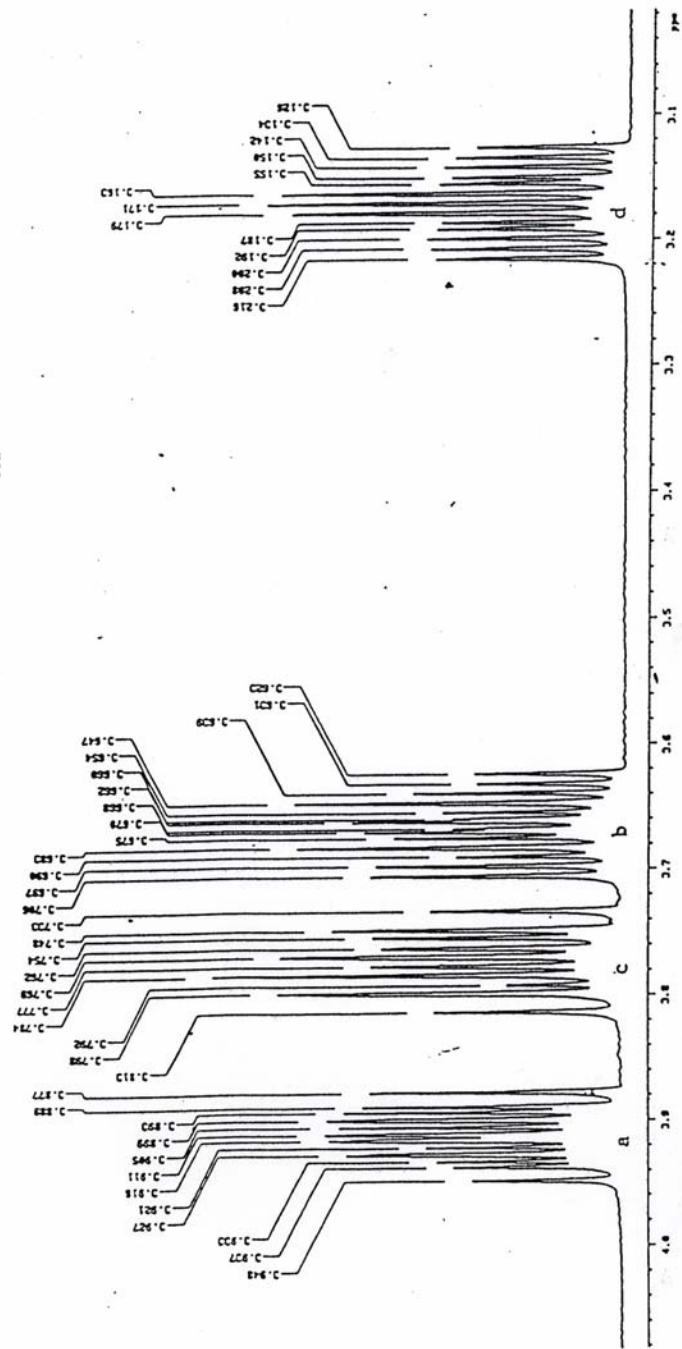


Figure 4. 2 ¹H NMR spectrum of P=O bicyclic compound, **3a**.

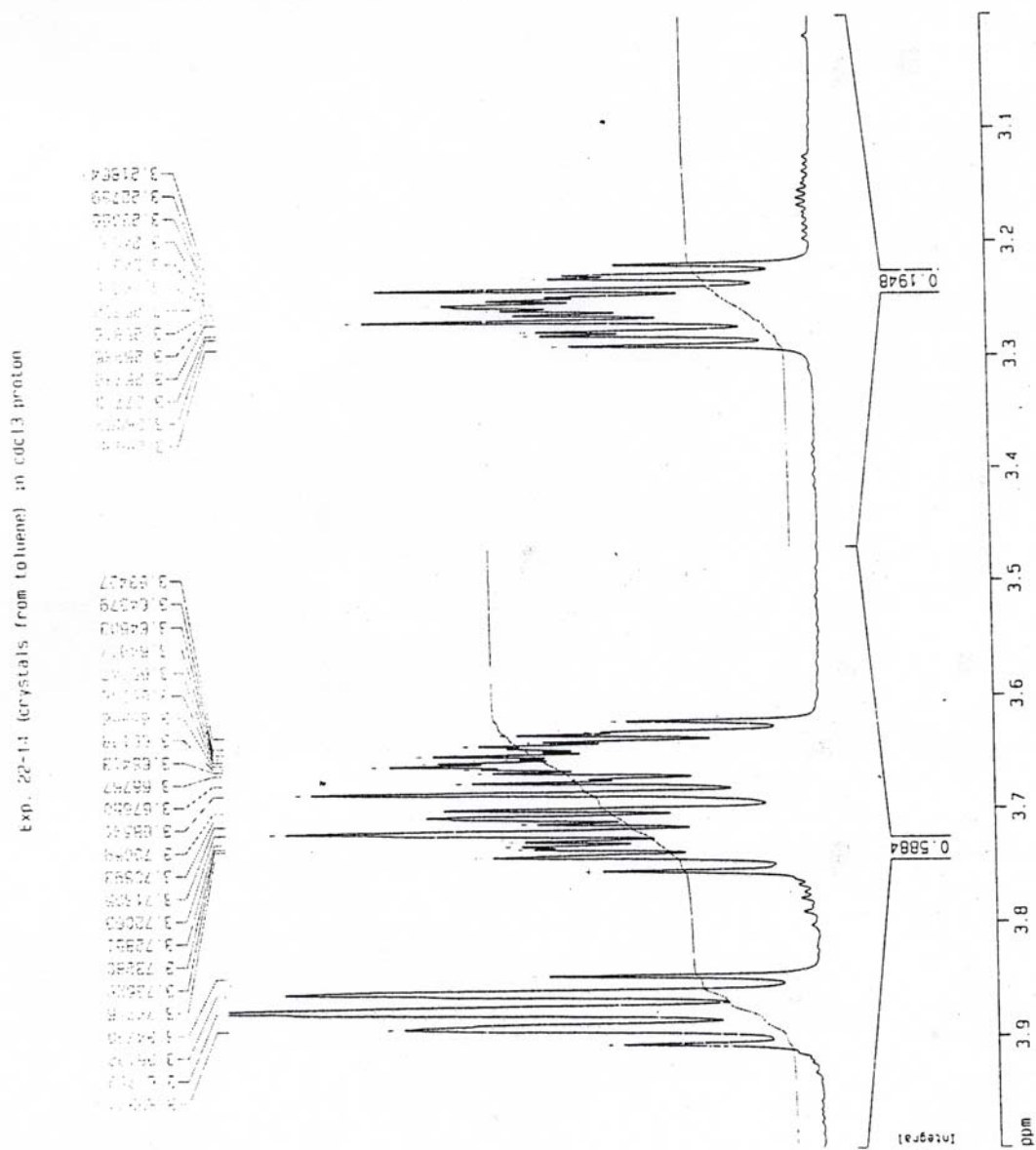


Figure 4. 3 ¹H NMR spectrum of P=S bicyclic compound, **11a**.

of symmetry. The plane of symmetry divides the protons into two groups of four protons of the vicinal system, which gives an ABCDX spin system, where X represents the ^{31}P nucleus. The existence of only one ABCDX splitting pattern in the aliphatic region, i.e. the two $\text{N-CH}_2\text{-CH}_2\text{-N}$ moieties, suggests that the two halves of the molecule are equivalent in terms of the NMR time scale.

Conformational equilibria and other dynamic processes influence the coupling constants of many molecules. The observed data are then average values that are formed on the basis of the mole fractions p , from the data of the individual conformers. In the simplest case of an equilibrium between two conformers A and B, **Equation 4.1** holds.

$$J_{\text{exp}} = p_A J_A + p_B J_B \qquad \text{Equation 4. 1}$$

Vicinal proton-proton couplings in saturated compounds have been studied extensively both experimentally and theoretically. Coupling constants, which are frequency difference in Hertz (Hz) between multiplets, unlike chemical shifts, are not affected or dependent on the strength of the magnetic field. It has been shown that the sign of $^3J_{\text{HH}}$ is always positive and the magnitude depends basically on four factors.

- i) dihedral bond angles
- ii) electronegativity of the substituents on the H-C-C-H moiety
- iii) bond length between the two carbon atoms bearing the protons
- iv) H-C-C valence angles, θ .

One of the most important factors that affect vicinal coupling relationships is the dihedral angle¹. Valence bond theory has been of great success in qualitatively describing trends in $^3J_{\text{HH}}$. The dihedral angle (torsion angle) can be defined as the angle of rotation about a carbon-carbon bond viewed end on with lower numbered carbon nearest to the viewer and hydrogen eclipsed; a clockwise rotation of the carbon farthest away corresponds to a positive dihedral angle. The dependence of

the coupling constant on dihedral angle can be approximately determined by the theoretically derived Karplus equation² as in **equations 4.2** and **4.3** and some of its variations. By employing an appropriate set of parameters, the Karplus equation can be used to describe some of the heterocyclic system conformations in terms of the dihedral angles. Normally the sign of the coupling constant has no effect on the appearance of the NMR spectra³ and therefore has no effect on the Karplus equation:

$${}^3J_{\text{HH}} = 8.5 \cos^2 \theta - 0.28 \text{ for } \theta = 0^\circ - 90^\circ \quad \text{Equation 4. 2}$$

$${}^3J_{\text{HH}} = 9.5 \cos^2 \theta - 0.28 \text{ for } \theta = 90^\circ - 180^\circ \quad \text{Equation 4. 3}$$

where the value of theta (θ) is the dihedral angle.

The relationship between the dihedral angle and vicinal coupling constant is of particular importance in the stereochemistry of groups attached to cyclic systems, e.g. triterpenoids, steroids, etc. In cyclohexane ring, the hydrogens are axial or equatorial, forming with their neighbours a dihedral angle of 60° or 180° , thus rendering the application of the Karplus equation and some of its variations a straightforward procedure to find out the stereochemistry of the products through coupling constant between vicinal hydrogens, which could otherwise not be determined easily.

Since the dihedral angle is the largest when the vicinal protons are diaxial with respect to one another, the coupling constant are accordingly larger, but when the vicinal protons are in an axial equatorial or equatorial-equatorial relationship, the dihedral angle is about 60 degrees or less and the coupling constant are correspondingly smaller⁴.

An estimation of coupling constant of dihedral angles constant by Karplus equation does not necessarily end up with only saturated systems, but also in olefins, where a modified Karplus equation predicts larger trans-coupling than cis-coupling.

One more factor that influences the determination of 3J is the presence of a heteronuclear atom that has a magnetic nucleus. The presence of the heteronuclear atom in the organic molecule can introduce additional signals in the spectrum, since this nucleus will take up spin with respect to the applied field in the same way a neighbouring proton does. Vicinal heteronuclear coupling constants also depend on the dihedral angles. Karplus-like curves have been developed for $^3J_{(\text{HCOP})}$ and $^3J_{(\text{NCCH})}$. In molecules where non-bonding electrons are localized in a specific direction, as in some nitrogen and phosphorus containing compounds, geminal couplings are also dependant on the angular orientation.

The Karplus equation is not limited to the conformation analysis of six-membered ring heterocyclic systems but to a large number of five-membered ring phosphorus heterocyclic systems which have also been analyzed by NMR techniques. The Karplus equation can be applied to confirm the conformation and configuration of heterocyclic systems since the coupling is transmitted through nitrogen (also oxygen and sulphur) provided that no exchange of protons attached to the heteroatom occurs.

The complexities of the structural analysis of the five-membered phosphorus heterocycles is the question of planarity or pyramidality of the nitrogens in the PNR moiety. The 1,2,3-dioxaphospholanes, 2-oxo and 2-thio-1,2,3-oxazaphosphorinane⁵ systems are examples of compounds which follow a similar Karplus-like relationship.

The most stable conformations of cyclopentane are the envelope and the half-chair. The implications in the conformational analysis of cyclopentanes are the barriers between the two conformations which make it impossible to freeze out to individual conformers. It is for this reason that cyclopentanes and heterocyclopentanes are totally different from cyclohexane derivatives in which their chair conformation is located in a deep energy valley. In cyclopentane there is little if any energy difference between the envelope and the half-chair. The molecule is

thus in rapid state of conformational flux through conformational interchange. Internal substitution of the five-member ring with a heteroatom seems to introduce a small energy barrier in the conformational circuit. A few studies on heterocyclic five-membered rings have been reviewed by Fuschs and Riddel.^{6,7} Both oxygen and nitrogen-containing rings, like cyclopentane itself, seem to interchange conformations freely. Equilibrium and NMR studies have been carried out for 2,4 disubstituted and 2,4,5-trisubstituted-1,3-dioxolanes⁸.

For cyclobutane and cyclopentane derivatives, because of their great flexibility, the dihedral angles are less well defined and an unambiguous assignment of the configuration on the basis of the 3J values is, in general, not possible.

The proton-proton coupling constants of a rigid system can be determined from the solution state NMR spectrum and used to calculate the dihedral angles with the Karplus⁹ equation.

4.1.2 Experimental

A study was already conducted on **3a**¹⁰ to calculate the dihedral angles from the coupling constants. A similar study was done on the thiophosphoryl analogue **11a** in order to compare the structures of the two systems in terms of NMR data as well as X-ray diffraction data.

Full ^1H , ^{13}C and ^{31}P NMR assignments were made for the two bicyclic systems. The ^1H NMR spectrum of **3a** is of first order (chemical shifts are large compared to the coupling constants) and therefore relatively easy to calculate the coupling constants and make assignments to the different protons. The spectrum of **11a** is of second order (the chemical shifts are of the same magnitude as the coupling constants). This type of spectrum is much more complicated to analyze because the chemical shifts and coupling constants can no longer both be measured directly from the spectrum. It was therefore necessary to do a complete analysis of the system¹¹.

4.1.3 Results and Discussion

On the NMR scale the molecules under consideration are symmetrical and have a highly rigid conformation due to the two fused five-membered rings. Our results indicated that the molecules are flexible to a great extent and that numerous conformations of a stable molecule is possible in these cases.

The dihedral angles obtained from single crystal XRD results reported in the next section, as well as the calculated dihedral angles are listed in **table 4.1**. From the crystal structures it is clear that the two halves (two five-membered rings) of the molecules **3a** and **11a** are remarkably different as far as the dihedral angles are concerned. There is a remarkable difference in the vicinal proton orientation for each ring. The NMR data represent an average of the two rings, so they appear identical on the NMR-scale.

Our results indicate that the method of comparing the dihedral angles determined from NMR data using the Karplus equation with the dihedral angles from x-ray diffraction data is in this case very approximate. There is very little correlation between the experimental and the calculated dihedral angles for compounds **3a** and **11a**.

		P=O			P=S		
Bond		J value (Hz)	Dihedral angle (θ) XRD	Dihedral angle (θ) Calc	J value (Hz)	Dihedral angle (θ) XRD	Dihedral angle (θ) Calc
J _{a-b} *	gem	11.8	-	-	11.35	-	-
J _{c-d} *	gem	9.3	-	-	-9.31	-	-
J _{a-c} *	cis	6.3	37.6	49.5	4.72	33.8	39.7
J _{a-d} *	trans	6.2	157.5	145.7	6.22	-86.0	146.2
J _{b-c} *	trans	3.3	83.4	145.7	6.22	154.2	145.7
J _{b-d} *	cis	3.3	36.4	49.5	7.32	34.4	19.4

Table 4.1 Experimental (from both NMR and single crystal XRD data) and calculated values for dihedral angles for the bicyclic compounds **3a** and **11a**. *The subscripts a,b,c,d refers to the atomic labels in Fig. 4.1 on page 71.

Coupling constants should be integrated over the whole rotation circuit of the molecules rather than just summed over the most stable conformation. A wide range of coupling constants arise from the different conformations of the systems under investigation, but only one set of coupling constants were used to calculate the dihedral angles. Therefore an average value of the dihedral angles which resulted from our NMR data is not in agreement with the observed crystal structure.

As the NMR data arise from molecules in solution state and single crystal XRD data arise from molecules in the solid state it is expected that the results may be different.

4.2 Crystal Structure Analysis

4.2.1 Introduction

*I held them in every light. I turned
them in every attitude, I surveyed
their characteristics. I dwelt upon
their peculiarities. I pondered upon
their conformation.*

*- Edgar Allan Poe**

Any aspect of science which depends upon a knowledge of the atomic positions in a molecule can profitably make use of X-ray crystallography. Where crystals of known chemical composition have been obtained, single crystal X-ray diffraction can be used to obtain their molecular structure. X-ray diffraction can derive precise structural information of the molecule, atom by atom as well as where the atoms are positioned in relation to each other. In the best cases X-ray diffraction is equivalent to taking a three dimensional photograph of the molecule.

* Edgar Allan Poe (1809 – 1849) was an American poet and writer.

The inherent periodicity of a crystal makes it possible to be used as a diffraction grating for an X-ray beam of wavelength comparable to interatomic distances. X-rays most commonly used for X-ray crystallography is between 0.5 and 2.5 Å.¹²

The magnitude of the interatomic distances involved in organic molecules is typically 1.54 Å for a C-C single bond.

The solution of a crystal structure depends upon recombining the diffracted X-rays to synthesize an image of the molecular structure by Fourier Transformation. A crystal structure is considered solved when it is possible to construct, from the diffraction data, a three dimensional electron density map showing the contents of the unit cell. The unit cell is the building block of the crystal lattice.

The crystal structures of the *N*-aryl substituted phosphoryl derivatives were available from previous studies, so it was possible to compare the structural features of some of the phosphoryl and thiophosphoryl analogues.

4.2.2 Experimental

The crystal structures of compounds **0** , **8** , **1f** and **11a** were determined.

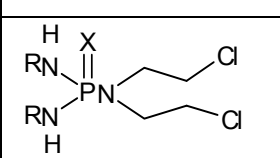
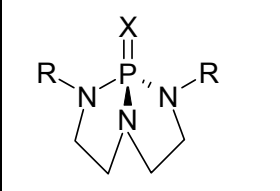
"username" of compound	Number of compound	Structure
Substrate	<u>0</u> X=O <u>8</u> X=S	$\text{Cl}_2\text{P}(\text{X})(\text{NCH}_2\text{CH}_2\text{Cl})_2$
Triamidate	<u>1f</u> X=O, R=Bz	
Bicyclic	<u>11a</u> X=S, R=Ph	

Figure 4. 4 Triamidates for which crystal structures were determined.

Crystallographic data acquisition and refinement details of compounds **0**, **8**, **1f**, **11a** are listed in **table 4.2**.

	0	8	1f	11a
Empirical formula	C ₄ H ₈ NPOCl ₂	C ₄ H ₈ NPSCl ₂	C ₁₈ H ₂₃ N ₃ O ₁ P ₁ Cl ₂	C ₁₆ H ₁₈ N ₃ PS
Molecular weight	258.9	275.0	399	315.36
Crystal dimension,		0.48 x 0.36 x 0.28	0.48 x 0.57 x 0.62	0.55 x 0.42 x 0.26
	Monoclinic	Monoclinic		Triclinic
Space group	P2 ₁ /c	P2 ₁ /c	P2 ₁ /n	P-1
Cell dimensions:				
a, Å	9.088(3)	13.2840	9.369(4)	8.2311(14)
b, Å	8.492(3)	5.9693	9.866(2)	10.4883(18)
c, Å	13.129(4)	14.1940	21.479(6)	10.6538(9)
α, °	90.00	90.000	90.000	115.417(11)
β, °	101.238(6)	104.024	94.85(3)	91.825(10)
γ, °	90.000	90.000	90.000	105.479(14)
Z	4	4	4	2
Volume, Å ³	993.8(5)	1092.0(4)	1978.2	789.2(2)
D (cal), g.cm ⁻¹	1.730	1.67	1.34	1.327
μ, cm ⁻¹			3.68	0.303
Radiation (λ, Å)	0.71073	0.71073	0.7107	0.71073
T, °C	293(2)		295	293(2) K
F(000)	520.0	552.00	824	332
Scan Range (θ°)		3 ≤ θ ≤ 30.05	3 ≤ θ ≤ 30	2.15to29.96
Zone collected:				
H	-7:12	-18:18	-13:13	-11:11
K	-11:11	-6:7	-13:0	-14:14
L	-17:17	-16:17	0:30	-14:14
Reflections collected		7213	6198	9131
Unique reflections used (> 3 σ(I))	2462	2679	3345	3558
R _{int}	0.0317	0.0178	0.0880	0.0880
Parameters refined	133	133	233	
Max. positional shift/esd	0.002	15.000	0.011	0.390
Residual electron density (eÅ ⁻³):				
Maximum	0.296	0.474	0.87	0.390
Minimum	-0.414	-0.295	-0.52	-0.276
U _{iso} (H), Å ²			0.090(4)	
R	0.0345	0.0331	0.0787	0.0397
wR ²	0.0955	0.0830	0.0514	0.1093

Table 4.2 Crystallographic data acquisition and refinement details of compound **0**, **8**, **1f**, **11a**.

PO triamidate, 1f (PhCH₂NH)₂P(O) N(CH₂CH₂Cl)₂

All diffraction measurements were obtained at room temperature and the data were collected on an Enraf Nonius CAD4 diffractometer with MoK α radiation. Accurate unit cell parameters were obtained by least squares methods from the position of 25 centered reflections for each crystal. Data were corrected for Lorentz and polarization effects and absorption corrections were applied.¹³ Intensity checks were carried out every second hour and an orientation control every 400 reflections. Three standard reflections were used to check orientation and crystal stability at regular intervals, and the decay during data collection was 4.1% (corrected). The structure was solved by direct methods.^{14, 15} Refinement was by full matrix least squares methods, using $\sigma^2(F_{\text{obs}})$ weights¹⁵. All the non-hydrogen atoms were refined anisotropically. All hydrogen atoms, except the experimentally located and refined H10 and H18, were placed in calculated positions and were included in the refinement with common isotropic thermal parameters. Atomic scattering factors were taken from the literature.¹⁶ A perspective view of the molecule, prepared with ORTEP¹⁷, is represented in **Figure 4.5**.

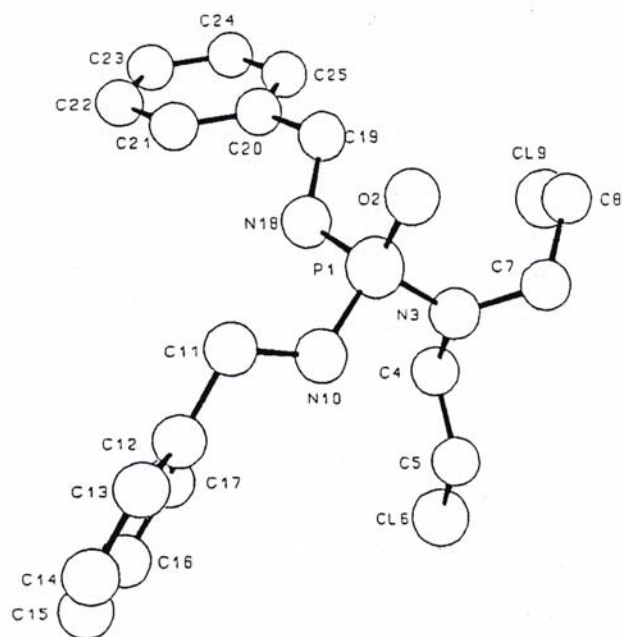


Figure 4.5 ORTEP drawing of 1f.

Atom	x/c	y/c	z/c	U_{eq} $=1/3 \sum_i \sum_j U_{ij} a_i^* a_j(a_i \cdot a_j)$
P(1)	3156(1)	7519(1)	2384(1)	33(1)
O(2)	3423(3)	6142(3)	2646(1)	44(1)
N(3)	4650(3)	8107(3)	2131(2)	37(1)
C(4)	4734(5)	9521(4)	1908(2)	43(1)
C(5)	4766(6)	9579(4)	1224(2)	63(1)
Cl(6)	5019(2)	11288(1)	985(1)	76(1)
C(7)	5977(4)	7335(5)	2212(2)	49(1)
C(8)	6731(5)	7329(5)	2857(3)	76(2)
Cl(9)	7232(2)	8951(2)	3157(1)	104(1)
N(10)	1990(4)	7716(4)	1782(2)	40(1)
C(11)	447(4)	7489(5)	1810(2)	57(1)
C(12)	-419(5)	8124(5)	1267(2)	47(1)
C(13)	-1325(5)	7419(6)	869(2)	57(1)
C(14)	-2120(6)	7992(6)	375(3)	67(2)
C(15)	-1941(7)	9386(7)	276(3)	90(2)
C(16)	-1040(7)	10097(6)	671(3)	97(2)
C(17)	-287(6)	9521(6)	1151(3)	72(2)
N(18)	2540(3)	8534(3)	2897(2)	34(1)
C(19)	3110(5)	8452(4)	3541(2)	46(1)
C(20)	2476(5)	9517(4)	3948(2)	39(1)
C(21)	1019(5)	9780(4)	3875(2)	48(1)
C(22)	473(7)	10765(5)	4265(3)	74(2)
C(23)	1353(8)	11402(6)	4716(3)	87(2)
C(24)	2779(7)	11114(6)	4776(3)	81(2)
C(25)	3359(6)	10150(5)	4404(2)	59(1)

Table 4. 3 Fractional atomic coordinates ($\times 10^4$) and equivalent thermal factors ($\times 10^3 \text{ \AA}^2$) for **1f**.

Atom	x/c	y/c	z/c	U_{eq} $=1/3 \sum_i \sum_j U_{ij} a_i^* a_j(a_i \cdot a_j)$
H(4A)	5696(5)	9984(4)	2124(2)	90(4)
H(4B)	3810(5)	10073(4)	2039(2)	90(4)
H(5A)	5637(6)	8961(4)	1085(2)	90(4)
H(5B)	3765(6)	9201(4)	1004(2)	90(4)
H(7A)	5732(4)	6297(5)	2084(2)	90(4)
H(7B)	6705(4)	7752(5)	1898(2)	90(4)
H(8A)	6027(5)	6868(5)	3170(3)	90(4)
H(8B)	7690(5)	6724(5)	2847(3)	90(4)
H(10)	2252(56)	7472(55)	1504(22)	90(4)
H(11A)	243(4)	6412(5)	1807(2)	90(4)
H(11B)	122(4)	7924(5)	2238(2)	90(4)
H(13)	-1430(5)	6342(6)	944(2)	90(4)
H(14)	-2855(6)	7396(6)	72(3)	90(4)
H(15)	-2524(7)	9884(7)	-115(3)	90(4)
H(16)	-926(7)	11173(6)	597(3)	90(4)

H(17)	434(6)	10128(6)	1454(3)	90(4)
H(18)	1852(47)	9099(46)	2766(22)	90(4)
H(19A)	2876(5)	7460(4)	3719(2)	90(4)
H(19B)	4256(5)	8593(4)	3562(2)	90(4)
H(21)	325(5)	9247(4)	3530(2)	90(4)
H(22)	-651(7)	11022(5)	4209(3)	90(4)
H(23)	916(8)	12132(6)	5023(3)	90(4)
H(24)	3471(7)	11648(6)	5121(3)	90(4)
H(25)	4484(6)	9897(5)	4470(2)	90(4)

Table 4. 4 Coordinates of the hydrogen atoms ($\times 10^4$) and isotropic thermal factors ($\times 10^3 \text{ \AA}$) for **1f**

PS Bicyclic, 11a

The data were collected on an Enraf-Nonius CAD4 diffractometer using Mo K_{α} radiation and an ω - 2θ scan. The structure was solved by direct methods using SHELX97-2¹⁸ in conjunction with WinGX¹⁹. Hydrogen atoms were introduced in calculated positions using the SHELX instruction HFIX 44 for the aromatic hydrogens and HFIX 24 for the hydrogens on the secondary carbon atoms. A drawing of **11a**²⁰ prepared using Platon is presented in **Figure 4.6**.

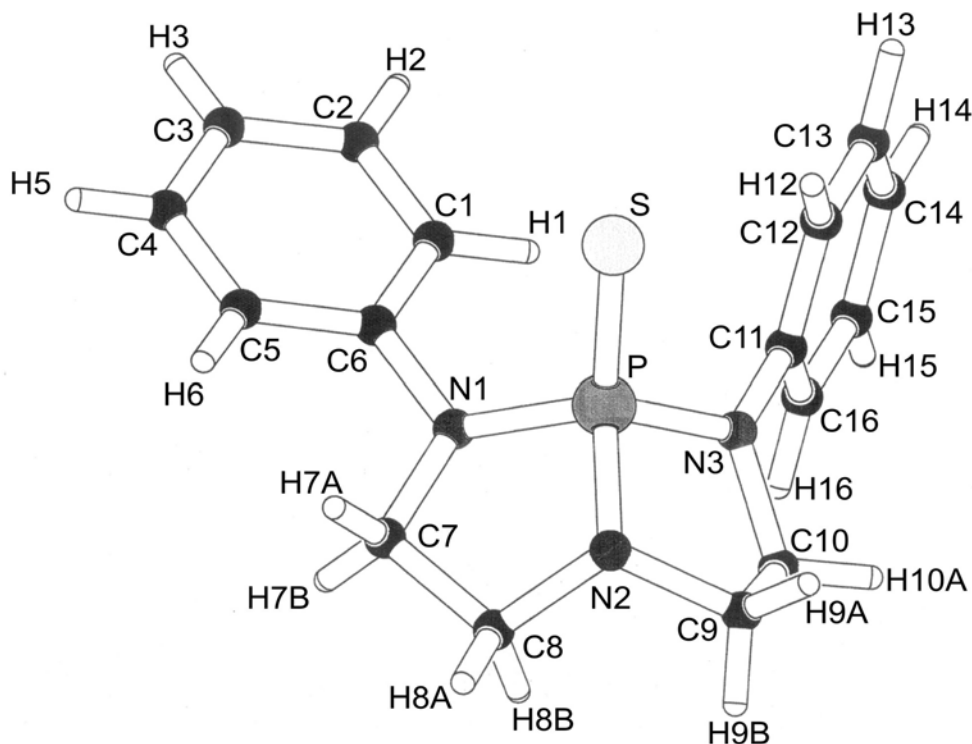


Figure 4.6 Platon drawing of **11a**.

Atom	X/c	y/c	z/c	U_{eq} $=1/3 \sum_i \sum_j U_{ij} a_i^* a_j (a_i \cdot a_j)$
P	8741(1)	7652(1)	685(1)	36(1)
S	10949(1)	8411(1)	1849(1)	49(1)
N(3)	7750(2)	8920(1)	972(1)	40(1)
N(1)	7516(2)	6042(1)	600(1)	42(1)
N(2)	8551(2)	7040(1)	-1061(1)	48(1)
C(11)	7320(2)	9837(1)	2270(1)	38(1)
C(4)	7502(2)	5726(2)	1772(2)	41(1)
C(16)	8556(2)	10752(2)	3464(2)	50(1)
C(10)	6913(3)	8744(2)	-363(2)	57(1)
C(12)	5642(2)	9841(2)	2349(2)	53(1)
C(5)	7222(2)	6734(2)	3046(2)	49(1)
C(14)	6439(3)	11625(2)	4781(2)	61(1)
C(7)	7330(3)	4834(2)	-820(2)	58(1)
C(3)	7712(3)	4418(2)	1662(2)	57(1)
C(15)	8101(2)	11628(2)	4712(2)	58(1)
C(8)	7375(3)	5514(2)	-1805(2)	67(1)
C(9)	8044(3)	8117(2)	-1405(2)	60(1)
C(1)	7355(3)	5118(3)	4067(2)	74(1)
C(6)	7157(3)	6425(2)	4185(2)	62(1)
C(2)	7637(3)	4125(2)	2816(2)	73(1)
C(13)	5217(3)	10731(2)	3594(2)	68(1)

Table 4. 5 Fractional atomic coordinates ($\times 10^4$) and equivalent thermal factors ($\times 10^3 \text{ \AA}^2$) for **11a**.

Atom	x/c	y/c	z/c	U_{eq} $=1/3 \sum_i \sum_j U_{ij} a_i^* a_j (a_i \cdot a_j)$
H(16)	9750(30)	10779(2)	3426(2)	59
H(10A)	6880(3)	9652(14)	-290(2)	69
H(10B)	5806(18)	8092(10)	-625(4)	69
H(12)	4754(19)	9205(14)	1514(18)	64
H(5)	7072(4)	7653(19)	3137(3)	58
H(14)	6134(8)	12241(15)	5650(20)	73
H(7A)	6278(16)	4070(12)	-1043(4)	69
H(7B)	8238(14)	4422(7)	-883(2)	69
H(3)	7891(5)	3784(16)	880(20)	68
H(15)	8980(20)	12260(14)	5558(19)	69
H(8A)	7780(7)	4938(10)	-2670(15)	80
H(8B)	6220(19)	5523(2)	-2072(5)	80
H(9A)	7439(10)	7639(8)	-2339(15)	72
H(9B)	9023(16)	8886(13)	-1324(2)	72
H(1)	7300(4)	4921(6)	4790(20)	88
H(6)	6978(5)	7102(17)	5030(20)	75
H(2)	7778(5)	3250(20)	2739(3)	87
H(13)	3950(30)	10728(2)	3636(3)	81

Table 4. 6 Coordinates of the hydrogen atoms ($\times 10^4$) and isotropic thermal factors ($\times 10^3 \text{ \AA}^2$) for **11a**.

PO substrate, 0

All diffraction measurements were obtained at room temperature and the data were collected on an Enraf Nonius CAD4 diffractometer with MoK α radiation. Atomic coordinates of compound 0 are listed in **tables 4.7** and **4.8**. A molecular drawing of the crystal structure is shown in **Figure 4.7**.

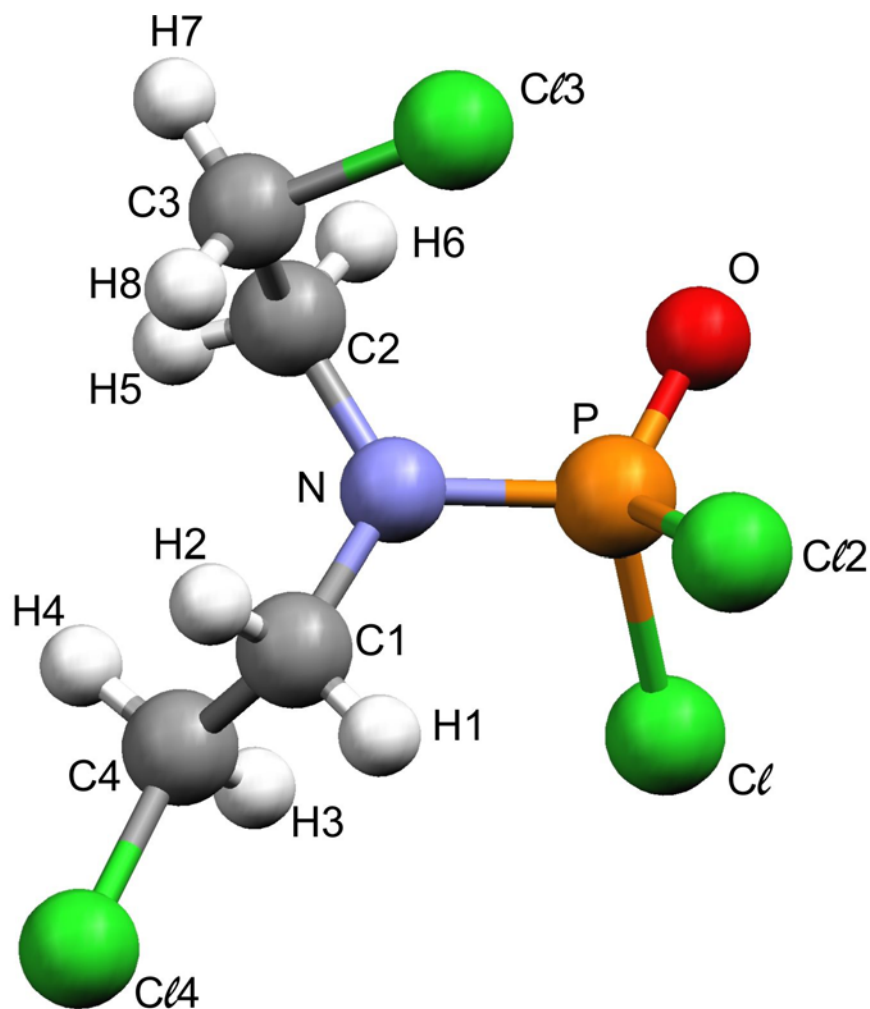


Figure 4.7 Molecular drawing of Cl₂P(O)N(CH₂CH₂Cl)₂, 0

Atom	x/c	y/c	z/c	U_{eq} $=1/3 \sum_i \sum_j U_{ij} a_i^* a_j (a_i \cdot a_j)$
P	2010(1)	1764(1)	4658(0)	38(1)
Cl2	1867(1)	-575(1)	4412(1)	57(1)
Cl	4101(1)	2156(1)	4423(1)	55(1)
Cl3	2703(1)	5643(1)	5590(1)	62(1)
Cl4	3518(1)	-1344(1)	8020(1)	66(1)
N	2019(2)	1993(2)	5882(1)	37(1)
O	875(2)	2633(2)	3939(1)	50(1)
C2	1139(3)	3256(3)	6253(2)	41(1)
C1	3044(3)	1066(3)	6666(2)	39(1)
C3	2026(3)	4713(3)	6621(2)	50(1)
C4	2201(3)	-166(3)	7158(2)	49(1)

Table 4.7 Fractional atomic coordinates ($\times 10^4$) and equivalent thermal factors ($\times 10^3 \text{ \AA}^2$) for **0**.

Atom	x/c	y/c	z/c	U_{eq} $=1/3 \sum_i \sum_j U_{ij} a_i^* a_j (a_i \cdot a_j)$
H1	3754(30)	5459(29)	6347(20)	49(7)
H2	3487(32)	1772(32)	7195(21)	58(8)
H3	1677(32)	-848(31)	6658(21)	55(8)
H4	1439(33)	311(32)	7536(23)	62(8)
H5	696(27)	2885(27)	6805(19)	41(6)
H6	275(30)	3511(3)	5690(2)	51(7)
H7	1328(30)	5488(31)	6861(20)	54(7)
H8	2923(32)	4463(30)	7153(22)	56(8)

Table 4.8 Coordinates of the hydrogen atoms ($\times 10^4$) and isotropic thermal factors ($\times 10^3 \text{ \AA}^2$) for **0**.

PS substrate, 8

All diffraction measurements were obtained at room temperature and the data were collected on an Enraf Nonius CAD4 diffractometer with MoK α radiation. Atomic coordinates of compound **8** are listed in **tables 4.9** and **4.10**. A molecular drawing of the crystal structure is shown in **Figure 4.8**.

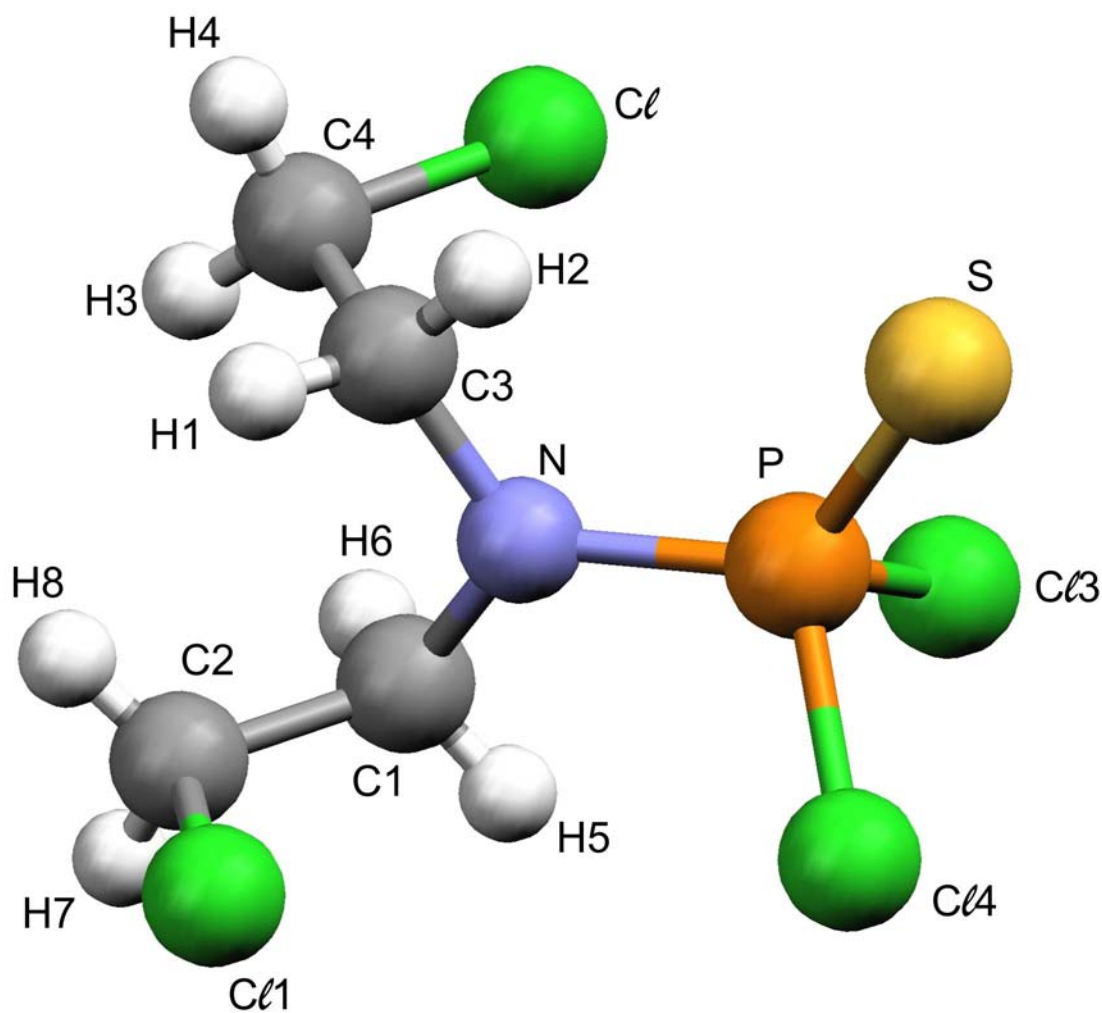


Figure 4.8 Molecular drawing of Cl₂P(S)N(CH₂CH₂Cl)₂, **8**

Atom	x/c	y/c	z/c	U_{eq} $=1/3 \sum_i \sum_j U_{ij} a_i^* a_j(a_i \cdot a_j)$
P	2658(5)	1065(11)	1541(5)	43(19)
Cl	593(6)	2798(15)	-632(7)	74(3)
Cl1	4240(6)	2796(13)	-49(7)	64(2)
Cl3	4059(6)	441(16)	2265(6)	69(3)
Cl4	2712(9)	4450(13)	1495(7)	79(3)
N	2534(14)	214(3)	352(15)	39(4)
S	1768(6)	-44(14)	2288(6)	58(2)
C2	3567(2)	-699(5)	-870(2)	50(6)
C1	3189(19)	1089(5)	-267(2)	44(5)
C3	1673(18)	-1025(5)	-202(2)	45(6)
C4	1020(20)	260(6)	-1078(2)	57(7)

Table 4.9 Fractional atomic coordinates ($\times 10^4$) and equivalent thermal factors ($\times 10^3 \text{ \AA}^2$) for **8**.

Atom	x/c	y/c	z/c	U_{eq} $=1/3 \sum_i \sum_j U_{ij} a_i^* a_j(a_i \cdot a_j)$
H1	1860(20)	-234(5)	490(2)	49(8)
H2	1330(20)	-1460(5)	285(19)	39(7)
H6	2860(20)	2150(50)	-780(20)	47(7)
H5	3700(20)	1820(50)	180(20)	45(7)
H8	3090(20)	-1410(60)	-1360(2)	52(9)
H3	1330(30)	710(60)	-1660(30)	60(10)
H7	4010(20)	20(50)	-1220(20)	51(7)
H4	480(30)	-570(60)	-1320(30)	71(10)

Table 4.10 Coordinates of the hydrogen atoms ($\times 10^4$) and isotropic thermal factors ($\times 10^3 \text{ \AA}$) for **8**

4.2.3 Results and Discussion

The ^1H NMR spectra of the two substrates, compounds **0** and **8** were very similar which indicated comparable geometries/conformation in solution state for the two compounds. However the chemical reactivities are very different. The phosphoryl compound is moderately reactive and undergo nucleophilic displacement at the phosphoryl centre quite easily. The thiophosphoryl analogue is very resistant to nucleophilic attack but not completely resistant. More harsh reaction conditions were necessary to displace the two chlorines at the thiophosphoryl centre. It was expected that a more detailed structural analysis of the two systems, will shed some light on the different chemical reactivities. Selected bond distances, bond angles and torsion angles are listed in **Table 4.11**.

The X-ray diffraction data revealed a few structural differences between the two compounds.

- The nitrogen atom in the thiophosphoryl analogue **8** is comparable with the nitrogen atom in the phosphoryl analogue **0**; both are planar.
- No intramolecular hydrogen bonding; no intermolecular hydrogen bonding.
- The bond angles in the $\text{Cl}_2\text{P}(\text{X})\text{N}$ moieties are slightly different:
- The angle Cl-P-S are slightly smaller than the Cl-P-O bond angle; the S=P-N angle is slightly bigger than the O=P-N bond angle. (We expected a *perfect* tetrahedral geometry for both, but it seems that the sulphur atom is 'bended' away from the mustard moiety);
- The bond angles involving nitrogen are different (C-N-C)
- The torsion angles involving the $\text{Cl}_2\text{P}(\text{X})\text{N}$ moiety are comparable
- The torsion angles of the two chloroethyl chains are different

Compounds **0** and **8** represent comparable geometry, and any differences in chemical reactivity should reflect the difference between the phosphoryl and thiophosphoryl center, and not the different geometries of the compounds.

Bond Distances / Å			
	<u>0</u>		<u>8</u>
P=O	1.4562(17)	P=S	1.8890(10)
P-N(1)	1.6177(19)	P-N(1)	1.7316(22)
P-Cl(2)	2.0126(10)	P-Cl(4)	2.0232(11)
P-Cl	2.0114(10)	P-Cl(3)	1.9318(10)
N(1)-C(1)	1.4740(28)	N(1)-C(3)	1.4276(10)
N(1)-C(2)	1.4753(29)	N(1)-C(1)	1.4733(31)
Bond Angles / °			
Y=P-N(1)	116.68(10)	Y=P-N(1)	121.30(7)
Cl-P-Cl	99.91(4)	Cl-P-Cl	99.96(5)
O-P-Cl(2)	112.37(8)	S-P-Cl(4)	113.55(5)
O-P-Cl	112.84(8)	S-P-Cl(3)	106.65(5)
C(1)-N(1)-C(2)	117.86(18)	C(1)-N(1)-C(3)	111.44(21)
C(1)-N(1)-P	120.64(15)	C(3)-N(1)-P	124.27(17)
C(2)-N(1)-P	121.11(15)	C(1)-N(1)-P	123.10(16)
Torsion Angles / °			
O-P-N-C(1)	175.04(16)	S-P-N-C(3)	11.49(23)
Cl-P-N-C(1)	-56.55(17)	Cl(3)-P-N-C(3)	135.16(19)
Cl(2)-P-N-C(1)	49.57(18)	Cl(4)-P-N-C(3)	-118.77(19)
O-P-N-C(2)	-12.26(21)	S-P-N-C(1)	177.97(16)
Cl-P-N-C(2)	116.14(16)	Cl3-P-N-C(1)	-58.36(20)
Cl(2)-P-N-C(2)	-137.73(16)	Cl(4)-P-N-C(1)	47.72(20)
C(1)-N-C(1)-C(3)	75.26(26)	C(3)-N-C(1)-C(2)	-54.70(28)
P-N-C(2)-C(3)	-97.63(23)	P-N-C(1)-C(2)	137.27(20)
N-C(2)-C(3)-Cl(3)	64.27(25)	N-C(1)-C(2)-Cl(1)	-56.07(26)
C(2)-N-C(1)-C(4)	78.84(26)	C(1)-N-C(3)-C(4)	-53.26(30)
P-N-C(1)-C(4)	-108.23(22)	P-N-C(3)-C(4)	114.60(24)
Cl(4)-C(4)-C(1)-N	175.44(17)	Cl-C(4)-C(3)-N	-56.80(27)

Table 4.11 Selected bond distances, bond angles and torsion angles for 0 and 8. Atomic labels are according to the structures in **Fig 4.7** and **4.8** respectively.

Since the X-ray structure of the bicyclic compound **3a** had been determined before²¹, it was now possible to compare the molecular parameters of the two systems i.e. **3a** and **11a**, closely related bicyclic structures. Selected bond angles and bond distances for both compounds are listed in **Table 4.12**. Selected torsion angles for these compounds are listed in **Table 4.1**.

Bond Lengths /Å					
	3a	11a		3a	11a
P=Y	1.926(2)	1.437(2)	N(2)-C(8)	1.470(2)	1.451(3)
P-N(1)	1.682(2)	1.676(3)	N(2)-C(9)	1.476(2)	1.475(2)
P-N(2)	1.674(3)	1.661(2)	N(3)-C(11)	1.426(2)	1.420(3)
P-N(3)	1.665(3)	1.653(3)	N(3)-C(10)	1.476(2)	1.473(2)
N(1)-C(4)	1.422(2)	1.407(3)	C(7)-C(8)	1.498(3)	1.497(3)
N(1)-C(7)	1.467(2)	1.470(2)	C(9)-C(10)	1.516(3)	1.504(2)
Bond Angles /°					
Y=P-N(1)	113.3(1)	114.4(2)	C(8)-N(2)-P	110.5(1)	109.2(2)
Y=P-N(2)	121.1(1)	121.3(1)	C(9)-N(2)-P	108.2(1)	110.9(1)
Y=P-N(3)	114.2(1)	112.7(1)	C(11)-N(3)-C(10)	119.3(1)	121.2(2)
N(1)-P-N(2)	95.4(1)	96.3(2)	C(11)-N(3)-P	127.6(1)	126.0(1)
N(1)-P-N(3)	114.9(1)	114.4(2)	C(10)-N(3)-P	111.3(1)	111.1(1)
N(2)-P-N(3)	95.8(1)	95.7(1)	N(1)-C(7)-C(8)	106.0(1)	104.5(1)
C(4)-N(1)-C(7)	119.1(1)	120.6(1)	N(2)-C(8)-C(7)	107.3(1)	107.1(1)
C(4)-N(1)-P	122.8(1)	127.4(2)	N(2)-C(9)-C(10)	106.9(1)	109.0(1)
C(7)-N(1)-P	109.6(1)	110.3(1)	N(3)-C(10)-C(9)	103.2(1)	106.3(2)
C(8)-N(2)-C(9)	114.2(1)	115.9(1)			

Table 4. 12 Selected Bond Lengths and Bond Angles for **3a** and **11a**.

It is clear that all parameters that describe the geometry of the 2,5,8-triaza-1 λ^5 -phosphabicyclo[3.3.0]octane system are in both cases approximately the same. The bond distances of the thiophosphoramidate (S=P-N) function does not show any unusual features, with the average P-N bond distance of 1.674 Å, a typical value reported²² for the amides of phosphoric acid. The length of the

thiophosphoryl bond (P=S, 1.926 Å) is also very typical. According to the Cambridge Structural Data Base, the average value of the P=S bond distance in 74 listed compounds of the (N,N',N'')P=S type is 1.929 Å. Compounds **3a** and **11a** represent similar geometry, and any differences in chemical reactivity should therefore reflect the difference between the phosphoryl and thiophosphoryl center, and not the different geometries of the bicyclic skeleton.

Both X-ray diffraction and NMR analysis supported the comparable molecular conformations for systems **3a** and **11a**.

4.3 References

1. D.H. Williams, I. Fleming, *Spectroscopic methods in organic chemistry*, 3rd Edition, McGraw-Hill Book, London, (1980).
2. H. Gunther, *NMR Spectroscopy*, John Wiley and sons, Chichester, 2nd Edition, 115 (1992).
3. L.M. Jackman, S. Sternhell, *Application of Nuclear Magnetic Resonance Spectroscopy in Organic Chemistry*, 2nd Edition, Pergamon Press, Elmsford, New York, 270-277 (1969).
4. Atta-ur-Rahman, *Nuclear Magnetic Resonance*, Springer-Verlag, New York, 82, (1986).
5. J. Nielsen, O. Dahl, *J. Chem. Soc. Perkin Trans.*, 2, 553 (1984).
6. B. Fuchs, *Top. Stereochem.*, 10, 1, (1978).
7. F.G. Riddell, *The Conformational Analysis of Heterocyclic compounds*, Academic, New York (1980).
8. W.E. Willy, G.Binsch, E.L. Eliel, *J. Am. Chem. Soc.*, 92, 5394 (1970).
9. M.J. Karplus, *Amer. Chem. Soc.*, 85, 2870 (1963).
10. R.M. Mampa, M.Sc. Dissertation, *X-ray and NMR Spectroscopic studies of selected Heterocyclic Compounds of Phosphorus and Nitrogen* (2000).
11. F. Scheinmann, *An Introduction to spectroscopic methods for the identification of organic compounds*, Vol.1, First Edition, 23 (1970).
12. A. Guinier, *X-Ray Diffraction*, W.H. Freeman and Company (1963).
13. A.C.T. North, D.C. Phillips, F.S. Matthews, *Acta Crystallogr.*, Sect A, **24**, 351

- (1968).
14. G.M. Sheldrick, SHELX86. *A program for the solution of crystal structures*. University of Göttingen: Göttingen, Germany (1986).
 15. G.M. Sheldrick, SHELX76. *Program for crystal structure determination*. University of Cambridge (1976).
 16. *International tables for X-ray crystallography*, Kynoch press., Birmingham (1974) Volume 4; D. T. Cromer and D. Liberman, *J. Chem. Phys.*, **4**, 1891 (1970).
 17. C.K. Johnson, ORTEP. Report ORNL-3794. Oak Ridge National Laboratory, Tennessee, USA (1965).
 18. G. Sheldrick, SHELXL-97: A program for Crystal Structure Refinement; University of Göttingen: Göttingen, Germany (1997).
 19. L.J. Farrugia, *J. Appl. Cryst.*, **32**, 837 (1999).
 20. S. Laurens, V.V.H. Ichharam, T.A. Modro, *Heteroatom Chemistry*, **12** (5), 327 (2001).
 21. S. Bourne, X.Y. Mbianda, T.A. Modro, L.R. Nassimbeni, H. Wan, *J. Chem. Soc., Perkin Trans. 2*, **83**, (1998).
 22. M.P. du Plessis, T.A. Modro, L.R. Nassimbeni, *J. Org. Chem.* , **47**, 2313 (1982).

CHAPTER 5

5. THEORETICAL CALCULATIONS

5.1 Introduction to Molecular Modeling

The goal of structural chemistry is to derive accurate information of the three-dimensional geometries of molecules. X-ray diffraction of single crystals is a powerful method to determine molecular structures but it does not provide information about individual molecules in unusual environments.

In many cases the morphology of the crystal is not suitable and does not lend itself to X-ray analysis. For many compounds, crystals suitable for X-ray analysis are difficult or impossible to prepare; therefore detailed structural information of these compounds remains unknown. Many of these compounds have been subjected to detailed analysis and the results have served to establish many theoretical concepts in physical chemistry. X-ray analysis of single crystals can be costly and time-consuming. Specialized equipment is involved and the theoretical aspects of X-ray diffraction can be difficult to comprehend. A possible solution to these problems is to extend structural information, already available from X-ray diffractometry, to new structures. Molecular Modeling is a way to address this problem.

Methods used to calculate three-dimensional molecular structures are called Molecular Modeling. Two main approaches are used to calculate molecular structures. One approach involves quantum mechanical calculations and the other, molecular mechanical calculations. Quantum mechanical calculations may require large computer resources and the results may be difficult to interpret. Quantum mechanics describes molecules in terms of interactions among nuclei and electrons, and molecular geometry in terms of minimum energy arrangements of nuclei. All the quantum mechanical methods can ultimately be traced back to the Schrödinger equation¹. For the special case of a hydrogen atom (a single particle in three dimensions), the Schrödinger equation may be solved exactly. Unfortunately, the multiple electron Schrödinger equation cannot be solved exactly even for the simplest multiple

electron system. Approximations need to be introduced to provide practical methods to solve the equation. Quantum mechanics is used to establish equilibrium geometries and conformations and also to supply quantitative thermo chemical and kinetic data^{1,2}.

Molecular mechanical calculations are simpler and the resulting structural parameters may be more reliable than those obtained from quantum mechanical calculations. No one method of calculation is ideal for all applications. Great effort has been directed at finding suitable methods for different applications. Molecular mechanical methods may be applied to molecules containing 1000 or more atoms. Molecular modeling is generally applied to classical coordination complexes of transition metals and metal ions in states of moderate oxidation as well as to organic compounds.

Chemists believe that molecular properties like thermodynamic, kinetic and electronic properties are directly related to molecular structure³. Molecular mechanical calculations are now routinely employed by chemists to establish molecular equilibrium geometries and conformations. Calculations are being used not only to interpret experimental data, but also to supplement limited data or even replace it entirely. The success of any particular model firstly depends on its ability to consistently reproduce experimental data.

The basic principle behind molecular mechanics is the high degree of transferability of geometrical parameters from one molecule to another, as well as the predictable dependence of the parameters on atomic hybridization.

There are numerous methods available to compute molecular structures, but Molecular Mechanics is an approach that can optimize structures with high accuracy and is not as costly in terms of computer resources.

Molecular Mechanics makes use of the bond concept. This appeal to traditional chemist's idea that a molecule is a sum of bonded atoms and that molecular properties can often be written as the sum of contributions from each bond. The chemical bond between a pair of atoms is a function of the

electron density distribution between atoms. In Molecular Mechanics this function is quantified in terms of the two atom types, which usually also define the bond order. Given atom types and bond orders imply a specific equilibrium (ideal) bond distance and a specific force is needed to distort this bond. Steric effects do not affect the bond order.

Molecular Mechanical calculations use the equations of classical mechanics to describe the potential energy surfaces and physical properties of molecules. A molecule is described as a collection of atoms held together by harmonic (elastic) forces. This description is called a force field. One component of a force field is the energy arising from compression and stretching of a bond. This component is often approximated as a harmonic oscillator and can be calculated using Hooke's law. The bond between two atoms is analogous to a spring connecting two masses. Using this analogy, Equation 5.1 gives the potential energy, V_{spring} , of the system as two masses joined by a spring and the force constant of the spring, K_r .

$$V_{\text{spring}} = \frac{1}{2} K_r (r-r_0)^2 \qquad \text{Equation 5. 1}$$

The equilibrium and the displaced distances of the atoms in a bond are r_0 and r . Both K_r and r_0 are constants for a specific pair of atoms connected by a certain spring. K_r and r_0 are force field parameters. The potential energy of a molecular system in a force field is the sum of individual components of the potential, such as bond distance, bond angle and Van der Waals potentials and coulombic interactions. The energies of the individual bonding components (bond distances, bond angles, dihedral angles) are functions of the deviation of a molecule from a hypothetical compound that has bonded interactions at minimum values.

Geometry optimizations find the coordinates of a molecular structure that represent a potential energy minimum. The absolute energy of a molecule in a molecular mechanical calculation has no intrinsic meaning. E_{Total} values are useful only for comparisons between molecules in the same chemical

environment. The relative energies relate to the relative thermodynamic stabilities i.e. the lower the energy, the more stable the compound.

Molecular mechanics cannot describe bond formation, bond breaking or systems in which electronic delocalization or molecular orbital interactions play a major role in determining geometry or properties⁴.

The aim of our molecular mechanical study was to establish the thermodynamic stabilities of the compounds involved in the eight-membered ring to five-membered ring rearrangement⁵ as well as the compounds involved in the thiono-thiolo rearrangement of the thiophosphoric ester⁶.

5.2 Experimental

The group of structurally related phosphoramidates, discussed in the preceding chapters, was further studied by molecular mechanical calculations.

Hyperchem software was used to perform the molecular mechanical calculations. The default force field in Hyperchem is MM+ (Mmplus). MM+ is an extension of MM2 which was developed by Allinger and co-workers.^{7,8,9}

Hyperchem's MM+ force field employs the latest MM2 (1991) parameters and atom types with the 1977 functional form^{7,8,9}.

The MM+ force field internally makes use of ergs for energy and reports its force constants in units of millidynes per Ångstrom. For example, a factor of 71.94 must be multiplied to MM+ stretching force constants for comparison with stretching force constants for the other force fields. Hyperchem reports all energy results in energy units of kcal/mol.

The interaction potential describes both bonding and non-bonding interactions. The interaction potential calculated by MM+ includes energy terms for bond stretching, bond dipoles, angle bending, dihedrals, Van der Waals interactions as well as a bond stretching and angle bending cross term.

A description of how the energetic terms are calculated is included as described in the Hyperchem Manual.

Bond Stretching

MM2 uses a cubic stretch term:

$$E_{\text{bond}} = 143.88 \sum 0.5 K_r (r-r_0)^2 [1 + CS(r-r_0)] \quad \text{Equation 5.2}$$

The cubic stretch term is a factor CS times the quadratic stretch term. This constant CS can be set to an arbitrary value. The default value for MM2 and MM+ is CS = -2.0.

Two r_0 values are given for each MM+ bond, r_0^A and r_0^B . If r_0^B is available (has a non-zero value in the parameter file) then it is used in preference to the normal r_0^A for bonds where atom i and j have at least two hydrogen atoms directly attached to them.

Bond Dipoles

MM+ calculations do not have an electrostatic charge-charge interaction nor define a set of atomic charges for atoms. The electrostatic contributions come from defining a set of bond dipole moments associated with polar bonds. The MM+ dipole is calculated by **Equation 5.3**.

$$E_{\text{dipole}} = 14.39418 \epsilon \sum \mu_i \mu_j [(\cos \chi - 3 \cos \alpha_i \cos \alpha_j) / R_{ij}^3] \quad \text{Equation 5.3}$$

The center of the dipole is defined to be the midpoint of the bond and two dipoles μ_i and μ_j , separated by R_{ij} (**Figure 5.1**).

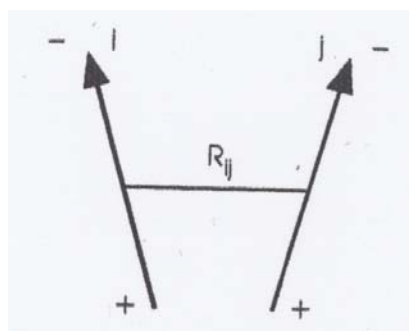


Figure 5.1

Where ϵ is the dielectric constant. Hyperchem uses the MM2 value of 1.5. The angle χ is the angle between the two dipole vectors and α_i and α_j are the angles that the two dipole vectors make with the R_{ij} vector. The constant 14.39418 converts ergs to kcal/mol.

Angle Bending

Equation 5.4 is used for the angle bending energy.

$$E_{\text{bond angle}} = 0.043828 \sum 0.5 K_{\theta} (\theta - \theta_0)^2 [1 + SF (\theta - \theta_0)^4] \quad \text{Equation 5. 4}$$

MM+ includes a sextic angle bending term. This term is a scale factor SF times the quadratic bending term. The constant 0.043828 converts the MM+ bending constants expressed in millidynes-A per radian² to kcal/mol per degree².

Bond Stretch and Angle Bending Cross Term

MM+ includes coupling between bond stretching and angle bending. If the angle is defined to include atoms i , j and k , where k is the central atom, then MM+ couples stretching of the ik and jk bonds with the angle:

$$E_{\text{stretch-bend}} = 2.51118 \sum K_{\text{sb}} (\theta - \theta_0)_{ijk} [(r - r_0)_{ik} + (r - r_0)_{ij}] \quad \text{Equation 5. 5}$$

If atoms i or j is a hydrogen, the deformation is considered to be zero. Thus, no stretch-bend interaction is defined for XH_2 . The stretch-bend force constants are incorporated into the programme and cannot be changed. If R is not a hydrogen, the following values are used for the stretch-bend force constants:

$K_{\text{sb}} = 0.120$ for XR_2 where X is in first long row

$K_{\text{sb}} = 0.090$ for XRH

$K_{\text{sb}} = 0.250$ for XR_2 where X is in second long row

$K_{sb} = -0.400$ for XRH

The constant 2.51118 converts between MM+ stretch-bend force constants expressed in millidynes per radian and Hyperchem's default, kcal per degree.

Out-of-Plane Bending

An sp^2 hybridized atom tends to be co-planar with its attached atoms. This effect is accounted for by improper torsions in other force fields and by out-of-plane-bending interactions in MM+.

Consider the situation illustrated in figure 5.2, involving an atom X that is sp^2 hybridized. Y is the projection of X onto the ABC plane.

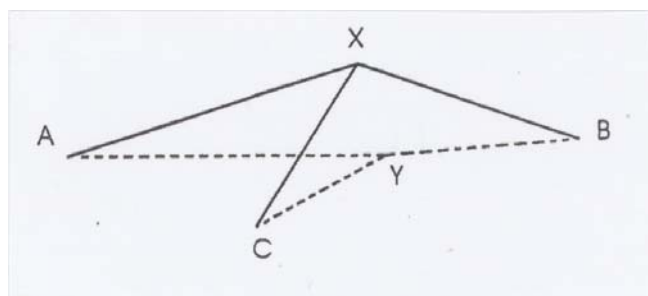


Figure 5. 2

When the central atom (X) is sp^2 hybridized, the angle bending calculations are modified to use the in-plane angles AYB, AYC and BYC in equation 5.4 with the standard force constants rather than the standard angles AXB, AXC and BXC. Out-of-plane components are computed as well, for the out-of-plane angles XAY, XBY and XCY. These last three calculations also use equation 5.4, but with θ_0 equal to 0 and special out-of-plane bending constants, K_θ .

Dihedrals

The dihedral angle or torsional energy interaction in MM+ is of the general form of equation 5.6 but explicitly includes $n=1,2$ and 3 with a phase angle of $\Phi_0 = 0$:

$$E_{\text{dihedral}} = \sum V_n/2 [1 + \cos (n\Phi - \Phi_0)] \quad \text{Equation 5. 6}$$

The MM+ force field uses special values for the torsional force constants when the atoms are in a four-membered ring.

Van der Waals

The MM+ van der Waals interactions do not use a Lennard-Jones potential but combine an exponential repulsion with an attractive $1/R^6$ dispersion interaction. The basic parameters are a van der Waals radius r_i^* for each atom type and a hardness parameter ϵ_i that determines the depth of the attractive well and how easy (or difficult) it is to push atoms close together. There are interactions for each nonbonded ij pair, including all 1-4 pairs. The parameters for a pair are obtained from individual atom parameters as follows:

$$r_{ij}^* = r_i^* + r_j^*$$

$$\epsilon_{ij} = (\epsilon_i \epsilon_j)^{0.5}$$

The van der Waals interaction is then calculated using **Equation 5.7**.

$$E_{\text{van der Waals}} = \sum_{ij \text{vdW}} \epsilon_{ij} (2.9 \times 10^5 \exp(-12.5 \rho_{ij}) - 2.25 \rho_{ij}^{-6}) \quad \text{Equation 5.7}$$

Hyperchem's MM+ does not include parameters for the phosphorous-nitrogen bond in the chemical environment of interest (**Figure 5.3**).

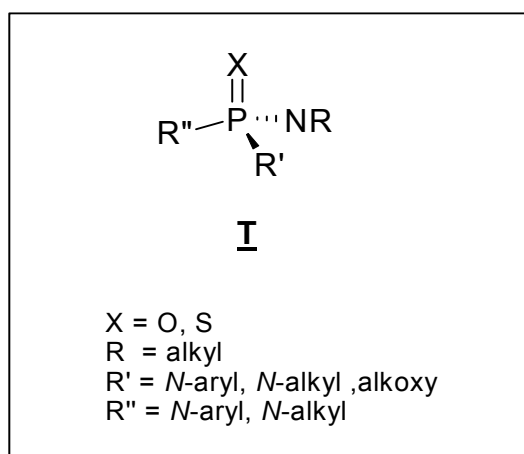


Figure 5.3 General structure of compounds discussed in this chapter.

The new atom types, which were introduced, are listed in **Table 5.6**. Column 3 in **Table 5.6** contains the lines that were added to describe the connectivities of the new atom types. All tables containing the new force field parameters are appended at the end of the chapter.

The geometries of all the compounds were optimized with MM+ using a conjugate gradient algorithm, Polak-Ribiere.

The structural data from the crystal structures were used to set up the new force field. Crystal structures were not available for all the compounds in the series and in such cases the structural data of a structurally closely related compound e.g. PELRED, SACWOI, SACYEA from the Cambridge Database¹⁰ were used.

The energies of a series of phosphoramidates were calculated. All the structures listed in **Table 5.1** were optimized in order to prepare a force field that can be applied to the phosphotriamidates in general.

5.3 Results and Discussion

The MM+ parameter files only included parameters for interactions with lone pairs on sp^3 oxygen (e.g. in alcohol), sp^3 nitrogen (e.g. in tertiary amine), furan oxygen, oxime nitrogen and pyridine nitrogen. No lone pairs were added to sp^2 oxygen, sp^2 nitrogen and sulphur or halogens. This is a matter of great uncertainty and confusion. Numerous authorities¹¹ on the subject of molecular modeling were consulted regarding the treatment of the lone pairs in Hyperchem. All agreed that in principle, the lone pairs should be added, but it seems that Hyperchem treats this differently. Hypercube^a was contacted in this regard with no success.

Structure optimization resulted in exactly the same geometry, regardless of the in- or exclusion of lone pairs to the appropriate atoms, but the calculated energies were completely different. A difference between these two scenarios

^a Company who developed HyperChem software

was expected since many more interactions are involved when lone pairs are added. The size of the electrostatic energy term increases significantly when the lone pairs are included. This is due to the interaction of all the pairs of dipoles in the compound. Another approach is to treat the lone pairs as if they were hydrogen atoms. Replacement of the lone pairs by hydrogen atoms resulted in the distortion of the bond distances and bond angles, where oxygen, sulphur and nitrogen are involved. The bending energy term overshadowed all the other energy terms.

All the structures of the compounds discussed in this chapter were optimized by the same force field; therefore the decision was made to leave out the lone pairs. Reliable results were obtained in the reproduction of the crystal structures, without the addition of lone pairs.

The new force field produced a reliable representation of the real geometries of the phosphoramidates in the different chemical environments under investigation. We were only interested in the relative thermodynamic stabilities of the compounds, especially the eight-membered ring and five-membered ring isomers.

Table 5.1 is included for a quick reference to the different structures that are discussed in this chapter. The same numbering system was used in the preceding chapters.

For the P(O)*N*-Phenyl series (column A) the ^1H , ^{31}P and ^{15}N –NMR as well as the crystal data revealed a decrease in the N-P-N bond angles and an increase in the P-N bond distances. The nitrogen atoms became less planar (more pyramidal) with the introduction of another ring. The planarity of the nitrogen is indicated by the sum of the three angles around nitrogen. A sum close to 360 degrees implicates a planar nitrogen as in the triamidate precursor **1**. The smaller sum of 326 degrees for the tricyclic compound **4**, indicated a more pyramidal nitrogen. The bond angles and bond distances of the triamidate series are listed in **table 5.2**

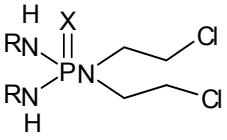
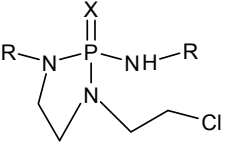
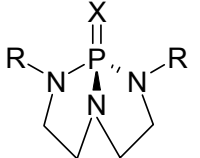
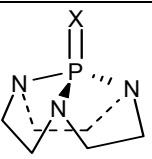
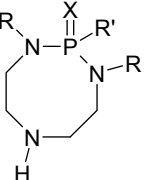
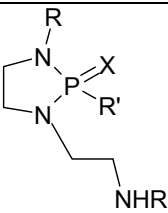
"username" of compound	Number of Compound	Structure
Substrate	<u>0</u> X=O <u>8</u> X=S	$\text{Cl}_2\text{P}(\text{X})(\text{NCH}_2\text{CH}_2\text{Cl})_2$
Triamidate	<u>1a</u> X=O, R=Ph <u>1f</u> X=O, R=Bz <u>*9a</u> X=S, R=Ph <u>9b</u> X=S, R=Bz	
Monocyclic	<u>2a</u> X=O, R=Ph <u>2f</u> X=O, R=Bz <u>*10</u> X=S, R=Ph <u>*10</u> X=S, R=Bz	
Bicyclic	<u>3a</u> X=O, R=Ph <u>3f</u> X=O, R=Bz <u>11a</u> X=S, R=Ph <u>*11b</u> X=S, R=Bz <u>*19</u> X= lone pair, R=Ph	
Tricyclic	<u>4</u> X=O <u>21</u> X=S	
8ring	<u>5a</u> X=O, R=Ph, R'=OEt <u>5f</u> X=O, R=Bz, R'=OMe <u>*15</u> X=S, R=Ph, R'=OMe (thiono) <u>*17</u> X=O, R'=SMe, R=Ph (thiolo)	
5ring	<u>6a</u> X=O, R=Ph, R'=OEt <u>6f</u> X=O, R=Bz, R'=OMe <u>16</u> X=S, R=Ph, R'=OMe (thiono) <u>17a</u> X=O, R'=SMe, R=Ph (thiolo)	

Table 5.1 List of the labelled structures of all compounds which were discussed in this chapter. *Compounds that were not isolated.

Compound	Triamidate	Monocyclic	Bicyclic	Tricyclic
Av P-N bond distance (Exp) /Å	1.639	1.646	1.663	1.673
Av P-N bond distance (Calc) /Å	1.651	1.6532	1.655	1.658
Av N-P-N angle (Exp) /°	105.7	105.53	102.1	100.9
Av N-P-N angle (Calc) /°	102.097	101.400	100.380	98.132
Sum of angles around endocyclic N exp	359.39	350.1	336.04	
Sum of angles around endocyclic N calc	359.51	357.27	347.13	332.59

Table 5. 2 Selected bond distances and bond angles for the P(O)N-Phenyl series.

This trend was also observed in the geometries of the calculated structures listed in **table 5.2**, however the changes in P-N bond distance and the bond angle were much more subtle. It was expected that the nonrigid triamidate **1a** and the highly strained bicyclic compound **3a** cannot be modeled exactly with the same set of parameters, because of the big differences in the geometry of the nitrogen atom. The changes in hybridization is also clear from the calculated geometries.

The geometries of the two compounds that were of interest, the eight-membered ring **5a** and five-membered ring **6a** compounds correspond very well with the experimental data. Selected bond distances, bond angles and torsion angles are listed in **Table 5.3**. All the calculated torsion angles involving the phosphorus tetrahedron or a nitrogen atom correspond with the experimental values. Some of the calculated torsion angles are of the same order of magnitude as the experimental values but of opposite sign. This can be explained as follows: when the two structures are superimposed, the orientation of the N-C bond are in opposite directions i.e. when it is “up” in the crystal structure, it is “down” in the calculated structure and vice versa. The sign of the torsion angles does not influence the energy calculation. No parameters were added for torsion angles. For the torsion angles where the new atom types were involved, the default values in Hyperchem were used.

The calculated values for the bond angles and bond distances are in good agreement with the experimental values. This result demonstrated that the amended force field is a reliable model to predict the geometries of the other derivatives of the eight-membered ring and the five-membered ring isomers.

8-RING 5a	EXP	CALC	5-RING 6a	EXP	CALC
Bond distances /Å					
P=O	1.466	1.446	P=O	1.476	1.442
P-N ₁	1.653	1.665	P-N ₁	1.662	1.661
P-N ₃	1.678	1.666	P-N ₂	1.648	1.648
P-O _{et}	1.574	1.594	P-O _{Et}	1.571	1.578
N ₁ -C	1.484	1.488	N ₁ -C	1.474	1.485
N ₃ -C	1.479	1.486	N ₃ -C	1.462/1.464	1.463/1.469
N ₁ -C _a	1.435	1.422	N ₁ -C _a	1.399	1.425
N ₃ -C _a	1.432	1.421	N ₃ -C _a	1.376	1.352
Bond angles /°					
P-O-C	119.2	125.7	P-O-C	121.5	124.9
O=P-O	114.2	110.2	O=P-O	107.2	113.2
O=P-N ₁	111.3	112.1	O=P-N ₁	116.7	112.3
O=P-N ₃	115.6	113.8	O=P-N ₂	118.4	117.1
O-P-N ₁	106.3	104.1	O-P-N ₁	110.2	108.1
O-P-N ₃	101.5	102.5	O-P-N ₂	109.2	109.2
C-N ₁ -C _a	118.5	118.5	C-N ₁ -C _a	121.2	121.6
C-N ₃ -C _a	117.9	120.3	C-N ₂ -C	119.0	122.5
P-N ₁ -C	116.1	116.2	P-N ₁ -C	112.7	109.5
P-N ₁ -C _a	124.7	122.7	P-N ₁ -C _a	125.1	126.1
P-N ₃ -C	118.9	115.7	P-N ₂ -C _{exo}	119.8	124.9
P-N ₃ -C _a	121.1	123.6	P-N ₂ -C _{endo}	111.3	112.6
C-N ₂ -C	117.5	114.5	C-N ₃ -C	125.1	119.9
N ₁ -P-N ₃	107.1	113.2	N-P-N	94.8	95.4
Torsion angles /°					
O=P-O-C	43.5	49.4	O=P-O-C	179.5	177.1
O=P-N ₁ -C	30.3	-42.1	O=P-N ₁ -C	-125.1	-101.3
O=P-N ₁ -C _a	-159.2	119.3	O=P-N ₁ -C _a	66.7	59.7
O=P-N ₃ -C	-108.3	40.8	O=P-N ₂ -C _{endo}	104.0	119.0
O=P-N ₃ -C _a	54.9	-146.3	O=P-N ₂ -C _{exo}	-41.4	-59.492
P-N ₁ -C-C	84.2	-51.4	P-N ₁ -C-C	18.2	34.632
P-N ₃ -C-C	83.3	94.9	P-N ₂ -C _{endo} -C	32.5	-20.745
C _a -N ₁ -C-C	-86.9	146.4	C _a -N ₁ -C-C	-173.0	163.379
C _a -N ₃ -C-C	-80.4	-78.4	C _{exo} -N ₂ -C-C	178.2	157.82
N ₁ -P-N ₃ -C	16.4	-88.8	N ₁ -P-N ₃ -C	0.6	-19.8
N ₃ -P-N ₁ -C	-96.9	88.4	N ₃ -P-N ₁ -C	20.9	0.1
C _a = aromatic carbon, C _{endo} = carbon inside five-membered ring, C _{exo} = carbon outside five-membered ring.					

Table 5.3 Selected bond angles, bond distances and torsion angles of eight (**5a**)- and five-membered (**6a**) ring compounds.

The calculated energies of the 8-membered ring to 5-membered ring isomers for all the different derivatives are listed in **Table 5.4**. The relative energies

confirmed that the rearrangement is thermodynamically controlled. The five-membered ring isomer has in each case a lower total strain energy than the eight-membered ring isomer.

“username”	Compound no.(Table 5.1)	Eight-membered ring kcal/mol	Compound no. (Table5.1)	Five-membered ring kcal/mol
P(O)N-Phenyl	<u>5a</u>	13.257	<u>6a</u>	7.163
P(O)N-Benzyl	<u>5f</u>	7.147	<u>6f</u>	5.731
P(S)N-Phenyl	<u>15</u>	13.974	<u>16</u>	6.661
P(S)N-Benzyl *	<u>15x</u>	10.866	<u>16x</u>	2.832

Table 5. 4 Calculated energies in kcal/mol for eight-membered ring and five-membered ring isomers.

The thiono-thiolo isomers had comparable potential energies. Rows A and B from **Table 5.5** indicate that for the *N*-Phenyl derivatives the thiolo isomer had a slightly lower potential energy than the thiono isomer for both the eight- and five-membered ring isomers. The last two rows in the table indicated more stable *N*-Benzyl substituted thiono isomers for both the five-membered and eight-membered ring isomers.

For the thiono as well as the thiolo isomers the calculated energies suggest that the five-membered ring isomer is thermodynamically more stable than the eight-membered ring compound. From **Table 5.5** it is clear that there is a consistency in the trend of the calculated results for the whole series of rearrangement products.

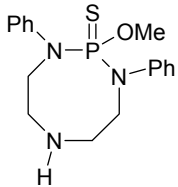
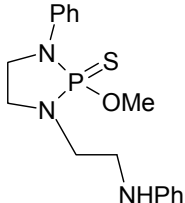
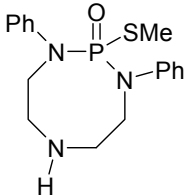
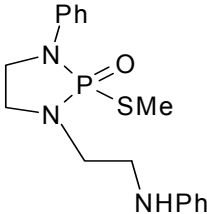
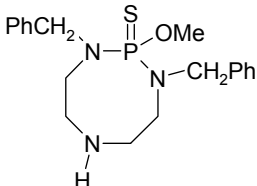
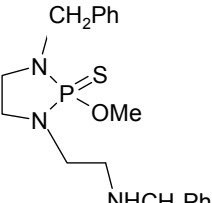
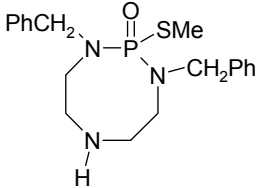
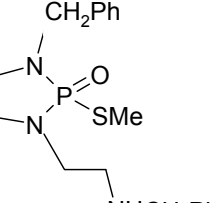
	“username”	E No.	F 8-ring Energies in kcal/mol	G no.	H 5-ring Energies in kcal/mol
A	P(S)N-Phenyl thiono	15a 	13.974	16a 	6.661
B	P(O)N-Phenyl thio	22 	12.407	23 	5.688
C	P(S)N-Benzyl thiono	15f 	10.866	16f 	2.832
D	P(O)N-Benzyl thio	24 	12.644	25 	6.060

Table 5.5 Calculated energies in kcal/mol for all thiono and thio phosphoric esters.

The following tables contain lists of all the parameters that were added to prepare the new force field.

Element	Description in chem.rul file
P	; phosphorus (P=O) connected to (=O)(-N)(-N)(-N)
P	; phosphorus (P=S) connected to (=S)(-N)(-N)(-N)?
P	; phosphorus P(O)NCI2 connected to (=O)(-N)(Cl)(-Cl)?
N	; phosphoramidate connected to (-C)(-C)(-P)?
N	; phosphoramidate connected to (-C)(-C)(-P)?
O	; phosphoryl connected to (=P)?
O	; phosphate ester connected to (-C)(-P)?
S	; thiophosphoryl connected to (=P)?
S	; phosphate thio ester connected to (-C)(-P)?

Table 5. 6 New atom types added to *chem.rul*

TYPE	MASS	REMARK
n5	14.003	73. N PHOSPHORAMIDE
n8	14.003	74. N PHOSPHORAMIDE
Po	30.994	77. P P=O phosphoryl
Ps	30.994	78. P P=S thiophosphoryl
Px	30.994	79. P P(O)NCI2
Op	15.994	80. O O=P
Sp	31.972	81. S S=P
Om	15.994	82. O P-OMe
Sm	31.972	83. S P-SMe

Table 5. 7 Changes made to *mmptype.txt* to list new atom types.

T1	T2	KS	L0	L1	DIPOLE
H	op	4.600	0.942	0.000	-1.115
H	sp	3.800	0.600	0.000	0.389
Px	op	6.500	1.456	0.000	-0.650
Px	sp	3.000	1.889	0.000	-0.650
Px	n5	6.400	1.618	0.000	0.950
Px	cl	3.200	2.012	0.000	1.950
Po	cl	3.200	2.012	0.000	1.950

Po	op	3.000	1.437	0.000	0.970
Ps	sp	3.100	1.930	0.000	0.900
Po	n5	6.200	1.637	0.000	0.950
Ps	n5	6.200	1.670	0.000	0.950
Po	n8	6.200	1.665	0.000	0.950
Ps	n8	6.200	1.670	0.000	0.950
n8	ca	6.320	1.410	0.000	1.300
n5	c4	5.100	1.460	0.000	0.040
n8	c4	5.100	1.470	0.000	1.470
Po	sm	2.900	1.800	0.000	0.970
Po	om	2.900	1.571	0.000	0.970
Ps	om	2.900	1.571	0.000	0.900
Om	c4	5.350	1.571	0.000	0.440
Sm	c4	3.200	1.815	0.000	0.000
Po	sm	3.100	2.024	0.000	0.830
n8	co	6.400	1.352	0.000	-0.290

Table 5. 8 Changes made to mmpstr.txt for bond stretching.

T1	T2	T3	KS	TYPE1	TYPE2	TYPE3
Op	po	n5	0.315	119.103	0.000	0.000
Op	px	n5	0.330	116.680	0.000	0.000
Op	po	n8	0.350	113.565	0.000	0.000
Sp	ps	n5	0.330	121.100	0.000	0.000
Sp	px	n5	0.300	121.300	0.000	0.000
Sp	ps	n8	0.300	113.850	0.000	0.000
Op	px	cl	0.560	112.650	0.000	0.000
Sp	px	cl	0.445	113.550	0.000	0.000
Sp	ps	cl	0.500	110.000	0.000	0.000
n8	ps	cl	0.500	108.000	0.000	0.000
n5	ps	cl	0.500	108.000	0.000	0.000
Op	po	cl	0.500	110.000	0.000	0.000
Cl	px	cl	0.710	99.910	99.960	0.000
Cl	po	cl	0.710	99.910	99.960	0.000
Cl	px	n5	0.450	108.00	105.00	0.000
Cl	po	n5	0.450	108.00	105.00	0.000
n8	po	n5	0.680	96.320	95.710	0.000
n8	po	n8	0.455	114.420	0.000	0.000
n8	ps	n5	0.690	95.410	0.000	0.000
n8	ps	n8	0.500	114.910	0.000	0.000
n5	po	n5	0.520	111.420	102.200	103.120
n5	ps	n5	0.520	111.420	102.200	103.120
Op	po	om	0.455	114.200	107.200	0.000
c4	n5	c4	0.380	119.000	111.340	0.000
Px	n5	c4	0.375	120.890	0.000	0.000
Po	n5	c4	0.375	120.890	110.300	0.000
Ps	n5	c4	0.320	123.600	109.350	0.000
Ps	n5	hv	0.440	110.000	0.000	0.000
Po	n8	ca	0.310	125.500	0.000	0.000
Ps	n8	ca	0.300	127.610	0.000	0.000
Ps	n8	c4	0.360	109.610	0.000	0.000
Po	n8	c4	0.530	110.020	0.000	0.000
Po	n8	hv	0.430	115.600	0.000	0.000
Ps	n8	hv	0.430	115.600	0.000	0.000

Po	n5	hv	0.440	110.000	0.000	0.000
c4	n5	hv	0.430	115.600	0.000	0.000
c4	n5	hn	0.695	106.690	0.000	0.000
Ca	n8	hv	0.420	116.000	0.000	0.000
c4	n8	ca	0.690	121.200	0.000	0.000
n5	c4	c4	0.450	112.890	0.000	0.000
n5	c4	ca	0.500	108.500	0.000	0.000
n5	c4	h	0.360	109.500	0.000	0.000
n8	c4	h	0.530	110.400	0.000	0.000
n8	ca	ca	0.695	120.000	0.000	0.000
Om	po	n5	0.530	111.300	115.6	0.000
Om	c4	h	0.695	109.470	0.000	0.000
Om	c4	c4	0.695	109.470	0.000	0.000
n8	c4	c4	0.500	105.600	0.000	0.000
n5	po	om	0.360	109.000	0.000	0.000
n8	po	om	0.500	106.300	101.500	110.200
Om	ps	n5	0.360	109.000	119.200	0.000
Sm	po	op	0.400	121.500	119.200	0.000
Ps	om	c4	0.400	121.500	119.200	0.000
Po	sm	c4	0.400	121.500	119.200	0.000
Po	om	c4	0.400	121.500	119.200	0.000

Table 5. 9 Changes made to *mmpben.txt* for angle bending.

C	A	COPB
Ca	n8	0.050
n8	Ca	0.050
n8	Hv	0.050
n8	Po	0.050
n8	Ps	0.050
n5	Hv	0.050
n5	c4	0.050
Po	Op	0.050
Ps	Sp	0.050
Op	Po	0.050
Sp	Ps	0.050
Px	Op	0.050
Op	Px	0.050
Px	Sp	0.050
Px	Sp	0.050
n5	Px	0.050
n5	Po	0.050
n5	Hn	0.050
n5	Ps	0.050
n8	c4	0.050
Sm	c4	0.050
Om	c4	0.050
Ps	Om	0.050
Ps	Sm	0.050
Po	Sm	0.050
Po	Om	0.050

Table 5.10 Changes made to *mmpoop.txt* for out-of-plane bending.

TYPE	RSTAR	EPS
Po	2.2000	0.1680
Ps	2.2000	0.1680
Px	2.2000	0.1680
Op	1.7400	0.0660
Sp	2.1100	0.2020
Om	1.7400	0.0500
Sm	2.1100	0.2020
n5	1.8200	0.0550
n8	1.8200	0.0550

Table 5.11 Changes made to *mmpnbd.txt* for van der Waals radii.

5. References

1. W.J. Hehre, J. Yu, P.E. Klunzinger, L. Lou, *A Brief Guide to Molecular Mechanics and Quantum Chemical Calculations* (1998).
2. A. Hinchliffe, *Chemical Modeling From Atoms to Liquids* (1999).
3. J.C.A. Boeyens, P. Comba, *Coordination Chemistry Reviews*, **212**, 3, (2001).
4. Hyperchem Manual, HyperChem® Release 7.0, Hypercube Inc., Florida, USA (2002).
5. X.Y. Mbianda, T.A. Modro, P.H. van Rooyen, *Chem. Commun.*, 741, (1998).
6. S. Laurens, V. Ichharam, T.A. Modro, *Heteroatom Chem.*, **12 (5)**, 327 (2001).
7. N.L Allinger, *J. Am. Chem. Soc.*, **99**, 8127 (1977).
8. N.L. Allinger; Y.H. Yuh, Quantum Chemistry Program exchange, Bloomington, Indiana, Program #395.
9. U. Burkert; N.L. Allinger, *Molecular Mechanics*, ACS Monograph 177 (1982).
10. The Cambridge Structural Database: a quarter of a million crystal structures arising, F.H. Allen, *Acta Crystallogr.*, **B58**, 380 (2002).
11. Personal communications with Dr. Marsicano (Wits), Prof. P.H. van Rooyen (UP), Prof. J. Dillen (US), Prof. J.C.A. Boeyens (UP), Prof. P. Comba (University of Heidelberg), other Hyperchem users (May 2004).

CHAPTER 6

6. CONCLUSION

The chemical reactivities of the different analogues were expected to be comparable however, it proved to be very different. Most of the phosphoryl derivatives in the series were relatively easy to prepare and isolate (R=Ar), others were more difficult (R=aliphatic) to prepare and some of the thiophosphoryl could not be synthesized successfully. The exact reaction conditions could not be found to prepare any of the phosphine derivatives.

Both the substrates for the phosphoryl and thiophosphoryl series were prepared, via the same synthetic route, under the same experimental conditions, except for the starting materials of $P(O)Cl_3$ and $P(S)Cl_3$ respectively. The phosphoryl derivatives with *N*-Phenyl substituents were also prepared and no stumbling blocks were anticipated in the preparation of the thiophosphoryl analogues. The thiophosphoryl substrate proved to be resistant to reaction with aniline however, the substrate reacted relatively easy with benzylamine. The second and third nitrogen atoms with a phenyl substituent could be introduced by another route. This result indicated that the thiophosphoryl center with one nitrogen attached to phosphorus is not completely resistant to nucleophilic attack.

The alcoholysis of the *N*-alkyl bicyclic substrates progressed differently from the *N*-aryl derivatives. In the case of the *N*-aryl substrates, the acidic alcoholysis resulted in the eight-membered ring product **5a** and the basic alcoholysis in the five-membered ring isomer **6a**. Both the acidic and basic alcoholysis of the *N*-alkyl substrates resulted in the same product namely the eight-membered ring compound **15**. The alcoholysis products were isolated and characterized. The hydrochloric salts were not suitable for X-ray determination. The free base of the alcoholysis product, the eight-membered ring, in both cases could not be isolated. The reaction kinetics of the alkyl derivative were studied. The free amine of the $P(S)N$ -Phenyl derivative was very unstable and resulted in a mixture

of unidentified phosphorus compounds. For this reason it was not possible to perform any kinetic studies on this compound.

A difference between the *N*-aryl and *N*-alkyl substrates was also observed for their reactivity in the related eight-membered to five-membered ring rearrangement.

From the crystal structures it was clear that the two halves (two five membered rings) of **3a** and **11a** had remarkably different dihedral angles. The NMR data represented an average of the two rings; therefore they appear identical on the NMR-scale.

Comparing the dihedral angles as determined from NMR data, by utilization of the Karplus equation, with the dihedral angles obtained from X-ray diffraction data was only approximate. There was very little correlation between the experimental and the calculated dihedral angles for compounds **3a** and **11a**. An average value of the dihedral angles, resulting from NMR data, was not in agreement with the crystal structures.

The analysis of the crystal structures did not reveal any significant differences in the geometries of the phosphoryl and thiophosphoryl analogues. The geometries around phosphorus and nitrogen were comparable. The thiophosphoryl substrate had a P=S bond distance of 1.889 Å, which is shorter than the average P=S bond length of 1.926 Å in similar compounds, The P-N bond distance (1.732 Å) was longer than the average P-N bond length of 1.65 Å. The nitrogen atoms in both substrates were planar i.e. the sum of the bond angles around nitrogen is 359.61° and 358.81° respectively. The two bicyclic analogues **3a** and **11a** also had comparable geometries and revealed no deviations from the normal bond angles or bond distances of this class of compound¹.

The reason for their different chemical reactivity must lie in the differences between the phosphoryl and thiophosphoryl centers.

Molecular mechanical calculations were used to optimize the geometries of all the phosphotriamidates discussed in this work. The Hyperchem MM+ force field in its original form, was not suitable for the type of compounds discussed in this manuscript. Parameters were added to prepare an improved force field to represent the compounds, under question. There were however a few limitations. There was no clear information on how to treat the lone pairs in Hyperchem. Hyperchem only adds lone pairs on sp^3 oxygen and sp^3 nitrogen. Hyperchem treated the sp^3 nitrogen, without the lone pair, as a sp^2 nitrogen and therefore an out-of-plane bending term were added to the total energy calculation. The reason for this selective use of the lone pairs might be to cancel the out-of-plane bending. The absence of the lone pairs did not influence the geometry, however it did add to the calculated electrostatic energy as well as the bond stretch energy. In the case of sp^3 oxygen and sp^3 sulphur, the addition of the lone pairs also did not influence the geometry but an out-of-plane bending term is involved. This out-of-plane bending for the sp^2 oxygen contributes significantly to the total energy.

The new force field was employed to optimize the geometries of the series of compounds listed in **Table 5.1**. The results indicated that it was a reliable model to use for similar compounds, for which no experimental data exists.

The molecular mechanical calculation results clearly confirmed the experimental result for the eight-membered to five-membered ring rearrangement. The five-membered ring is thermodynamically more favoured than the eight-membered ring. Similar results were obtained for the thiophosphoryl analogues of both the *N*-phenyl and *N*-benzyl derivatives, i.e. the calculated energy for the five-membered ring compound was lower in each case.

The structures in the thiono-thiolo rearrangement had comparable energies, with that of the thiono isomer of the *N*-Benzyl derivative slightly lower than that of the thiolo isomer. It can be argued that in the case of the *N*-Benzyl derivative the thiono isomer is thermodynamically more favourable in energy than the thiolo isomer.

To perform a more thorough and complete study of the chemical behaviour of the phosphotriamidates and the differences between the phosphoryl and thiophosphoryl analogues, it will be required to perform quantum mechanical calculations. This will yield more information on the thermodynamics, reaction kinetics, as well as the activation energies of these compounds.

The mechanism of the eight-membered to five-membered ring rearrangement is also a matter that is worth a thorough investigation. Molecular mechanical methods are not sufficient to study this mechanism since MM+ was not developed to accommodate atomic charges. The postulated mechanism for the rearrangement, as discussed in the introductory chapter, progressed via a trigonal bipyramidal intermediate^{2,3}. No experimental data were available for the trigonal bipyramidal structures of the phosphotriamidates to test any calculation results.

The thiono-thiolo rearrangement is a temperature dependent reaction and proceeds via a bimolecular reaction mechanism. Quantum mechanical calculations could be utilised to get more information on this process.

6.1 References

1. S. Laurens, V. Ichharam, T.A. Modro, *Heteroatom Chem.*, **12 (5)**, 327 (2001).
2. Z. He, S. Laurens, X.Y. Mbianda, A.M. Modro, T.A. Modro, *J. Chem. Soc. Perkin Trans. II*, 2589, (1999).
3. X.Y. Mbianda, T.A. Modro, P.H. van Rooyen, *Chem. Commun.*, 741, (1998).

Publications originated from this work:

1. Z. He, S. Laurens, X.Y. Mbianda, A.M. Modro, T.A. Modro, *J. Chem. Soc. Perkin Trans. II*, 2589, (1999).
2. S. Laurens, V.V.H. Ichharam, T.A. Modro, *Heteroatom Chem.*, **12 (5)**, 327 (2001).